THE MESSENGER

EL MENSAJERO

Munich

Paranal
La Silla
La Serena
Santiago

No. 84 – June 1996

TELESCOPES AND INSTRUMENTATION

Main Structure: Progress and First Test Results

M. QUATTRI, ESO

The assembly of the main structure is progressing very fast in Milan, and the telescope will finally be completed and functional at the end of September. At this stage of the mounting, one can say that the tasks which were considered the most difficult, from the assembly point of view, have been carried out by AES's crew under the supervision of Mr.

Figure 1: The M1/M3 concrete dummy is positioned on the fork.

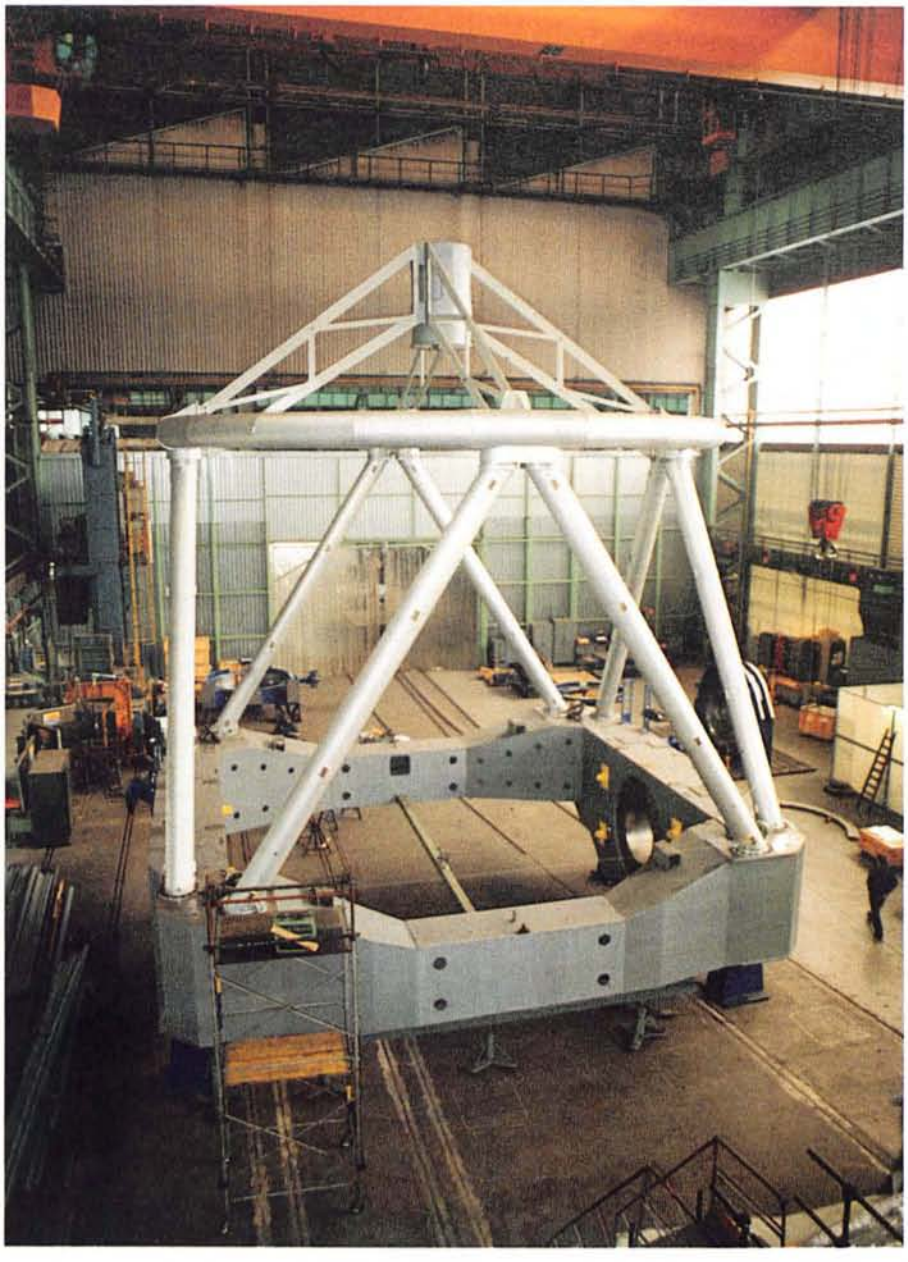

Figure 2: The tube is placed on supports for the Top Unit dynamic test. ◄

would have played a major role in the overall long-time stability of the telescope, also impacting on the functionality of the hydrostatic bearing system which needs plane journals to work at its best performance. Also the encoders could have been affected by instability of the mounting due, for instance, to temperature gradients in the mechanics, and this would have influenced the repeatability of the system degrading the final performances.

All these concerns have now been ruled out by the results obtained in Milan. The precision of alignment of the azimuth bearing journals, both positioning and run-out, as well as planarity, have been met better than specified, as already mentioned in previous articles. Their stability has proved to be so good that during all the surveying time until now (and it will continue until the dismounting of the main structure) no modifications have been detected, and the azimuth hydrostatic bearing system runs in a smooth and stable manner.

The positioning and alignment of the large mechanics have been carried out with outstanding precision and reproducibility even after multiple dismounting and mounting. The reference pinning of the different pieces has made it feasible and will make the assembling of the structure in Chile faster and "easier".

The altitude encoder has been completely assembled in a laboratory built on purpose next to the telescope, and its mounting stability is kept under control. It shows that no modifications of the relative position of the measuring elements take place due to temperature cycling or micro-vibration induced into the system

Bartolamei, obtaining far better results than specified and eliminating all the concerns that these operations had caused the designer.

As a matter of fact, even though during the conceptual and final design phases all the difficulties related to the machining and alignment of large pieces had been thoroughly investigated, the designers were waiting for the real operation to test on the field that the assumptions used would have given the foreseen results.

In fact, the major concerns which accompanied us during the phases of assembly were related to the alignment precision and its stability in time, both required to meet the final specified alignment of the axes of the telescope. The concrete foundations long-term stability

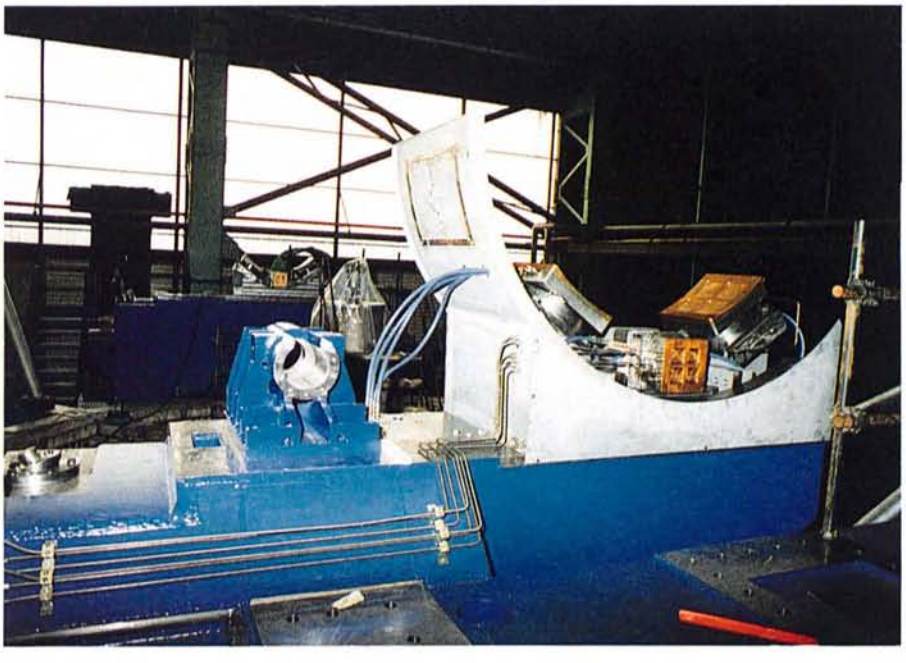

Figure 3: Altitude hydrostatic bearing pads and locking pin support. ►

Figure 4: Altitude drive pre-assembling. ►

by the "dirty" industrial environment (one should not forget that heavy tool machines are operated in the same building).

After a first assembling of the tube on the main structure to perform a number of alignments, the telescope has again been taken apart as one can see in Fig. 1 and 2. This operation was necessary to carry out a modification of the altitude hydrostatic pads to facilitate the maintenance (mainly to make accessible pressure transducers and check valves as seen in Figure 3) and perform the final alignment of the altitude axis. At the same time the M1/M3 unit concrete dummy has been placed on the fork and centred with respect to the azimuth axis (Fig. 1), ready now to be bolted on the tube structure.

At the same time the altitude drives (2.8 m diameter) are being pre-assembled ready to be lifted on the Nasmyth platform (Fig. 4).

Now the tube structure has been repositioned on the fork, and the dummy has been mounted, making the main structure ready to undergo the dynamic tests during week 22.

The first test results though have been obtained during the month of March 1996. In fact, one of the reason to dismount the tube from the fork and place it on supports was precisely to test the dynamic performance of the M2 dummy, which forms with top ring and spider the so-called telescope Top Unit.

The eigenfrequencies of the M2 along the optical axis and around the axis perpendicular to it will define the performance of the M2 unit under the wind action (important for the Optical Path Variation in the interferometric mode) and while

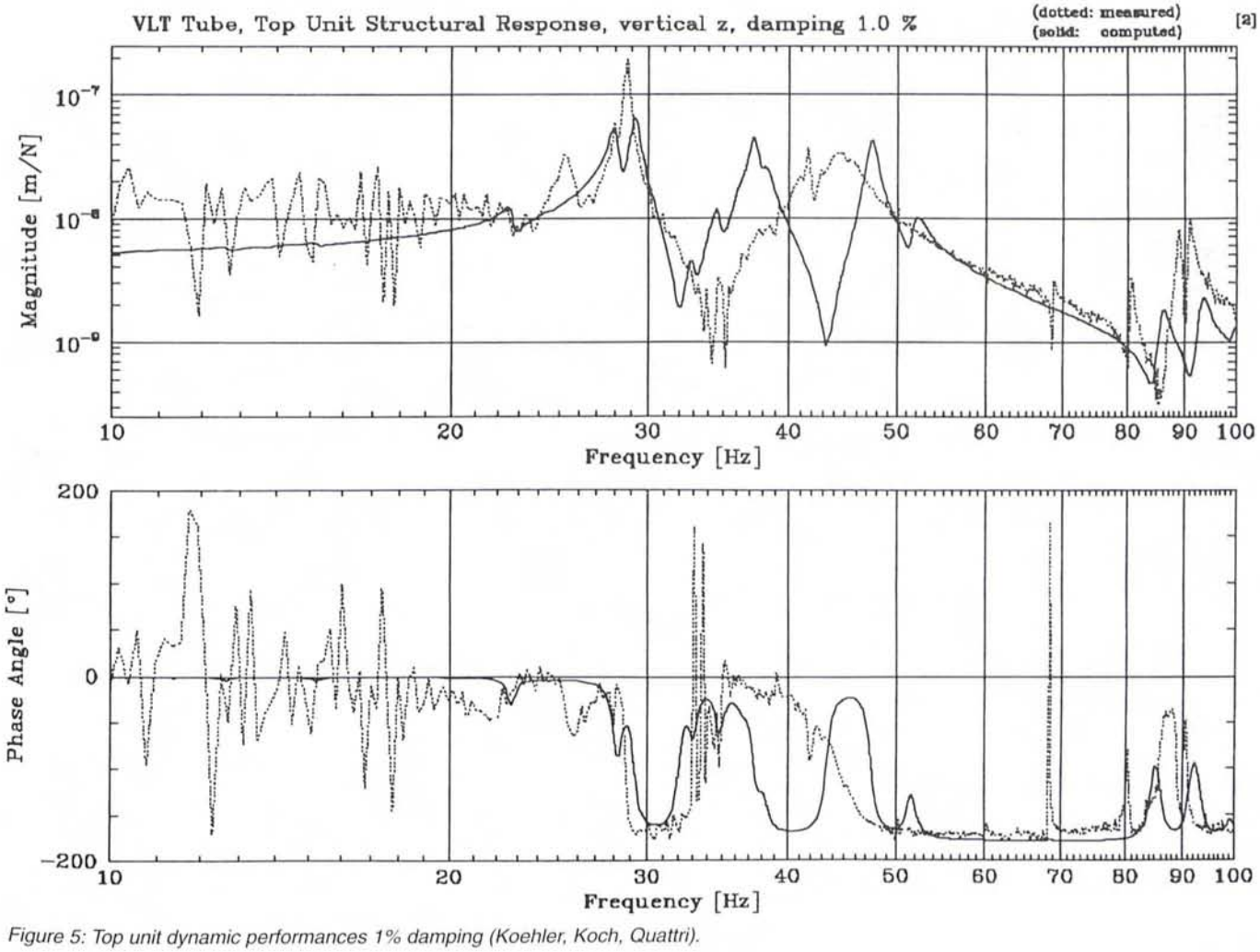

Figure 5: Top unit dynamic performances 1% damping (Koehler, Koch, Quattri).

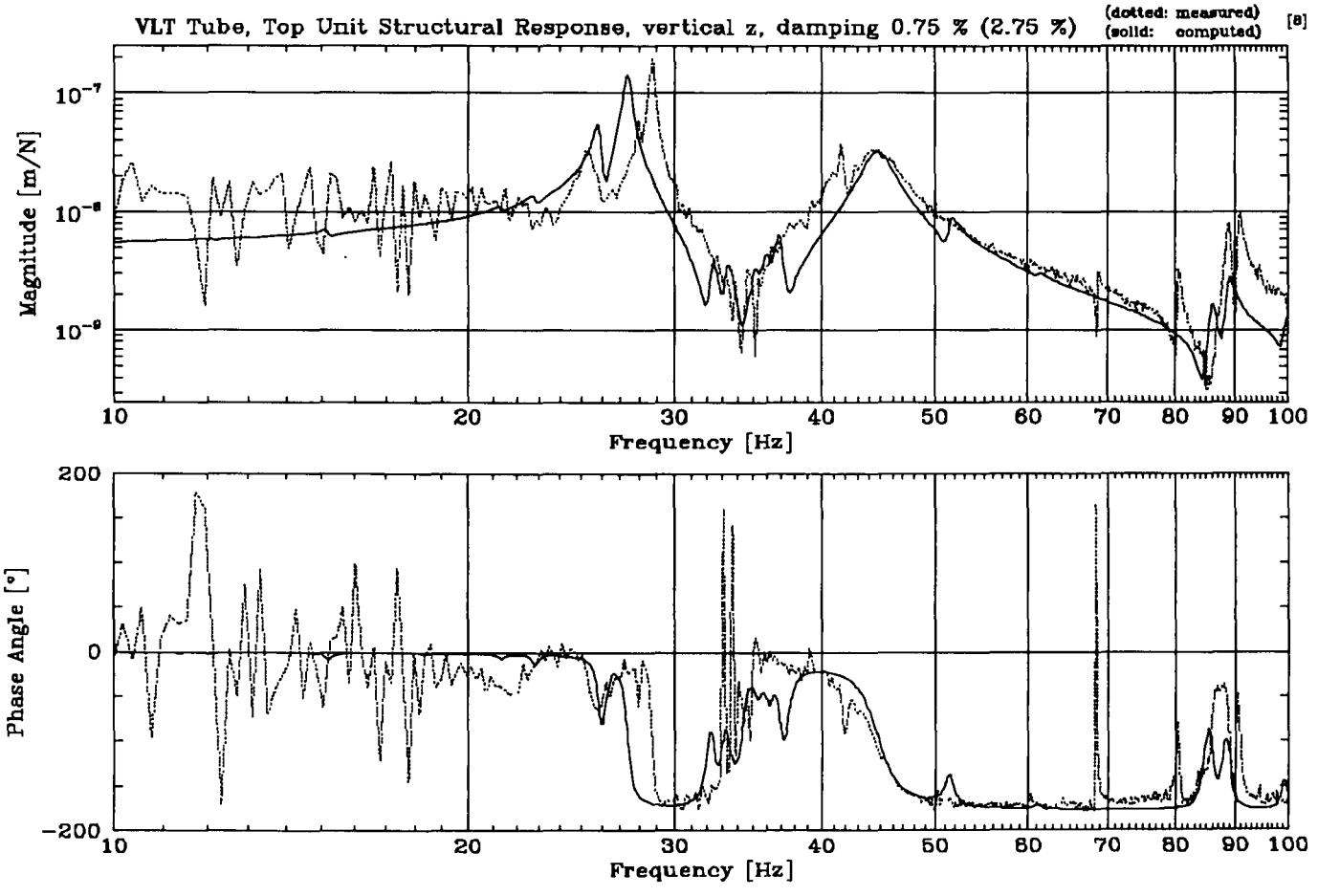

Figure 6: Top unit dynamic performance 0.75% and 2.75 % damping (Koehler, Koch, Quattri).

chopping or tip-tilting. The value specified, and determined according to the interferometric and infrared requirements, were 20 Hz along the optical axis and 26 Hz in rotation. The design calculation had shown better performances (27 and 36 Hz respectively) after the modification of the top ring using a stiffer section.

Last March the tube was equipped with accelerometers, and, using an electronic hammer, the impulsive excitation was applied to the M2 dummy both along the optical axis and the axes perpendicular to it. The results are shown in Figure 5: the dotted line shows the recorded spectrum of the displacement of the M2 dummy. B. Koehler and F. Koch have compared the experimental results with the calculated spectrum, shown in Fig. 5 with the solid line, and have found a very good agreement among the two, which tells how reliable the calculations performed by AES are.

It was very interesting to see that the curves had even a better agreement after having applied a higher damping factor to that mode in which the spiders move on the bolted attachments to the top ring (see Fig. 6).

The fact that the effective damping is the same as the one used in the analysis, and generally used for welded structures, gives an idea of how good the bolted junctions in the structure have been designed and realised. On the other hand, the fact that the vibration modes which involve bolted parts are better damped gives the feeling that the behaviour of the structure during seismic events could be better than the one calculated with the very conservative damping factor of 0.75%.

In the next months, till end of July, the main structure will be thoroughly tested in all its components, and a complete picture of its performances will be available. The start is positive and very encouraging.

Marco Quattri
e-mail: mquattri@eso.org

The VLT Software Review

P. QUINN, G. RAFFI, ESO

A Status Review of the VLT control software was held in ESO, Garching, from April 24–26, 1996. The purpose of the Review was to provide the ESO Management and the Divisions involved in using the VLT software with a quantitative report on the status of the software, close to important milestones of the VLT programme.

ESO representatives of the different "VLT software User" Groups/Divisions were present, including Instrumentation, La Silla and of course DMD and VLT (Software Engineering, NTT Upgrade, VLTI). A team of external Reviewers was appointed from the international scientific community: Drs. R. Doxsey (STSci), Chairman, A. Daneels (CERN), S. Wampler (Gemini) and T. Axelrod (MSSSO). They provided already a number of relevant comments and remarks during and at the end of the Review. A written report will also be forwarded to ESO.

The review had a dense three-day agenda, involving not only the VLT control software aspects but also the Data

Flow software. The aspects considered covered:

– the software development cycle from requirements to implementation

– maintainability, ease of integration and scalability of software

– test procedures, documentation and user's support

– operational aspects

– interfaces between VLT control and Data Flow software

The VLT Control Software

The programme was based on presentations and several demonstrations, as quite a large portion of the software is ready at least in a first version or in a prototype form.

The VLT common software was first introduced. This is by now a well-established product, developed in an incremental way through a series of Releases since 1994, typically twice or three times per year. It contains now an amount of code of about 500 Klines and is distributed to Instrument Consortia and VLT Contractors. In addition, a complete CCD control software package is now available, which is also distributed to Consortia. This is going to be used now both for technical and scientific CCDs.

The part which is becoming more critical now in the VLT programme is obviously the telescope control software, both the subsystem control and the coordinating software. This software is basically the same on the NTT upgrade and on the VLT. It will be tested in parallel during the so-called NTT Big Bang starting in July at La Silla (recommissioning of the NTT with the new software) and with the first telescope structure at the manufacturing site in Milano.

The presentations about the Instrumentation standards used by ESO, but also by the Instrumentation Consortia, concluded the presentations on VLT control software.

It was clear from all this that ESO developments are well aligned with the VLT milestones, although still quite some work has to be done. This was also the subject of presentations covering the telescope integration and commissioning periods, from the point of view of the control software. Looking at planning, while still quite some effort will go into completing the common software this year, more and more effort will be shifted towards telescope control software in the medium range. On the longer run control software for instruments will take more and more effort, although this is to a large extent a collective effort by the Astronomical Community of member countries channelled through the Consortia.

The ongoing training of the Paranal software support team, well integrated with the VLT software development team, was also explained. This is part of the strategy to cope with the software support and maintenance activities at Paranal.

An interesting presentation was given also on the VLT Interferometer software plans, a new potential "customer" of the VLT software standards.

The DMD Data Flow Software

On the final day of the Review, DMD presented an overview of the design and implementation status of the VLT Data Flow System (DFS) (see this issue's article on the DMD for a general discussion of the DFS). The DMD presentation was preceded by a discussion of interface issues between the DFS and the VLT Control Software (VCS). An outline of software needs of instrument developers and operators was also presented.

The DMD presentation showed the system breakdown of the DFS into components of the observing cycle from proposal entry to archival research. The concept of Observation Blocks as the quantum of data that flows in the DFS was outlined. Observation Blocks will be passed to the VCS for execution. VCS will request services from the DFS such as catalogue support and archival storage of calibration and raw data. DFS will request site and instrument status data from the VCS so that the short-term scheduling of Observation Blocks can be done to optimise the scientific throughput of the VLT. Since the DFS design process began only in 1995, there is a significant difference in the developmental status of VCS and DFS. Many important pieces of software infrastructure were developed within the VLT software effort before the DFS was defined. Hence there is a critical need for DMD, INS and VLT software groups to work together to define and address the various open interface issues between the DFS and VCS. In September 1995, a Data Flow Project Team was formed with members from VLT, DMD, INS and Science divisions. This team will play a vital role in the successful union of VCS and DFS. The work of the team will be critical in the NTT prototyping programme. By the beginning of 1997, DMD in collaboration with VLT plan to run prototypes for DFS archive, pipeline and scheduling systems on the NTT.

Conclusion

The general feeling was that ESO is well on track both with respect to the technology used and in relation to the next VLT milestones. The effort made by ESO in the NTT upgrade project, used also as a testbed for the VLT and DMD software, was appreciated and encouraged. Still a number of areas exist where the ongoing developments have to be checked and improved. We look forward to the written report by the Reviewers to then start a number of corrective actions.

The VLT software group has been running VLT control software workshops in the last two years, to strengthen the collaboration with Consortia and Contractors. The above Review was clearly not meant to be a replacement for this year's Workshop. This is expected to be held in the second week of September, in collaboration with the DMD and INS Division. Invitations will be sent out to the VLT partners before the summer.

Gianni Raffi
e-mail: graffi@eso.org

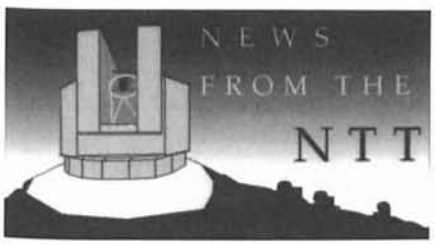

The NTT upgrade project has the following goals:

1. *Establish a robust operating procedure for the telescope to minimise down time and maximise the scientific output.*
2. *Test the VLT control system in real operations prior to installation on UT1.*
3. *Test the VLT operations scheme and the data flow from proposal preparation to final product.*

J. SPYROMILIO, ESO

By the time this issue of the Messenger appears in print, the NTT will be in the big-bang phase of the upgrade. Since this article is being written some time in advance, it is difficult to give you an update on how we are doing with the big bang. Right now the preparations are in their final hectic days. I would, however, like to concentrate more on what we plan to do at the time you will be reading this article.

Big Bang

The first thing we plan to do in the big bang is the re-aluminisation of the secondary mirror of the NTT. This will be done while the old control system is still in place so that we can verify the optical alignment of the M2 unit before removing any other optical element. Following the reintegration of the M2 unit we will start the control system upgrade. This is split into four parts. In the big bang part 1 we shall upgrade the major telescope subsystems (building, altitude, azimuth, M1, M2 and M3) and the adapter rotator on side A (the SUSI side). This work will last until the middle of September and we expect that the re-aluminisation of the primary as well as a number of maintenance activities will also occur during this time. Following this part 1, we will begin to integrate the various subsystems into the NTT control system. At the same time side B (the EMMI side) and the instruments will be upgraded. In this second part of the big bang we plan to have a period of complete system integration of all control functions.

With the end of the big bang part 2 we plan to re-align the telescope and re-aluminise the tertiary mirror of the telescope (which has to be removed in any case for the alignment). At the same time we shall be installing the new CCD controllers (ACE) on EMMI and SUSI. The completion of part 3 will allow us to begin the commissioning phase for the new control system and the instruments. We expect to be doing this during December and January of 1996/97. When we have a global understanding of the control system we shall then plug this system into the VLT data flow system which will handle all parts of observing external to the direct control of the instrument/telescope.

Bringing the NTT Back to the Users

A number of applications having been submitted, we are awaiting the OPC approval for service programmes with the NTT in February/March 1997. Assuming the aforementioned phases of the big bang go according to the plan, we expect that we shall be doing some very limited service observing on the NTT during that period. As was made clear in the announcement of opportunity, this observing is strictly shared risks. As anyone who has commissioned an instrument or a telescope will be well aware, the number of problems that we shall face cannot be overestimated. Depending on the progress with the big bang, a decision will be made on what may be made available to the community during period 59. However, we do want to welcome users back to the telescope before the official end of the big bang in July 1997. This is a critical part of the prototyping the NTT is supposed to perform in advance of the arrival of UT1.

We expect that the NTT that comes out of the big bang will be better than what we had before. The problem discussed in the last issue of the *Messenger* regarding the sensitivity of EMMI has now been traced to the long period between aluminisations of the telescope mirrors and also to the bad state of the RILD mode selection mirror which seems to suffer from acne. A similar problem has been found in the SUSI M4 mirror. Although the latter should be replaced before the big bang, the former cannot be replaced so soon. We hope for a significant improvement in sensitivity for the whole telescope after the upgrade.

What will the NTT Scientific User See

For a start we plan to replace the NTT console for one more functional. Users familiar with the remote control room can expect a similar look and feel. A number of new workstations will be in place both for the control of instrument and telescope but also to provide access to data flow tools such as pipeline and scheduler within the control room. The somewhat uncomfortable situation of having to do data analysis on the same workstation that is taking the data will hopefully be a thing of the past with a dedicated workstation planned for off-line use by the astronomer.

The new control system will come with a new operations scheme, and people who have applied for NTT SUSI service time and whose proposals are selected by the OPC shall be using a phase II proposal preparation tool to specify their observations in more detail. At phase II observing blocks (OB) will be created. These OBs marry targets and observations into a single entity that can be scheduled and executed. The observing blocks will be run by the NTT team in service mode and checked against the requirements before we send the data to the applicant.

We strongly value the comments and suggestions from the community at all times. Moreover, during this rapid prototyping phase, the user community can be most influential and helpful. Therefore, all users of the NTT are strongly encouraged to help us make an NTT that suits their scientific needs.

Comings and Goings

The NTT team composition has been fairly stable over the last few years; but now, as the big bang approaches, some changes have taken place. Pierre Martin has arrived as a new NTT fellow and Stephane Brillant has also joined the team as a student. Also Marco Chiesa and Thahn Phan Duc, both of whom are software engineers, have transferred from Garching to La Silla to be closer to the action. Sadly, Roberto Aviles, one of the NTT instrument operators, is no longer with the team.

Jason Spyromilio
jspyromi@eso.org

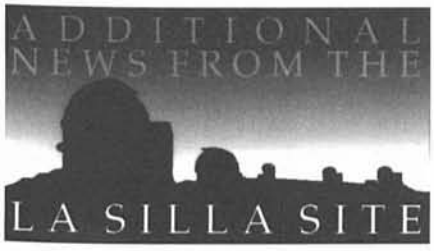

The La Silla News Page

The editors of the La Silla News Page would like to welcome readers of the fourth edition of a page devoted to reporting on technical updates and observational achievements at La Silla. We would like this page to inform the astronomical community to changes made to telescopes, instruments, operations, and of instrumental performances that cannot be reported conveniently elsewhere. Contributions and inquiries to this page from the community are most welcome. (P. Bouchet, R. Gredel, C. Lidman)

A New CCD for the B&C Spectrograph on the ESO 1.52-m Telescope

C. LIDMAN

During the beginning of March, a new CCD (#39) was installed at the ESO 1.52-m telescope. This CCD is intended for use with the B&C Spectrograph. The new CCD is a UV-flooded, thinned, Loral CCD and is a 2048 × 2048 array of 15 micron pixels.

Compared to the old Ford CCD (#24), the new CCD has a five-fold increase in sensitivity at 4000 Å and a two-fold increase in sensitivity at 6000 Å. This large increase in sensitivity is gained at the expense of a slight decrease in the resolution of the instrument, particularly in the blue. This is demonstrated in Table 1 which lists the FWHM (Full Width at Half Maximum) for various spectral lines at different slit widths. With the holographic grating (#32) this translates to a resolution of 2500 at 3700 Å.

The dark current of the new CCD is 5.2 ADU (6.2 electrons) per hour and the read noise is 5.8 ADU. The pixel scale along the slit is 0.82 arc seconds per pixel.

TABLE 1.

Slit width arc sec.	3888 Å		4922 Å		7635 Å	
	#24 (old)	#39 (new)	#24 (old)	#39 (new)	#24 (old)	#39 (new)
1.0	1.64	2.50	1.41	2.27	1.40	1.79
1.5	1.97	2.70	1.67	2.48	1.70	2.01
2.0	2.39	2.99	2.04	2.77	2.09	2.30
2.5	2.83	3.33	2.55	3.10	2.46	2.66
3.0	3.34	3.73	3.04	3.47	2.81	3.09
4.0	4.25	4.51	3.96	4.28	3.68	3.85

The FWHM of chosen spectral lines, as measured in pixels, for various slit widths. The pixel size of the old and new CCDs are identical. Grating #7 was used.

At the time of writing this article, the new CCD has now been in operation for two months. The quality of the UV flood is continually monitored and to date there is no degradation in the efficiency of the CCD nor in the uniformity of the response. With proper care, the UV flood can be maintained for five months or longer, as has been demonstrated by the CES CCD.

The installation of the new CCD has only been possible through the combined efforts of many people both at La Silla and Garching. This includes the CCD group in Garching, in particular S. Deiries and O. Iwert, the optical detector group at La Silla, the 2.2-m team, and C. Ledoux and H. Duerbeck who took all of the initial test observations.

News at the Danish 1.54-m Telescope

J. STORM

The DFOSC CCD Upgrade

In July we will be upgrading the thinned LORAL CCD currently mounted on DFOSC to a UV-sensitive device. This upgrade will be done by Copenhagen University Observatory, who has provided the camera and controller, together with the ESO optical detector team. This upgrade is expected to improve the quantum efficiency (QE) very significantly, not only in the UV but over the full optical wavelength range. The QE of the detector will be very similar to the one of the chip currently mounted at the Boller and Chivens spectrograph on the ESO 1.52-m telescope, i.e. above 80% QE from 350 nm to 750 nm and above 50% down to 320 nm and up to 850 nm.

The Danish 1.54-m TCS Upgrade

The graphical user interface for the Telescope Control System has also been significantly redesigned, and is now based on one fixed window. The interface is now easier to use and more transparent than the previous one. New functionality has also been added, including a graphical user interface to the object catalogue handling. We plan to install and commission the new version in the coming months.

The DFOSC Control System Upgrade

At the same time as the TCS upgrade, the Data Acquisition Integrated SYstem (DAISY), developed originally for the Dutch telescope, will be ported to the

newly-installed dual screen HP-735 at the Danish 1.54-m. The graphical user interface will resemble the one at the Dutch telescope but the functionality will of course be expanded to allow the control of the significantly more complex DFOSC instrument. DAISY will interface to the DFOSC controller (slit, filter, and grism wheels, camera focus) as well as with the telescope focus unit, the filter and shutter unit (FASU), and the CCD controller. Thus DAISY will provide an integrated interface to the complete instrument.

The new HP-735 workstation and the newly installed 150 MHz Pentium PC, which controls the CCD, are now capable of reading out a full 2k × 2k CCD frame (when using a single read-out amplifier) and display it on the MIDAS display on the workstation in less than 90 seconds. In the coming year we will experiment with using two amplifiers simultaneously. This should reduce the read-out time to well under 1 minute.

EFOSC-2 CCD Upgrade

In the last week of July we plan to install a UV-sensitive CCD in EFOSC2. The device will be a thinned LORAL 2k × 2k chip of the platinum flash gate type. This means that the device will not need UV flooding to achieve the high quantum efficiency (a significant operational advantage), but otherwise the specifications are very similar to the ones of the chip currently in operation at the ESO 1.52-m telescope (see above). The new CCD will be significantly larger than the Thompson chip currently in use but the pixels will be slightly smaller (15 μm compared to 19.5 μm). The field of view will thus increase, but we expect that the image quality will degrade towards the edges of the field as EFOSC2 was not designed for such a large-format detector.

With this upgrade, the optical instruments mounted on the three main telescopes operated by the 2.2+1.5-m Telescope Team will all have high-quantum-efficiency, large-format CCDs, making them truly competitive for the coming years.

IRAC1 – Back in Good Shape

C. LIDMAN and H. GEMPERLEIN

IRAC1 is ESO's 1–5-micron imager on the 2.2-m telescope. It has been operating in its present form since 1994.

For IRAC1, 1995 was a disappointing year. Apart from its infrequent use by the community, the camera had suffered from significantly reduced throughput and significantly higher backgrounds than what was found during the initial test observations of 1994.

During the new year, it was discovered that an oily liquid was deposited on the inside of the entrance window lens. The origin of this liquid is unclear, but may be due to the evaporation of overheated insulating material when the detector is baked inside the dewar. The liquid was removed and baking is performed now with greater care. Since that time there have been two observing runs with the camera. The performance of IRAC1 has returned to that measured in 1994.

The Mechanical Support Team (MST)

G. IHLE

Everyone who observes at, or visits, La Silla would have come into contact with the Mechanical Support Team. Some of the time, it is a last-minute modification to a well-prepared experiment; at others, it is a broken pair of spectacles or a broken luggage handle that needs repairing.

The day starts with the eight-o'clock meeting with the other teams. This is where and when the previous night's problems are discussed. Back to the workshop, and after a short discussion, the mechanics plan the day's activities. The stand-by mechanic takes care of all the emergency calls while the other mechanics are dedicated to continuing projects or maintenance. The dome mechanics continue to check daily the condition of the domes, compressors and hydraulic systems of all the telescopes. The cryogenic experts produce the cryogenic liquids vital to the continuing operation of modern detector systems.

At ten o'clock, there is a break: it's coffee time. The famous *CAD* (*C*afé *A* las *D*iez) is held in the design and engineering office. Issues of importance are discussed. If you happen to arrive you will probably find interesting conversation and a good provision of chocolates or cookies that many times are provided by our friends in Garching.

Problems of varying complexity and bewildering variety appear continuously, and most of the time they have to be solved as soon as possible.

During the whole year there are other jobs that require special attention. The aluminisation of telescope mirrors is one of great importance. This delicate job is handled by the MST until the mirror is left at the aluminisation plant, where the Optical Group takes over. After cleaning and aluminisation, the MST take care of its re-installation.

The different projects that are developed by the MST at La Silla start from an idea that is expressed as detailed design to the manufacturing of parts to a precision, when required, of no less than a few microns. The MST have conceived projects as the Schmidt guider and film holder, EFOSC2, the 1.52-m telescope mechanical upgrade, the NTT telescope installation, the CCD adapter flange for the CES, the mechanical improvements for different telescopes, etc. They have been carried to reality by a group of mechanics with a vast experience and a willingness to make things to the highest quality.

▲ ***VLT enclosures 1 and 2*** *photographed by H. Zodet in May 1996.*

▶ ***The primary mirror cell of the VLT (Unit 1)*** *is turned at the St-Chamond GIAT factory, prior to undergoing dimensional check and painting (16/07/96).*
The structure of the primary mirror cell has been assembled face down on a dedicated jig, by welding together a number of sub-assemblies previously generated by means of laser cutting and welding technology.
(Photographer: H.-H. Heyer)

The Early Universe with the VLT

HIGHLIGHTS OF THE ESO WORKSHOP, APRIL 1–4, 1996

A. RENZINI, ESO

Progress in science is not a steady process. Occasionally, when a fundamental breakthrough takes place, the frontier of our knowledge of Nature moves suddenly ahead more than it had in years before. Those who last April attended in Garching the workshop "The Early Universe with the VLT" were left with the feeling that one of these *quantum jumps* is indeed taking place right now in observational cosmology. The main breakthrough is probably represented by the success of a simple but robust photometric criterion for the identification of high-redshift galaxies, that has allowed to find star-forming galaxies all the way to $z = 3.5$, and that may well work also beyond (cf. Steidel *et al.*, 1995, *AJ*, 110, 2519; see also Macchetto and Giavalisco, 1995, *The Messenger*, 81, 14). M. Giavalisco showed a series of impressive Keck telescope spectra of these galaxies, selected in both the generic field and the *Hubble Deep Field* (HDF), and together with D. Macchetto argued for these objects being the precursors of present-day spheroidals caught in the act of their formation. Figure 1 (also shown by Giavalisco, from Madau *et al.*, 1996, preprint) gives an idea of the kind of high-level information on the evolution of the universe that we can now grasp from these data. The global star-formation rate (SFR) per unit comoving volume appears to climb a factor ~ 10 from $z = 0$ to $z \simeq 1$, a result that comes from the Canada-France Redshift Survey that was presented by F. Hammer. Beyond $z = 1$, one now has a set of lower limits established by HDF and Keck spectroscopic data. These limits are likely to move up somewhat as new data will soon become available, with the expectation that in a few years the whole diagram will be filled all the way to $z \simeq 5$ with determinations as accurate as those now available for $z \lesssim 1$. The product will be the accurate reconstruction of the whole global star-formation history of the universe. Theoretical work on the *chemical evolution of the universe* (hopefully a closed box indeed) that parallel these observations was presented at the meeting by M. Fall, while complementary constraints on the early SFR that can be obtained from far-infrared observations by FIRAS/COBE and ISO, were discussed by J.L. Puget, M. Rowan-Robinson, and A. Franceschini.

Searching for very high redshift galaxies, either by Lyα imaging or photometrically locating breaks in the spectral energy distribution, was further discussed by K. Meisenheimer, E. Thommes, and E. Giallongo, the latter reporting the discovery of the so far most distant star-forming galaxy at $z = 4.7$, about 2″ away from a quasar with the same redshift (see Fig. 2). 3D spectroscopic observations of this object were also presented by G. Adam, and the merits for high-redshift studies of a 3D, adaptive optics fed spectrograph on the VLT were further illustrated by G. Comte. Yet another way of finding high-redshift galaxies was illustrated by Y. Mellier, who advocated strong gravitational lensing by massive clusters offering the advantage of amplifying the light of distant galaxies, thus helping their detailed study.

While the very high redshift galaxies played the *primadonna* role at the meeting, very impressive was also the progress of systematic studies of the redshift and morphology of galaxies at more moderately high redshifts (R. Ellis, M. Colless, and W. Couch). The HDF images have now allowed to morphologically classify galaxies as faint as $I = 24.5$, and have shown once more that the well-known excess in faint galaxy counts is mainly due to blue, irregular, star-forming galaxies. So, the ratio of blue to red galaxies appears to increase with redshift, both in the field as well as in clusters (the latter being the Butchler-Oemler effect), and it remains to be quantitatively established what difference exists (if any) between field and clusters as far as the evolution with z of the B/R ratio is concerned.

Intriguingly, Figure 1 suggests that the global SFR may peak somewhere around $z = 2$, tantalisingly close to the well-known peak in the QSO redshift distribution that was reviewed by S. Cristiani. However, the distribution itself remains somewhat uncertain beyond $z = 2$, and various speakers (R. McMahon, R. Webster, A. Omont, and P. Shaver) reported on current efforts to put it on firmer grounds, with special emphasis on prospects to detect QSOs beyond the $z = 5$ *wall*. What relation is there between the peak in the QSO activity and the expected peak in the global SFR? Hence, what relation is there between the formation of galactic spheroids, and that of massive central black holes, the likely powerhouse of QSO emission? These questions did not receive answers at the meeting, but several speakers (H. Röttgering, A. Cimatti, and S. di Serego Alighieri) discussed the latest results – especially from HST – concerning high-redshift radio galaxies, and the perspectives to understand the connection between galaxy formation and nuclear activity. The relative contribution of QSO's and primeval galaxies in reionising the universe was then explored by A. Blanchard.

A complementary approach to gather insight into the formation of galactic spheroids (i.e., ellipticals and the bulge

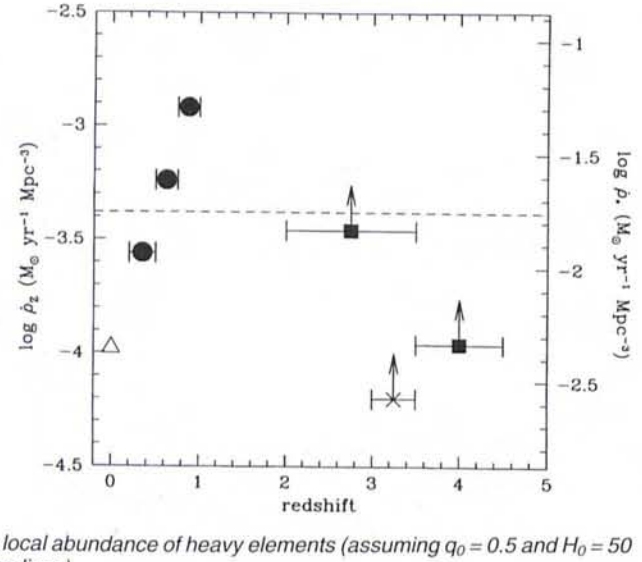

*Figure 1: The global star formation and metal production rates per unit comoving volume (right scale and left scale, respectively) as a function of redshift (from Madau et al. 1996, preprint). The open triangle gives the local value (from Gallego et al. 1995, ApJ, **455**, L1); filled circles are from the Canada-France Redshift Survey (Lilly et al., 1996, ApJ, **460**, L1); the cross is from Steidel et al. (1996, ApJ. in press); and the filled squares are for galaxies in the Hubble Deep Field. The horizontal line is the cosmic-time average rate as derived from the local abundance of heavy elements (assuming $q_0 = 0.5$ and $H_0 = 50$ (paper presented by M. Giavalisco).*

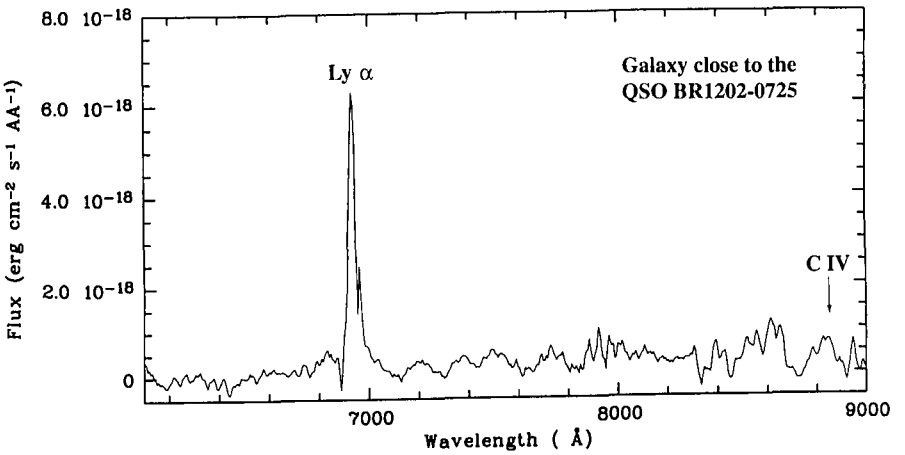

*Figure 2: A 3.5-hour integration on the galaxy ~ 2″ from the z = 4.7 QSO BR1202-0725 obtained with the EMMI spectrograph at the ESO 3.5-m NTT (courtesy of S. D'Odorico). The spectrum shows a strong emission line identified as Lyα at z = 4.702, and a continuum level in agreement with the integrated magnitude of this object (I = 24.1, Fontana et al., 1996, MNRAS **279**, L27). This level of the rest frame ultraviolet continuum indicates a star-formation rate of ~ 30 $M_\odot$ yr^{-1}. The C IV emission doublet is not detected, which sets an upper limit to its intensity of ~ 1/10 that of Lyα. The object is one of the-high redshift candidates from a deep, four-colour study of the galaxies in the field of the QSO (paper presented by E. Giallongo).*

of spirals) is to follow their evolution with redshift. R. Bender and M. Franx reported about the construction of the fundamental plane relation for cluster ellipticals up to $z \simeq 0.4$, thus setting a tight lower limit ($z \gtrsim 2$) for the formation epoch of the bulk of the present-day stellar content in these galaxies. Combining HST imaging (giving accurate effective radii and surface brightness distributions) with 8–10-m-telescope spectroscopy (giving velocity dispersions and metallicity indices) is the winning strategy in this field, and D. Koo reported recent Keck observations of high-z ellipticals as well as spirals and faint blue galaxies. The evolution of the fundamental plane and Tully-Fisher relations involve both dynamical and stellar population properties of galaxies. As such, they can constrain the formation epoch of the stars in these galaxies, but still allow a variety of galaxy-build-up scenarios. For example, in some CDM simulations of galaxy formation and evolution (reported by G. Kauffmann and M. Steinmetz) the bulk of stars may well form at very high z, but their assembly to build up the big galaxies of today does not complete the process before $z \lesssim 1$. Thus, even more fundamental than the fundamental plane itself may eventually be the empirical construction of the *distribution functions* of the velocity widths and velocity dispersions at various redshifts. Velocities – better than luminosities – indeed represent a rather direct measure of the depth of galaxy potential wells, and their distribution traces the assembly of dark matter halos on galaxy scales, the firmer result of CDM simulations.

Next to galaxies on the mass scale, galaxy clusters at high redshift also received wide coverage at the meeting, including X-ray searches (H. Böhringer) and their optical counterparts (G. Chincarini), group and cluster detection from QSO absorption line systems (P. Petitjean and M. Haehnelt) and from gravitational shear (P. Schneider and B. Fort). While systematic studies of moderate redshift clusters (unfortunately mostly limited to the northern hemisphere) are now well under way (R. Carlberg), successful detections of clusters around powerful AGNs were reported. These included a cluster at $z = 1.2$, that combined HST and Keck data show to contain already red (i.e. old) ellipticals (M. Dickinson), and the detection of clustering at a redshift as high as ~ 2.4 (P. Francis). Tracing the evolution of large-scale structure (LSS) at high redshift was then illustrated both by present and planned galaxy redshift surveys (V. De Lapparent and G. Vettolani), and by gravitational shear (P. Schneider and B. Fort).

While the emphasis of the meeting was obviously on high-redshift objects, D. Tytler in his comprehensive general introduction emphasized that a great deal about the early universe can be understood by looking at nearby objects. For example, dating the oldest stars and mapping the age, chemical and kinematic structure in our own Galaxy and in nearby galaxies, getting stellar abundances for residues of the Big Bang nucleosynthesis, etc. One crucial aspect of the local universe still worth investigating concerns *normalisations*. While getting rich samples of galaxies at high redshifts, one would like to compare them to fair samples at $z \simeq 0$, so as to gauge the change that has intervened in between. This includes e.g. the local luminosity function for morphologically typed galaxies (G. Vettolani reported on the ESO redshift survey results), supernovae of Type Ia, where observation of high-z counterparts can help determine q_0 (B. Leibundgut), and of course the local LSS with its walls, filaments, and voids that may or may not persist to high redshifts depending on the cosmological model.

Altogether, this wealth of data needs to be framed in a world model to make sense to us. As S. White pointed out, the current (standard) world model is based on a fairly limited set of basic assumptions, namely: (1) most matter is in some "dark" nonbaryonic form, (2) ordinary baryons are present in the amount predicted by Big Bang nucleosynthesis, (3) primordial density fluctuation are gaussian and were generated by quantum effects during inflation, (4) structures grow solely through the effect of gravity, and (5) galaxies form by dissipative collapse within massive halos made of dark matter. Within this frame the observations should allow us to unambiguously determine a consistent set of the main model parameters: H_0 Ω_0) Ω_b, Ω_{CDM}, Λ, and n, the spectral index of the primordial fluctuations. As S. White emphasised, should this effort fail, we will have to give up some of the five basic assumptions.

The role that the VLT will be able to play in observational cosmology will ultimately depend (besides the commitment of the ESO community) on its complement of focal instruments and on their efficiency. For this reason VLT instruments were on stage both at the beginning and at the closure of the meeting, with the PI's of the first-generation instruments and of those under consideration illustrating their scientific drivers and their technical performances. Thus, I. Appenzeller, S. D'Odorico, P. Felenbok, O. LeFèvre, R. Lenzen, A. Moorwood, and K. Taylor presented respectively FORS, UVES, FUEGOS, VIRMOS, CONICA, ISAAC, AUSTRALIS, and SINFONI, all acronyms that will become familiar to us like today are SUSI and EMMI and TIMMI, etc. Some limitations of the first-generation instruments emerged clearly at the meeting, especially concerning the multiobject and area spectroscopy, and G. Monnet in its closure talk illustrated how ESO is going to cope with this in selecting the next-generation instruments.

In the end, what lessons did we learn from this most exciting meeting, that may be relevant for planning the future science at the VLT? The first lesson was that VLT-grade projects need extensive preparation, both in terms of finding and selecting the appropriate targets, and in terms of dedicated scientific software to handle enormous data cubes. The second lesson comes from the tremendous success of a combined HST and Keck approach to so many astrophysical problems, with HST providing high-resolution imaging on fairly wide fields and/or UV spectroscopy, and the 10-m telescope providing spectra of sufficient resolution of the same objects. By the year 2000 about a dozen 8-m-class telescopes will be in operation world-wide,

and European astronomers will held about a 50% share of the whole stack. Maintaining adequate access to HST, and especially to the Next-Generation Space Telescope now under study, is vital for European astronomy to get full profit from its investments on ground-based as well as space-borne telescopes (e.g. VLT, GEMINI, LBT, COBRAS/SAMBA, ISO, XMM, etc.). Only if such access will be secured (and expanded) will European astronomy remain fully competitive. The third lesson also comes from the HST experience. With the HDF, for the first time a huge amount of high-quality, frontier-science data are made public just days after having been obtained. This example is likely to be contagious, and a growing fraction of astronomical data is likely to be distributed in a similar way in the future. We should prepare and be prepared for that, and anticipate the sociological changes that such a new operation mode will bring along. The fourth lesson, perhaps a hardly new one, was that a large variety of observational capabilities is required to make progress in observational cosmology, and it is somewhat reassuring to appreciate once more that the current VLT instrumentation plan offers in fact the needed diversification. However, and this was the fifth lesson, the explosion we are now witnessing thanks primarily to HST and Keck can only accelerate further as more 8–10-m-class telescopes come into line. Hence, timing becomes essential. With progress being so fast, maintaining the schedule and deploying focal instruments in the shortest possible time is a top priority for the VLT project.

Alvio Renzini
e-mail: arenzini@eso.org

Aerial view of Paranal taken by H. Zodet in May 1996.

First Ground-Based Mapping of the Asteroid Vesta

C. DUMAS (Observatoire de Paris-Meudon (DESPA) and University of Hawaii (IfA))
O.R. HAINAUT (University of Hawaii (IfA))

Asteroid 4 Vesta has been imaged in the Near-Infrared using the ESO 3.6-m telescope equipped with the Come-On-Plus adaptive optics system. The result of these observations is the first mineralogic map of a minor planet obtained from ground-based observations. We will discuss the data acquisition and reduction techniques that we used and developed, and present our ground-based observational prospects.

1. Introduction: Vesta

With a mean diameter of 520 km[20], Vesta is the third largest asteroid. Its orbit is located in the Main Belt, at 2.4 AU from the Sun. Its surface albedo is very high (0.38) compared to other asteroids whose albedo does usually not exceed 0.15. Vesta is large enough to have experienced a differentiation phase during its accretion: the heaviest elements like Iron separated to sink towards the core of the primordial body. While it cooled down, basaltic lava flows erupted on Vesta's surface through the cracks in the forming crust. At that time, highly energetic collisions between asteroids were very frequent, redistributing the material all over the surface. Previous observations[2,10,18,19] showed that the surface of most of the minor planets appears uniform, with little or no albedo variation. Surprisingly, spectrophotometric observations of Vesta[15] revealed a spectrum dominated by some strong absorption bands whose intensity varies with the rotation of the asteroid[9], implying that the surface of Vesta has some dark and bright areas. The dark regions are interpreted as some old material darkened by the erosion processes (solar wind and photo-dissociation) over its lifetime, while the brighter spots are considered to be some fresher material excavated by cratering impacts with smaller bodies. During such impacts, some fragments reached a sufficient velocity to escape the gravitational field of Vesta and be released in the inner solar system. It is generally accepted that these fragments are at the origin of the basaltic achondrite (HED) meteorites[15].

With the availability of the Hubble Space Telescope and its corrected optics, and with the development of Adaptive Optics on telescopes of the 4-m class, we are now able to obtain direct images resolving the disk of the biggest asteroids. Speckle Interferometry provides a similar resolving power[5], but requires extremely heavy and complex image reconstruction techniques. The original goal of our AO observations was to obtain resolved images of the whole visible surface of Vesta at 12 wavelengths sampling the 2.0 μm pyroxene band. Constraining this dataset with the spectra obtained from laboratory samples of HED meteorites, we would have obtained some crucial indications on the distribution of the pyroxene band strength, on the pyroxene chemical composition and grain size distribution[11]. The location of the impacting zones on Vesta could then have been determined with a very high accuracy, leading to a better understanding of the chemical and physical processes undergone by Vesta during its lifetime.

2. Observations

During its December 1994 opposition, we observed Vesta in the Near-Infrared with Come-On-Plus (CO+). The images were obtained on the Nicmos SHARP II camera through a Continuously Variable Filter ($\lambda/\Delta\lambda \simeq 60$). The pixel size was 0.05″, ensuring us a sufficient sampling of the image in order to satisfy the Shanon's principle. We did not select a smaller pixel size because the broad "wings" of the objects would not have fit in the corresponding field. At the time of the observations, the inclination of Vesta's rotational axis with respect to the line of sight was such that we could see almost 80% of its surface during an entire rotation period. Its angular diameter was 0.44″, almost 9 pixels across the chip. Because of some scheduling conflicts we could not observe Vesta during its transit, but only after, when it was at higher airmasses, pushing CO+ beyond its nominal limit of 60° of zenithal distance. We could only secure 3^h50^{min} of data, instead of the 10^h originally attributed to achieve our goals. Moreover, the

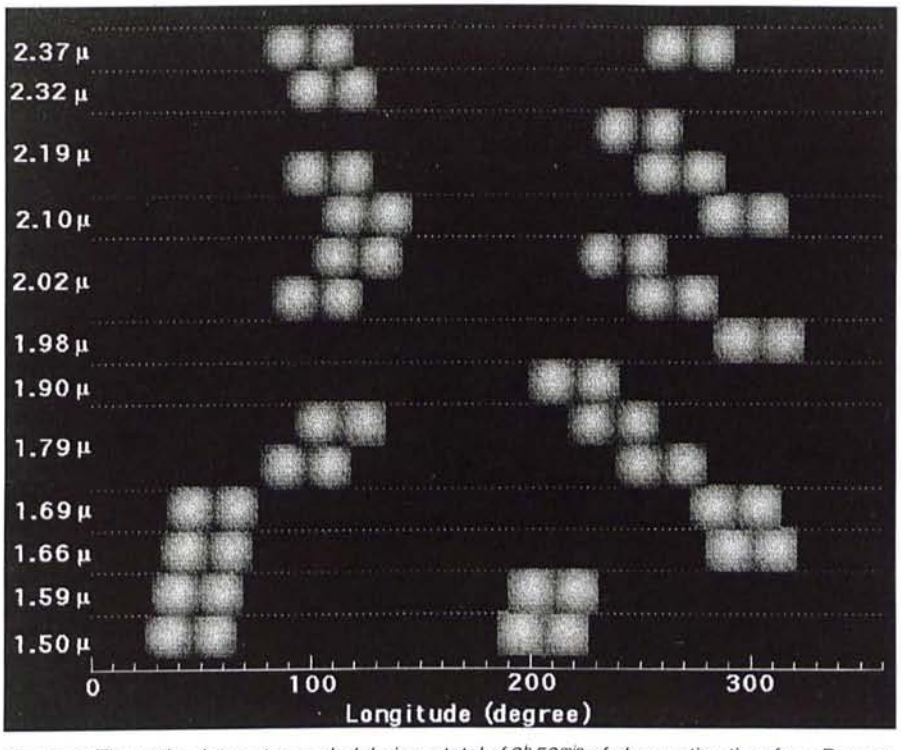

Figure 1: The entire data set recorded during a total of 3^h50^{min} of observation time from December 9–13, 1994. The x-abscissa is the central longitude of Vesta and the y-abscissa is the wavelength of the CVF at which Vesta was imaged. For each exposure, we obtain two images. The images shown are the raw images, i.e. no restoration has yet been applied to recover the optimal resolution of the instrument. We have recorded images at different wavelengths, from 1.5 to 2.37 μm, in order to scan the 2.0 μm pyroxene band. We do not have a complete longitudinal coverage of Vesta. Our images are roughly centred on the Vesta longitude 100° and 250°. Some features at the surface are already visible in the raw images. The rotation period of Vesta is 5.3^h and its angular diameter was 0.44″ for the 1994 opposition.

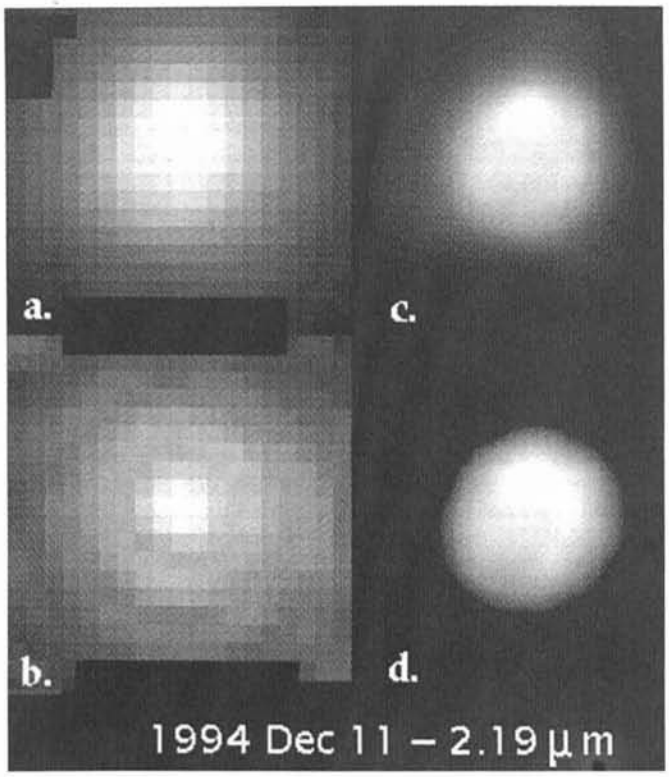

Figure 2:
– a: raw image
– b: PSF (logarithm grey-scale)
– c: Vesta image deconvolved by Lucy-Richardson (50 iterations)
– d: result of the wavelet transformation applied to the raw image. There is an excellent agreement between the result of Lucy-Richardson deconvolution (which use a PSF) and the wavelet transformation (simple spatial filtering).

weather was far from ideal (poor seeing and/or non photometric) during 3 of the 4 nights when we observed, and finally the camera displayed a systematic pattern noise. As a consequence, the dataset (illustrated in Fig. 1) does not cover the whole visible surface, and the regions observed do not have an equal coverage in wavelength. In order to establish a map of Vesta we had to combine some images recorded at different wavelengths. This has the same disturbing effect as looking at a landscape through a stained glass window. Each observation of Vesta consisted in a series of 30–50 short exposures (5 sec each) obtained in two different quadrants of the SHARP II camera, ensuring that the minor planet and the background are recorded simultaneously. We also obtained images of the solar-type star SAO 78355, which was chosen for its angular proximity to Vesta and its magnitude close to that of our object, in order to be used as reference Point-Spread-Function for further deconvolution, as well as a rough photometric calibrator.

3. Data Reduction

A bad pixel map was produced for each night, and the corresponding pixels were interpolated over in every individual image. For each object (Vesta and star) the data are distributed in two "cubes" of images: two object-cubes and two sky-cubes, one for each quadrant used during the exposure. For each quadrant, a unique sky frame is obtained by taking the median of the sky-cube. This sky frame is then subtracted from each image of the corresponding object-cube. Images of the dome were obtained through the same CVF. They were normalised and combined to generate a template flat-field, which is applied to each image of the data cube. However, we do not have suitable frames at each of our wavelength. We then found that the short-scale structures do not change much with the wavelength in the 1.5–2.5 µm range, allowing us to use the flat-fields obtained at a nearby wavelength. Each object image is then recentred on the central pixel of the frame. This is performed by zeroing the average phase of the image in the Fourier space. This technique proved to be much more accurate than the methods based on the centre-of-mass determination. Once the centring is done, we average the object cube in order to get a final and unique image for each quadrant. For every wavelength we end up with a set of two images of Vesta and two images of the star. In what follows, we refer to these as "raw images", in the sense that only the standard processing and no restoration technique has been applied. The images containing a pattern of systematic noise (induced by the reading of the camera) at a non-negligible level, have been filtered in the Fourier space[21].

None of the four nights was photometric, therefore no spectrophotometric calibration star was imaged. The images have been calibrated relatively to each other by adjusting the total integrated flux of each raw image to the measured flux of a spectrum of Vesta at the same wavelength.

To recover the optimal image resolution, we applied different restoration techniques:

– *Wiener filtering*, which is a simple division of the object by the PSF in the Fourier space, taking in account a certain level of noise present in the images.

– *Richardson-Lucy deconvolution*, using a new-generation algorithm by Hook and Lucy[1] based on an iterative maximum likelihood optimisation. We performed some tests on synthetic and real images of Vesta and of the PSF. They show that the best restoration is obtained after 50 iterations. A smaller number of iterations does not restore all the details of the image, while continuing over 50 iterations tends to create a "hole" in the centre of the minor planet disk and enhance its limb.

– *Wavelets spatial filtering*: the image is transformed in the wavelet space[16], from which some spatial frequencies are extracted to build the restored images. The advantage of this technique is that it does not require a PSF. It should how-

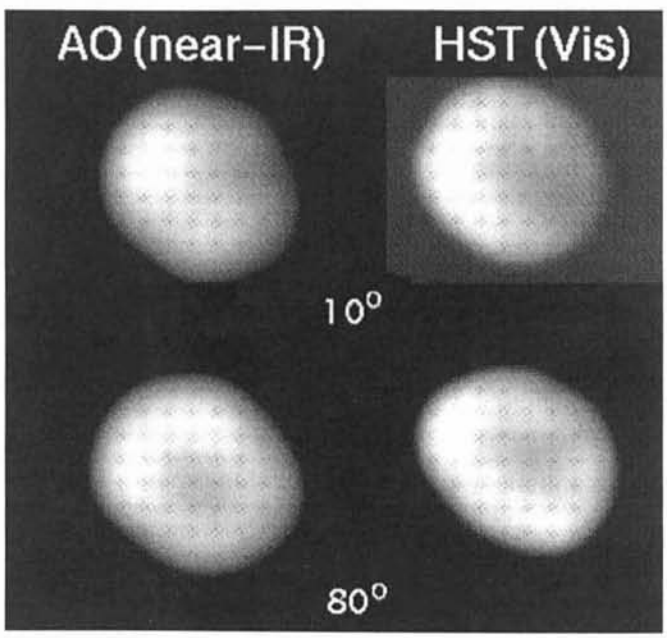

Figure 3: Adaptive Optics observations of Vesta from ESO (near-infrared) and HST (visible) – (Zellner B., Storr A., priv. comm.). These two images were recorded at nearly the same central longitude. The overall shape of the asteroid is the same as well as the main albedo features. On the AO images, Vesta is about 9 pixels across the chip. The AO images have been deconvolved using 50 iterations of the Lucy-Richardson algorithm.

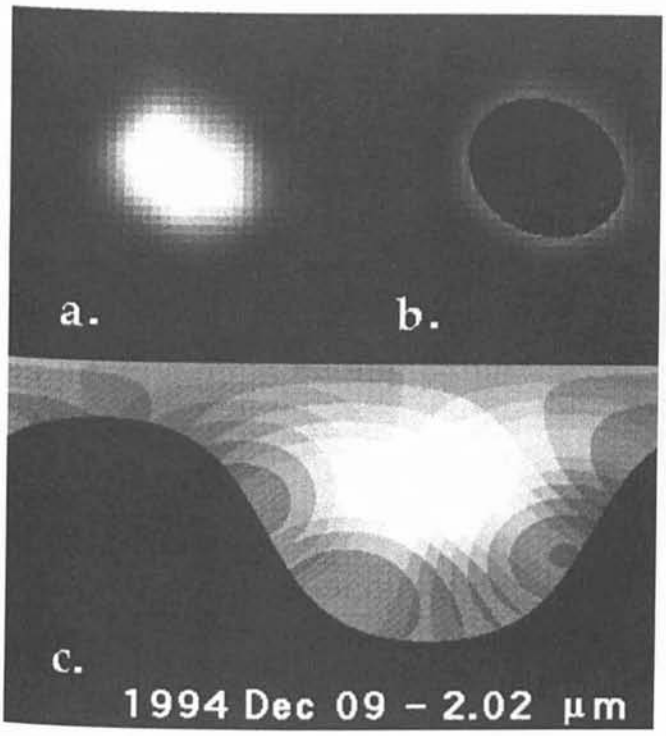

Figure 4: The map extraction is done by assuming a spheroidal shape for Vesta, with a ratio of 1.2 between the two diameters.
– a: image of Vesta after 50 iterations of Lucy-Richardson
– b: residual after subtraction of the spheroidal model
– c: map extracted. Similar maps were produced for all the images of our data set. During the 1994 opposition only 80% of Vesta's surface was visible. The unseen regions are black. Note the limb darkening present in the extracted map.

ever be noted that the enhancement in resolution achieved by this technique is not as good as that of the Lucy deconvolution.

The data have been processed using the Interactive Data Language (IDL), except the wavelet restoration which was performed with the ESO-MIDAS "wavelets" context. The results of these three restoration techniques show an excellent agreement in most cases (Fig. 2) – the disagreeing ones can all be explained either by a very bad raw image of Vesta, or a bad PSF. We are therefore confident that the features seen on Vesta are not artifacts introduced during the restoration process but rather some real albedo variations over the surface, due to some change in the nature of the minerals that form the asteroid regolith. It is interesting to note that HST observed Vesta nearly simultaneously in the visible wavelengths (WFPC Zellner et al., FOC Albrecht et al.). The WFPC team kindly made their raw and restored images available to our group, allowing us to compare our results. Figure 3 shows the comparison of HST (visible) and ESO (near-infrared) Vesta images recorded at nearly the same central longitude of the asteroid. Although some differences have to be expected because of the different wavelength ranges, the main albedo features are identical as well as the overall shape of the asteroid. As the instrumental set-up was completely different and the data processing totally independent, we take this as an additional confirmation of the reality of these features.

We extracted a map from each Vesta image by modelling the minor planet with an oblate spheroid whose eccentricity was adjusted to fit the images (Fig. 4). We used the orientation of the rotation axis set in the Magnusson's synthesis of the published pole solutions[14]. Our data are in perfect agreement with that orientation but cannot refine it. The local divergence of Vesta with a pure ellipsoid will produce some errors in the projection for the region close to the limb. As described later, this portion of the images is not taken into account in the final map and therefore is of little consequence. It should be noted that one single pixel on a Vesta image may be projected into an area that strongly varies depending on the angle θ between the normal to the surface of the asteroid and the line of sight. More specifically, a pixel close to the limb will correspond to a huge region of the minor planet that is seen in very poor conditions. This effect is taken into account by affecting a "weight" to each data-point: this weight is maximum for the sub-Earth pixel, and is equal to zero for the pixels where $\theta = 90°$. Each individual map is corrected for the limb darkening effect, using a simple $\cos(\theta)^{\kappa}$ law[4], where the exponent κ is adjusted to the data. This simple correction tends to over-correct the extreme edges of the limb, and will have to be refined. The final maps are obtained by taking the weighted median of the individual maps.

4. Results

Since our longitudinal coverage is not complete, we cannot confirm the triaxial shape measured from speckle interferometry[6] and HST[20] . But the two diameters measured from our images are in very good agreement with the HST measurements (560 km × 450 km). As mentioned before, we could not obtain a complete longitude coverage of Vesta at each wavelength. Still, a rough estimate of the pyroxene distribution can be assessed by combining all the data into two maps – the first one summing all the individual maps obtained at wavelengths outside the pyroxene band – the second, all those obtained inside the band. These two maps are reproduced in Figure 5. The black area corresponds to some "Terra Incognita" that was not visible at the time of the observations. It must be noted that, because we could not obtain a good coverage of Vesta, the reliability of the map varies much with the longitude. The regions of the map around 90° and 270° have been imaged several times and can be relied on, while the regions around 0° and even more around 180° are built from just a few pixels close to the limb. In a similar way, the maps of the regions below –15° and over 80° of latitude are not reliable. Among the features visible in the reliable parts of the maps, there is a strong albedo variation from one hemisphere to the other, variation even enhanced on the map corresponding to wavelengths in the bottom of the pyroxene band. This confirms previous photometric observations of the existence of a dark and a bright hemisphere on Vesta[3]. The difference of contrast between these two hemispheres from one map to the other indicates an enhancement of the pyroxene content of the left hemisphere (longitude below 180°) . Smaller details can be seen: the left hemisphere shows for example two bright spots separated by a dark region. Also the bright area visible on the right hemisphere is elongated and might correspond to a large impact zone on Vesta. A more detailed analysis of these maps is beyond the scope of this paper, and will be given in Dumas and Hainaut (1996).

The most encouraging result remains that even with poor seeing and weather, at high airmass and during a non-optimal opposition, we could obtain such a detailed map. The next step is of course to complete the pyroxene map of Vesta, and to extend it to the feldspar and olivine bands. The May 1996 opposition is one of the most favourable in terms of angular diameter (0.65″, 1.4 × its diameter in 1994) and aspect angle (more than 99% of the surface will be visible). We also wish to extend this programme to Ceres and Pallas in order to map the water of hydration that their surface is suspected to have retained since the asteroid belt formed[13]. Also in the case of Ceres some observational results[12] and calculations[8] sustain the fact that this asteroid might have some polar caps whose thickness varies with the seasonal variations induced by the inclination of its rotation axis[17]. Ceres and Pallas will be at opposition at about the same time as Vesta, making of May 1996 a fantastic period for the study of asteroid mineralogy. Unfortunately, no time was allo-

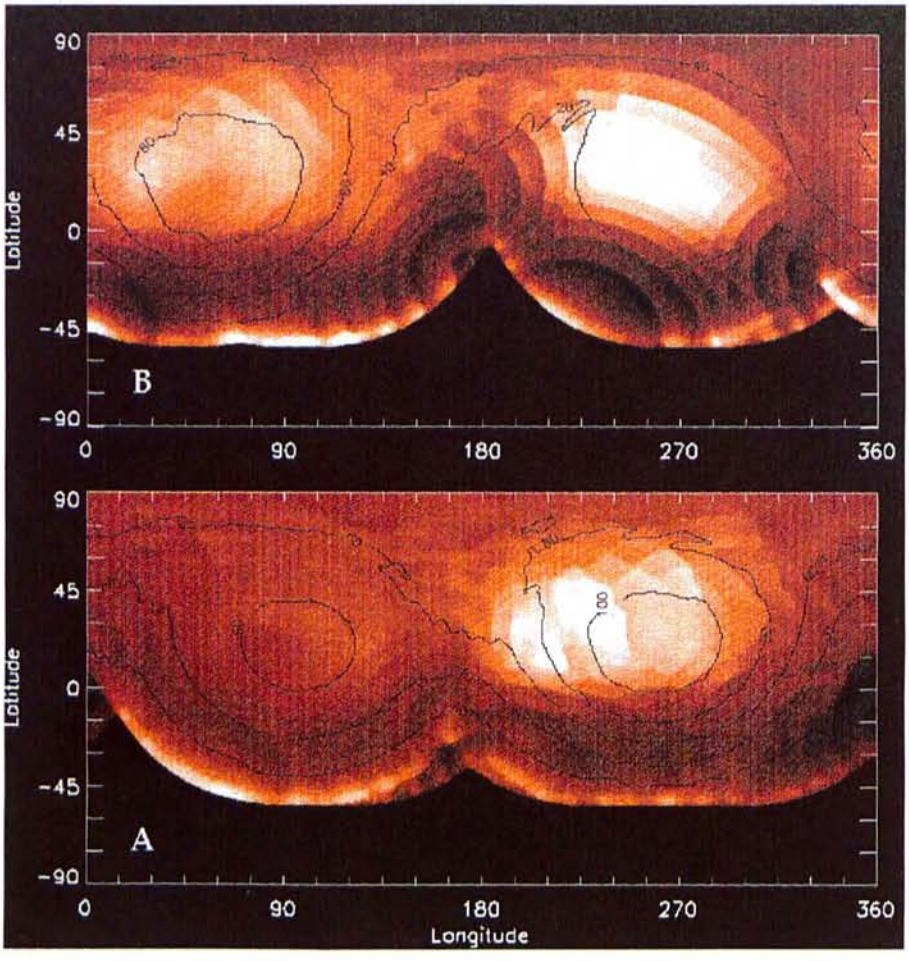

Figure 5: Map of the pyroxene distribution on Vesta. This is the first mineralogic map of Vesta based on direct observations. Map A: extracted from the images whose wavelength corresponds to the bottom of the pyroxene band. Map B: extracted from the images whose wavelength is outside the pyroxene band. The contour level is a measurement of the reliability of the data. The correction of the limb darkening introduces an artificial enhancement in the intensity of the two maps close to the limb. Map A shows clearly the existence of a pyroxene dominated hemisphere on Vesta (for longitude below 180°). This hemisphere becomes bright in the top map corresponding to the spectral range outside the pyroxene band. Some smaller structures are visible in each hemisphere. The range below –15° and above +80° of latitude, should be considered with caution since these data result from pixels located close to the limb of Vesta. Also, our longitudinal coverage being incomplete, the points on these maps close to longitude 0° and 180° have been obtained only from a small number of pixels, also localised close to the limb. Considering the bottom map, the bright hemisphere might correspond to a region where the largest number of impacts on Vesta occurred, the dark hemisphere to some older material, unaltered since the Vesta formation.

cated for this programme at ESO, and we will not be able to test the capabilities of ADONIS (Come-On-Plus' upgrade) under such good conditions before a long time (e.g. July 2000 will be almost as good for Vesta). ADONIS is the best instrument available to carry out this programme, thanks to the large spectral coverage offered by its cameras (COMIC, sensitive from 1.0 to 5.0 μm and an upgraded version of SHARP II), and the possibility to use a CVF. This programme was awarded one night on the Canada-France-Hawaii Telescope. The infrared camera used with this instrument is not sensitive above 2.5 μm and it is not equipped with a CVF. Despite a too short allocated time to complete our scientific objectives, these observations will refine the current map of Vesta and perform some exploratory observations of the water distribution over Ceres and Pallas.

Acknowledgements

We are very grateful to R. Albrecht, H. Schobert and the COME-ON+ team for their help at the telescope during the observations, B. Zellner for keeping us informed of the results of his team and giving us access to the HST images of Vesta, A. Barucci and D. Jewitt for kindly reviewing this article and for all the improvements they suggested, C. Roddier for her precious advise regarding the image analysis techniques we used, T. Encrenaz and T. Owen for their support during all these months spent working on this project and for their suggestions and encouragements concerning the future of this programme.

References

[1] Adorf, H. M. 1990, *ST-ECF Newsletter* **14**, 8–12.
[2] Albrecht, R. 1992, "HST Observations of 1 Ceres", *BAAS* **24** (3), 970.
[3] Bobrovnikoff, N. T. 1929, "The Spectra of Minor Planets", *Lick Obs. Bull.* **14**, 18–27.
[4] Buil, C. 1991, "CCD Astronomy", 209, Willmann-Bell, Richmond.
[5] Drummond, J.D., E.K. Hege 1989, "Speckle Interferometry of Asteroids", in *Asteroids II* (R. P. Binzel, T. Gehrels, M. S. Matthews Eds), 171–191, Univ. of Arizona Press, Tucson.
[6] Drummond, J., A. Eckart, E.K. Hege 1988, "Speckle Interferometry of Asteroids – IV. Reconstructed Images of 4 Vesta", *Icarus* **73**, 1–14.
[7] Dumas, C., O.R. Hainaut 1996, "Ground-Based Mapping of the Asteroid 4 Vesta" (in preparation to be submitted to *Icarus*).
[8] Fanale, F.P., J.R. Salvail 1989, "The Water Regime of Asteroid 1 Ceres", *Icarus* **82**, 87–110.
[9] Gaffey, M. J., W. Hall 1995, "Surface Lithogic Heterogeneity of Asteroid 4 Vesta", submitted to *Icarus*.
[10] Hainaut, O. 1994, thesis dissertation, Université de Liège and ESO, 154–161.
[11] Hiroi, T., R.P. Binzel, J.M. Sunshine C. M. Pieters, H. Takeda 1995, "Grain Sizes and Mineral Compositions of Surface regoliths of Vesta-Like Asteroids", *Icarus* **115**, 374–386.
[12] Lebofsky, L.A., M.A. Feierberg, A.T. Tokunaga, H.P. Larson, J.R. Johnson 1981, "The 1.7 μm – 4.2 μm Spectrum of Asteroid 1 Ceres: Evidence for Structural Water in Clay Minerals", *Icarus* **48**, 453–459.
[13] Lebofsky, L.A. 1980, "Infrared Reflectance Spectra of Asteroids: a Search for Water of Hydration", *Astron.J.* **85**, 573–585.
[14] Magnusson, P. 1989, "Pole Determinations of Asteroids", in *Asteroids II* (R.P. Binzel, T. Gehrels, M.S. Matthews Eds), 1180–1190, Univ. of Arizona Press, Tucson.
[15] McCord, T.B., J.B. Adams, T.V. Thomson 1970, "Asteroid Vesta: Spectral Reflectivity and Compositional Implications", *Science* **168**, 1445–1447.
[16] Meyer, Y. 1989, "Wavelets", Combes J. M. et al. Eds, 21, Springer Verlag, Berlin.
[17] Millis, R.L., L.H. Wasserman, O.G. Franz, R.A. Nye et al. 1987, "The Size, Shape, Density, and Albedo of Ceres from its Occultation of BD+8.471°", *Icarus* **72**, 507–518.
[18] St Pé, O., M. Combes, F. Ribaut, Tomasko M., Fulchignoni M. 1993, "Demonstration of Adaptive Optics for Resolved Imagery of Solar System Objects: Preliminary Results on Pallas and Titan", *Icarus* **105**, 263–270.
[19] St Pé, O., M. Combes, F. Ribaut 1993, "Ceres Surface Properties by High-Resolution Imaging from Earth", *Icarus* **105**, 271–281.
[20] Thomas, P.C., R.P. Binzel, M.J. Gaffey, A. Storrs, E.N. Wells, B. Zellner, 1995, "Vesta: HST Observations of Shape, Spin Pole and Surface Features", Abstract DPS Meeting.
[21] Wampler, E.J. 1992, "FFT Removal of Pattern Noise in CCD Images", *The Messenger* **70**, 82.

C. Dumas
e-mail: dumas@galileo.IFA.Hawaii.Edu

A Massive Galaxy Cluster at the Core of the Great Attractor

R.C. KRAAN-KORTEWEG [1], P.A. WOUDT [2], V. CAYATTE [1], A.P. FAIRALL[2], C. BALKOWSKI [1], and P.A. HENNING [3]

[1]Observatoire de Paris, DAEC, Unité associée au CNRS, D0173, et à l'Université Paris 7, Meudon, France
[2]Department of Astronomy, University of Cape Town, Rondebosch, South Africa
[3]Department of Physics and Astronomy, University of New Mexico, Albuquerque, USA

A deep survey for partially-obscured galaxies behind the southern Milky Way using the IIIaJ film copies of the ESO/SERC sky survey reveals the cluster A3627 at Galactic co-ordinates l = 325°, b = –7° to be the most prominent cluster in the southern hemisphere, were its galaxies not overlaid by the dust and stars of the Milky Way. Subsequent follow-up observations find this strongly obscured galaxy cluster to be the nearest, rich, massive cluster in the Universe, comparable to the well-known Coma cluster identified already by Wolf in 1906. Moreover, this massive cluster lies – within its errors – at the centre of the Great Attractor and most likely constitutes the previously unidentified bottom of this potential well (cf. Kraan-Korteweg et al., 1996 for further details).

Systematic deviations of galaxies from the uniform expansion field indicate the existence of a "Great Attractor" (GA) – a large mass concentration of ~ 5×10^{16} $M_\odot$, at a redshift v ~ 4500 km/s, close to or behind the southern Milky Way (Lynden-Bell et al., 1988). The nature and extent of the GA has been the quest of many optical and IRAS galaxy surveys, as well as X-ray searches. While there is a considerable excess of optical-IRAS galaxies in this region, the absence of a dominant rich cluster at its centre remained peculiar.

However, our Milky Way cuts across the central part of the large-scale overdensity of the GA (cf. Fig. 3b and 6b in Kolatt et al., 1995). Even if the core of the GA were in the form of luminous matter, it would be overlaid by the dust and the numerous foreground stars of our Milky Way – our Galaxy blocks the view of about 25% of the extragalactic sky.

For some years, two of us (RCKK and PAW) have led a dedicated effort to unveil the distribution of galaxies behind the southern Milky Way making use of the IIIaJ ESO/SERC survey. The films are inspected by eye with a 50 times magnification. All galaxies larger than D = 0.2 arcmin are recorded, i.e. a factor five smaller compared to the ESO/Uppsala Catalogue of Galaxies of the southern hemisphere. Although heavily crowded with the images of the stars of our Galaxy, careful scrutiny has revealed over 10,000 previously unknown galaxies – leaving, however, the innermost strip of the Milky Way completely opaque.

The cluster of galaxies Abell 3627 is close to that innermost strip. It had been catalogued in 1989 in the extended catalogue of rich clusters, because of the foreground obscuration only about 50 of the larger galaxies were noted. The true significance of the cluster became unveiled with the identification of over 600 additional cluster members, many of which are just below the Lauberts diameter limit of 1 arcmin. Correcting the observed properties of the galaxies for the foreground extinction would make this cluster the most prominent overdensity in the southern skies.

To arrive at the distribution of the uncovered galaxies in redshift space, observations have been made at the 3.6-m telescope of ESO using the multifiber system MEFOS built at the Paris-Meudon Observatory (cf. Felenbok et al., 1996), individual spectroscopy at the 1.9-m telescope of the SAAO (South African Astronomical Observatory), and HI observations of low surface brightness

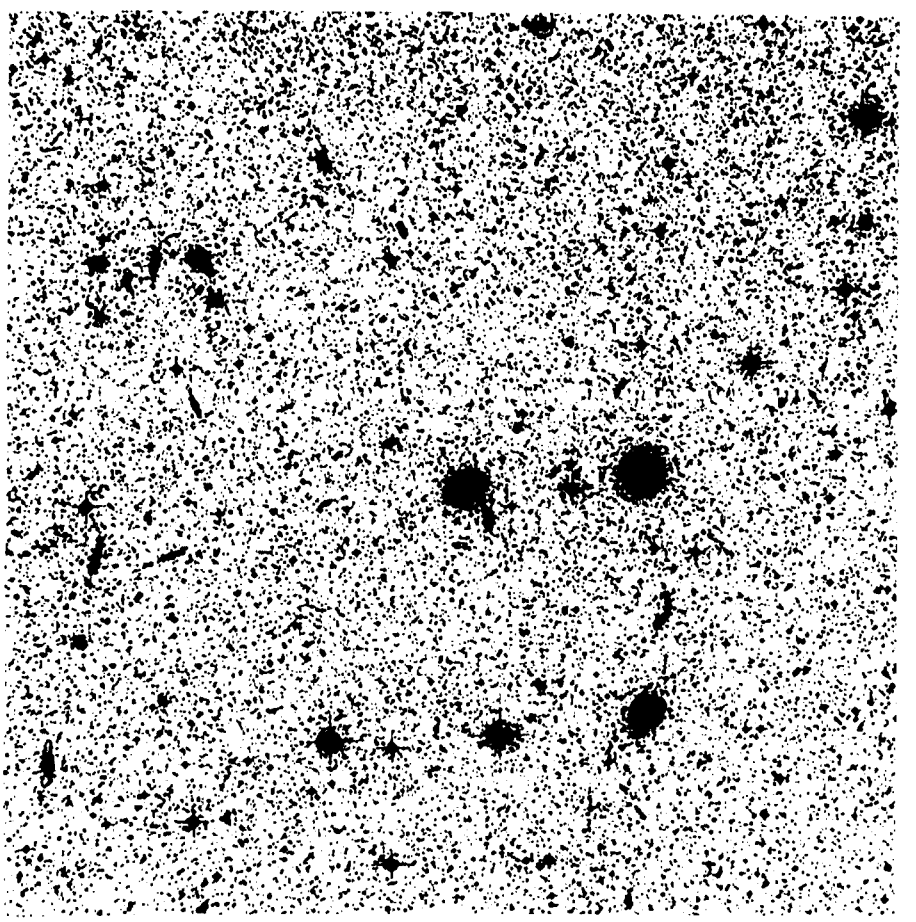

A photograph of the innermost part of the cluster ACO 3627 (25 × 25 arcmin), i.e. approximately the region within the core radius $R_c \leq 10.4$ arcmin, as seen on the ESO/SERC IIIaJ field 137. The central bright elliptical galaxy (a cD galaxy with blue magnitude $B_J = 14.4$) is the well-known radio source PKS 1610-60, one of the strongest radio sources in the southern hemisphere. Another cD galaxy is located to the left of the radio source ($B_J = 14.0$). Careful inspection will reveal 59 cluster members present in this photograph, a large fraction of those are early-type galaxies. Note furthermore the huge number of galactic foreground stars, which will give some inkling about the inherent difficulties in mapping the galaxy distribution across the Milky Way.

spiral galaxies with the 64-m Parkes Radio Telescope.

Within the Abell radius of the cluster A3627, 109 velocities have so far been reduced leading to a mean velocity of $< v_{obs} > = 4882$ km/s and a dispersion of $\sigma = 903$ km/s. This puts the cluster well within the predicted velocity range of the GA. The large dispersion of A3627 suggests it to be quite massive. Applying the virial theorem yields a mass of $\sim 5 \times 10^{15}$ $M_{\odot}$, i.e. a cluster on par with the rich, well-known Coma cluster – yet considerably closer. In fact, simulations show, that if Coma were at the position of A3627 in velocity space and subjected to the same foreground obscuration, the two clusters would be indistinguishable. A3627 even has – like Coma – 2 dominant cD galaxies at its core.

The most intriguing aspect of the recognition of the new cluster is its position at the approximate centre of the GA overdensity. Although very massive as a cluster, its mass contributes only about 10% of the total mass predicted for the Great Attractor. Hence, it is not "the" Great Attractor as such, but it is the prime candidate for being the hitherto unidentified centre of this large-scale overdensity. This is supported by the recent analysis of the ROSAT PSPC data of A3627 by Böhringer et al. (1996) which finds this cluster to be the 6th brightest X-ray cluster in the sky for the ROSAT spectral band and confirms its virial mass.

The results from our programme within the whole search area in combination with the Southern Redshift Catalogue suggest furthermore that A3627 is the dominant component of an apparent "great wall" structure – similar to the Coma cluster in the (northern) Great Wall – including the nearby Pavo, Indus clusters below the Galactic plane and the shallow overdensity in Vela above the Galactic plane at 6000 km/s. This whole large-scale structure embodies what has been dubbed in 1987 the then unseen Great Attractor.

References

Böhringer, H., Neumann, D.M., Schindler, S., & Kraan-Korteweg, R.C., 1996, *ApJ*, in press.

Felenbok, P, Guérin, J., Fernandez, A., Cayatte, V., Balkowski, C., & Kraan-Korteweg, R.C., 1996, *A&A*, submitted.

Kolatt, T., Dekel, A., & Lahav, O., 1995, *MNRAS* **275**,797.

Kraan-Korteweg, R.C., Woudt, P.A., Cayatte, V., Fairall, A.P., Balkowski, C., & Henning, P.A., 1996, *Nature*, **379**,519.

Lynden-Bell, D., Faber, S.M., Burstein, D., Davies, R.L., Dressler, A., Terlevich, R.J. & Wegner, G.,1988, *ApJ* **326**,19.

10- and 17-μm Test Images of the Galactic Centre: Massive Protostars Near SgrA*?

H. ZINNECKER, Astrophysikalisches Institut Potsdam
T. STANKE, Astronomisches Institut, Universität Würzburg; H.U. KÄUFL, ESO-Garching

Abstract

We have obtained 10 and 17 micron (N and Q band) images of the central square-parsec of the Galaxy. The images were taken with ESO's mid-infrared 64 × 64 pixel array camera TIMMI (Käufl et al., 1992, 1994) at the 3.6-m telescope on La Silla. The reduced images are displayed in Figure 1a,b: in total, 4 images are shown, two at each wavelength (i.e. a linear and a logarithmic stretch) in order to emphasise the full dynamic range. The images represent 1.5 and 7 minutes net on chip integration time at each wavelength, respectively. The images indicate that the morphological structure of the innermost parsec of the Galactic Centre is rather similar at both wavelengths, but differs significantly at certain locations, in particular at the position of IRS3. This compact source projected about 2 arcsec west and 4 arcsec north of SgrA* is found to have an extinction corrected spectral energy distribution νF_{ν} peaked near 10 microns and may be a massive protostar ($L_{bol} > 10^4 L_{\odot}$) or a cluster of protostars near the Galactic Centre. This might be possible, as there is indeed some dense gas in the innermost parsec from which stars can form (Jackson et al., 1993). In none of our images, mid-infrared emission from SgrA* is detected. Likewise, the strongest 2-micron source (IRS7) could not be detected, neither at 10 nor at 17 microns, to a 3-sigma limiting flux of about 0.3 and 4 Jy per arcsec^{-2}, respectively.

Technical Details

The N band images ($\lambda = 10.1$ micron, $\delta_{\lambda} = 4.0$ micron) were taken with a pixel scale of 0.66 arcsec/pixel in 1.2 arcsec seeing. Due to the high thermal background (sky and telescope) the on-chip integration time of the individual frames had to be very short (7 ms). Otherwise standard infrared techniques were employed, i.e. chopping the secondary mirror (2.5 Hz) and nodding the telescope. Sky frames were taken in a location clear of 10-micron sources. The Q band images ($\lambda = 17.15$ micron, $\Delta\lambda = 1.5$ micron) were taken with a smaller pixel scale (0.33 arcsec/pixel), a necessity due to the even higher thermal background at the longer wavelength. At 17 micron, the seeing FWHM was 1.5 arcsec – i.e. close to the diffraction limit at this wavelength at this telescope. Again, hundreds of short exposure frames were coadded, this time with an individual on-chip exposure time of 12 ms. The same chopping and nodding as for the N band images was employed, and approximately the same sky position was used. The overall on-source observing efficiency for the N and Q band integrations was 40%.

We note that the sky is fairly clear of sources at mid-infrared wavelengths, so that it is easy to find an empty sky position. The very Galactic Centre is the exception in this respect; there is no other clustering of strong mid-infrared sources in the Galaxy that rivals the innermost parsec.

The images shown have not been flat-fielded, as this appears to be unnecessary: the overall gradient in sensitivity across the array is less than 10%, and the pixel-to-pixel variations are even smaller (Käufl, 1995).

The star βGru was used as a point source calibrator (N = –3.55, Q = –3.58) and also to measure the seeing at mid-infrared wavelengths; α Cen (N = –1.52, Q = –1.55) was used, too.

Significance of the Images

A major goal of our observation was to compare the 17-micron image to the 10-micron image in order to find out which of the well-known 10-micron sources in the Galactic Centre (Gezari et al., 1985) have a rising flux density distribution towards longer wavelengths. The high spatial resolution mid-infrared TIMMI array data are superior to earlier single-beam raster-scan observations (Becklin et al., 1978, Rieke et al., 1978). The idea behind all this was to try to search for dust-enshrouded massive protostars, similar in kind to the Becklin-Neugebauer and IRc2 objects in

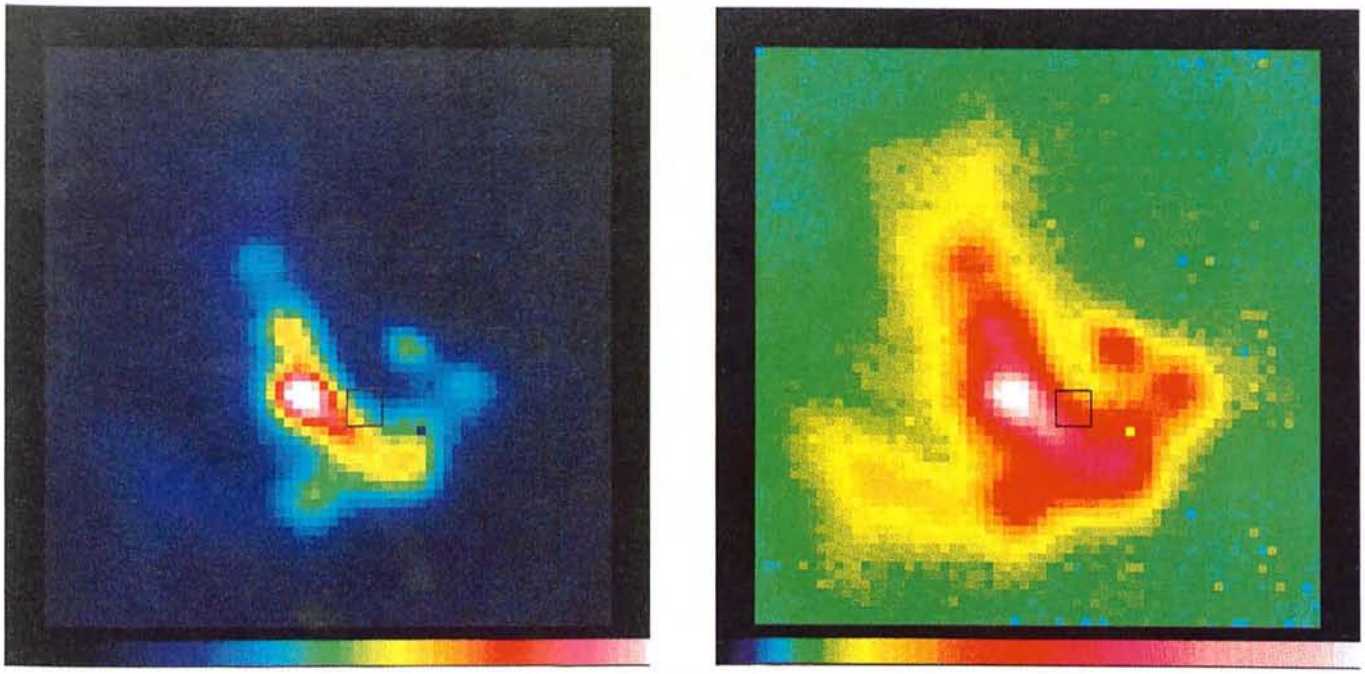

Figure 1a (left = intensity linear, right = log intensity): TIMMI 10-micron image ($\lambda/\Delta\lambda = 2.5$) of the central 40 × 40″ of the Galaxy. The image scale is 0.66″ per pixel. North is up, east to the left. The box indicates the position of SgrA, which is however not detected to a limiting 3-sigma sensitivity of about 0.3 Jy/sq″. While much of the mid-infrared emission is due to diffuse non-stellar emission, the two isolated sources north-west of SgrA* (IRS3 and IRS6) are almost certainly powered by embedded stellar objects.*

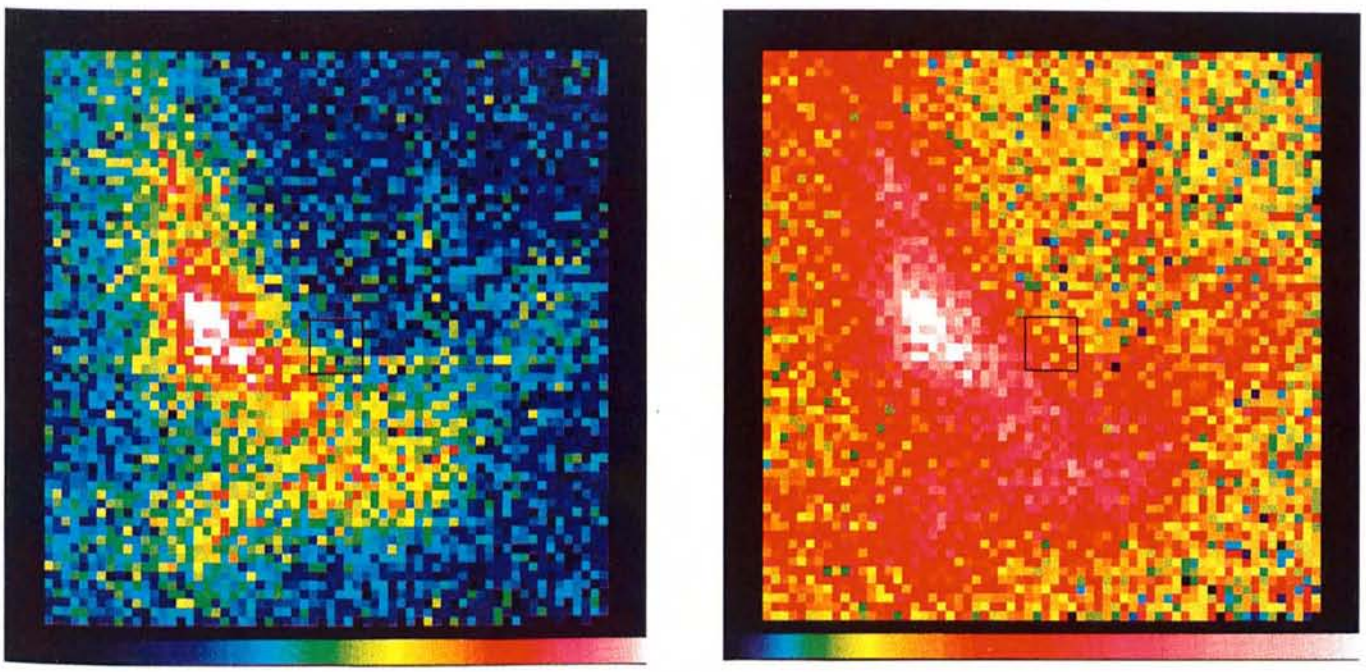

Figure 1b (left = intensity linear, right = log intensity): TIMMI 17-micron image ($\lambda/\Delta\lambda = 11.5$) of the central 20 × 20″ of the Galaxy. The image scale is 0.33″ per pixel. Note the overall similarity to the 10-micron image, except for the cocoon source IRS3 which appears to be heavily self-absorbed due to silicate dust. It is unclear whether IRS3 is a luminous evolved star or a deeply embedded massive protostar.

the Orion Nebula (Wynn-Williams et al., 1984). Those sources would have about 0.4 and 0.2 Jy at 10 microns and similar values at 17 microns, if displaced from Orion to the distance of the Galactic Centre (8.5 kpc). This takes into account a foreground extinction of around 1 mag in the broad N band and 0.5 mag in the Q band toward the Galactic Centre (corresponding to A_v = 27 mag, see e.g. Rieke and Lebofsky, 1985 for the interstellar extinction law towards the Galactic Centre). It is useful to compare our mid-infrared images to the K, L′, and M-band images of the Galactic Centre by Herbst et al. (1993) in order to more clearly isolate sources with flux density distributions rising toward longer wavelengths. A combined inspection of K, L′, M, N and Q-band images suggests at least one compact such source within a 12 × 12 arcsec (0.5 × 0.5 pc) field around the SgrA* position: IRS3! It is a very red source in the K, L′, M images, and is bright at 10 microns (7 Jy) and even brighter at 17 microns (approx. 10 Jy). Notice that the 17-micron detection is at a much lower signal-to-noise level than the 10-micron detection. IRS3 is known to have a noticeable 9.7-micron silicate absorption feature (Becklin et al., 1978, Rieke et al., 1978), indicating a temperature gradient in a dust shell or cocoon and considerable local extinction. The question whether IRS3 is indeed a deeply embedded massive protostar or

a very young embedded cluster of protostars near the Galactic Centre is thrown open here, although other explanations (a luminous evolved star such as an OH/IR star or a dust-enshrouded supergiant; Becklin et al., 1978, Rieke et al., 1978) have been considered in the past. Yet the fact that there are massive young stars such as WR stars and a cluster of HeI stars in the IRS16 complex near SgrA* (see the review of Genzel et al., 1995[1]) begs the question whether massive star formation continues in the Galactic-Centre region, even though no compact radio sources or ultracompact HII regions have been found.

It would be particularly worthwhile to extend the current 10-micron search for massive protostars to the Galactic Centre circumnuclear disk of dense molecular gas (e.g. Genzel, 1989).

A 5 × 5 mosaic of 10-micron TIMMI images would cover most of the relevant area. This TIMMI project would benefit greatly from the successful implementation of the 3.6-m refurbishment plan (M2 mirror), as it would probably enable us to reach the 10-micron diffraction limit of 0.7 arcsec. This would much improve the 10-micron point source sensitivity and the chance of detecting massive protostellar objects in the circumnuclear ring. On the other hand, ISOCAM images may soon reveal the presence (or absence) of young stellar sources in the circumnuclear disk region, albeit with poorer spatial resolution. Follow-up diffraction-limited imaging with TIMMI is likely to be needed. We hope for the best possible image quality at the 3.6-m by then.

Finally, we briefly discuss our results on IRS7 and SgrA* (which are in agreement with those of Gezari et al., 1994a,b). IRS7 – the brightest source in the 2.2-micron K-band – is not detected in our images, suggesting that this red supergiant lacks a warm optically thick dust shell. However, IRS7 is clearly detected at 7.8 and 12.4 micron (see Gezari et al., 1994a), suggesting that our non-detection at 10.1 microns may be due to absorption in the silicon feature around 9.7 microns, either locally or along the line of sight. As for SgrA*, we see no mid-infrared source at its position, which may imply that there is no or very little warm dust in the immediate vicinity of the Galactic-Centre monster. However, SgrA* has been claimed to be detected in deep 8.7-micron images (S. Stolovy, data presented at the recent ESO/CTIO conference in La Serena).

P.S. We have also obtained 10.4-micron [SI V] and 12.8-micron [Ne II] narrow-band images of the innermost Galactic-Centre region, in an attempt to study the spatial distribution of the energy and excitation sources in this region.

[1]In this review, Genzel et al. display a K-band spectrum of IRS3 obtained with their 3D spectrometer at the ESO-MPIA 2.2-m telescope. This spectrum shows a hint of weak HeI 2.06-micron emission on an otherwise featureless rising continuum, indicative of a highly reddened hot massive star. Krabbe et al. (1995) also mention that IRS3 could be a young massive star, although in their paper the HeI feature in IRS3 is barely discernible. Long ago, Rieke et al. (1978) already suspected that IRS3 could be a very young stellar object.

References

Becklin, E. et al., 1978, *ApJ* **219**, 121.

Genzel, R., 1989, IAU Symp 136 (ed. M. Morris).

Genzel, R., Eckart, A., Krabbe, A., 1995, *Ann. N.Y. Acad. Sci.* **759**, 38 (eds. Böhringer, H., Morfill, G.E., Trümper, J. (Proc. 17th Texas Symposium Munich).

Gezari, D. et al., 1985, *ApJ* **299**, 1007.

Gezari, D. et al., 1994a, in: *The Nuclei of Normal Galaxies: Lessons from the Galactic Center*, eds. R. Genzel and A. Harrig, Kluwer, p. 343.

Gezari, D. et al., 1994b, *ibidem*, p. 427.

Herbst, T.M., Beckwith, S.V.W., Shure, M., 1993, *ApJ* **411**, L21.

Jackson, J.M. et al., 1993, *ApJ* **402**, 173.

Käufl, H.U. et al., 1992, *The Messenger* **70**, 67.

Käufl, H.U. et al., 1994, *Infrared Phys. Technol.* **33**, 203.

Käufl, H.U. 1995, in *ESO/ST-ECF Workshop on Calibration and Understanding HST and ESO Instruments*, ed. P. Benvenuti, p. 99.

Krabbe, A., et al. 1995, *ApJ* **447**, L95.

Rieke, G. et al., 1978, *ApJ* **220**, 556.

Rieke, G., Lebofsky, M., 1985, *ApJ* **288**, 616. (Tab. 3).

Wynn-Williams, G. et al. (1984). *ApJ* **281**, 172.

Hans Zinnecker
e-mail: hzinnecker@aip.de

Redshift and Photometric Survey of the X-Ray Cluster of Galaxies Abell 85

F. DURRET[1, 2], P. FELENBOK[2], D. GERBAL[2], J. GUIBERT[3], C. LOBO[1, 4] and E. SLEZAK[5]

[1]Institut d'Astrophysique de Paris; [2]DAEC, Observatoire de Paris-Meudon; [3]CAI, Observatoire de Paris; [4]CAUP, Porto; [5]O.C.A., Nice

As the largest gravitationally bound systems in the Universe, clusters of galaxies have attracted much interest since the pioneering works of Zwicky, who evidenced the existence of dark matter in these objects, and later of Abell, who achieved the first large catalogue of clusters.

Clusters of galaxies are now analysed through three different and complementary approaches: optical imaging and spectroscopy, which allow to derive the galaxy content, X-ray imaging and spectroscopy, giving information on the physical properties of the X-ray gas embedded in the cluster, and from which the total dynamical mass of the cluster can be estimated, under the assumption of hydrostatic equilibrium, and, for clusters of redshifts $z \geq 0.31$ deep optical imaging of arcs and arclets in clusters.

As a complementary approach to that of large cluster surveys such as the ENACS (ESO Nearby Abell Cluster Survey) ESO key programme, we have chosen to analyse in detail a few clusters of galaxies, by combining optical and X-ray data. We present here results on the first of the two clusters observed at ESO: Abell 85.

This cluster is rich and located at a redshift $z \sim 0.055$, corresponding to a spatial scale of 97.0 kpc/arcmin ($H_0 = 50$ km/s/Mpc). Previously published data on this cluster include partial CCD imaging by Murphy (1984), redshift catalogues by Beers et al. (1991) and Malumuth et al. (1992), totalling 150 redshifts; these authors evidenced the existence of substructure in Abell 85 as well as the presence of a foreground group of galaxies. Abell 85 has a double structure in X-rays (Gerbal et al., 1992 and references therein), and is therefore not fully relaxed, as many other clusters indeed, contrarily to what was previously believed.

Observations

We first obtained a photometric catalogue of 4232 galaxies (hereafter the MAMA catalogue) in a region of ±1° around the cluster centre, by scanning a b_J photographic plate with the MAMA

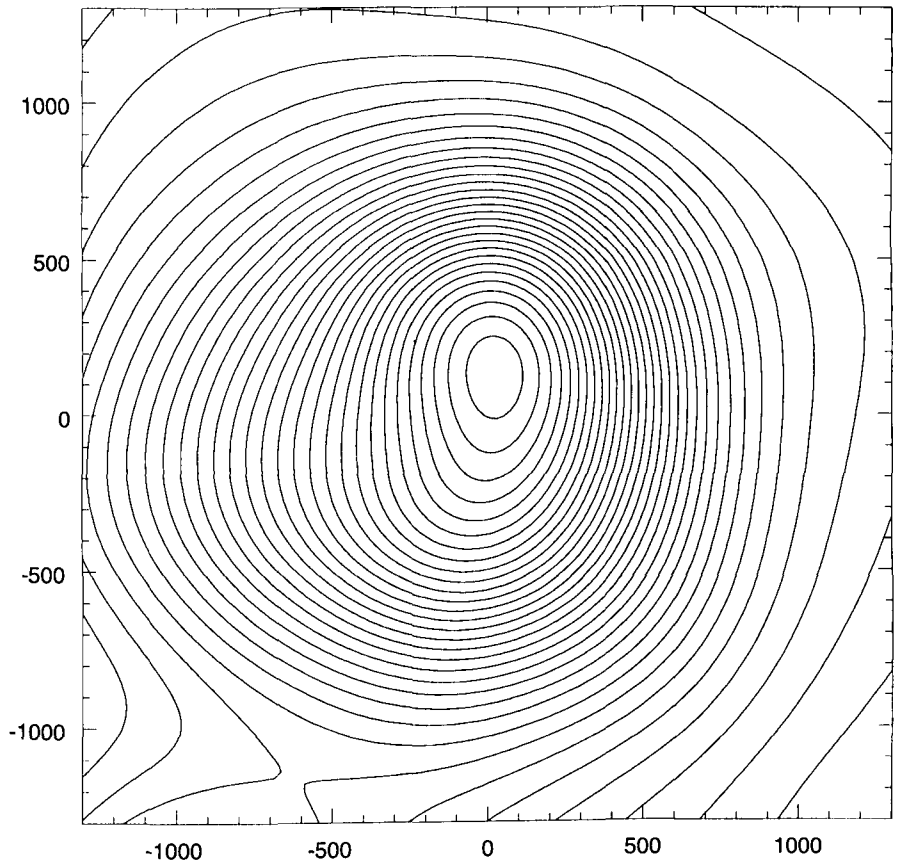

Figure 1. Kernel map distribution of the galaxies in the central regions of the MAMA photometric catalogue of Abell 85 (as defined in text), obtained with 10 bootstrap resamplings. Co-ordinates are in arcseconds relative to the centre.

measuring machine at the CAI, Observatoire de Paris. This catalogue is complete for $b_J \leq 18.0$; the galaxy positions obtained are very accurate (1–2″) while magnitudes are not due to usual problems with photographic plates.

We therefore made observations of six fields of 6.4 × 6.4′ in the central regions of the cluster with the Danish 1.5-m telescope in the V and R bands. Reductions were made with IRAF and using the software developed by O. Le Fèvre. This allowed us to recalibrate the magnitudes of our MAMA catalogue, and also to obtain a deeper photometric catalogue in V and R of the central regions of the cluster (hereafter the CCD catalogue).

Spectroscopic observations were performed with the ESO 3.6-m telescope equipped with MEFOS, and a dispersion of 224 Å/mm in the wavelength region 3820–6100 Å, during 6 and 2 nights in November 1994 and 1995. We obtained 421 reliable redshifts, leading to a spectroscopic catalogue of 592 objects in this region, 551 of them being galaxies (including the 150 published by Beers et al., 1991 and Malumuth et al., 1992). The reduction was made with IRAF and velocities were measured using cross-correlation techniques.

Projected Galaxy Distribution

We performed a kernel analysis of the MAMA photometric catalogue described above and display the result in Figure 1. The main structure of the cluster appears very smooth, with a clear elongation towards the south in the central region coinciding with the presence of the South blob observed in X-rays (see Gerbal et al., 1992). This confirms the idea that Abell 85 is bimodal, with a main body in which both the galaxies and the hot intracluster gas appear smoothly distributed, and a blob south of the central zone.

Velocity Distribution

The velocity distribution of the 551 galaxies of our redshift catalogue is displayed in Figure 2 as a function of distance to the cluster centre. We can see from this figure that there is indeed a "sheet" of galaxies with velocities of about 6000 km/s, as mentioned by previous authors. Behind the cluster, there is a large number of galaxies following a velocity distribution suggestive of a certain periodicity that could correspond to voids and sheets of galaxies and could therefore be used as an indicator of large-scale structures in this direction.

A good agreement between the mean and median values of the velocities is

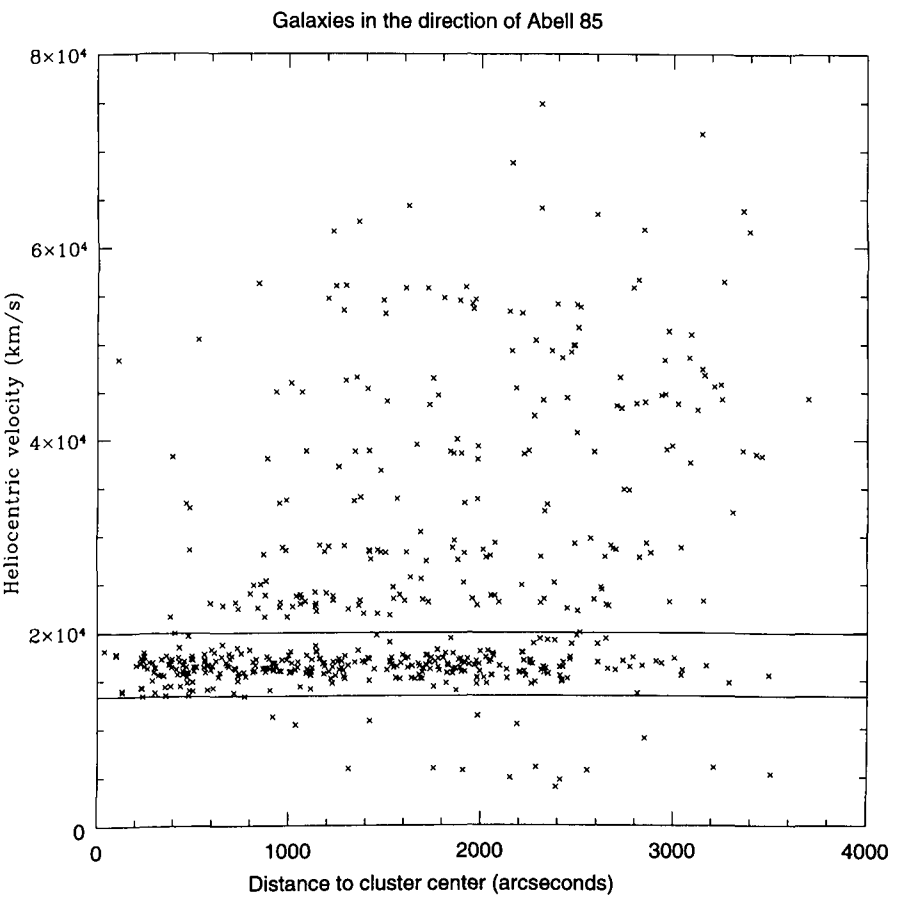

Figure 2. Velocity distribution as a function of distance to the cluster centre, with two lines indicating the velocity range in the cluster.

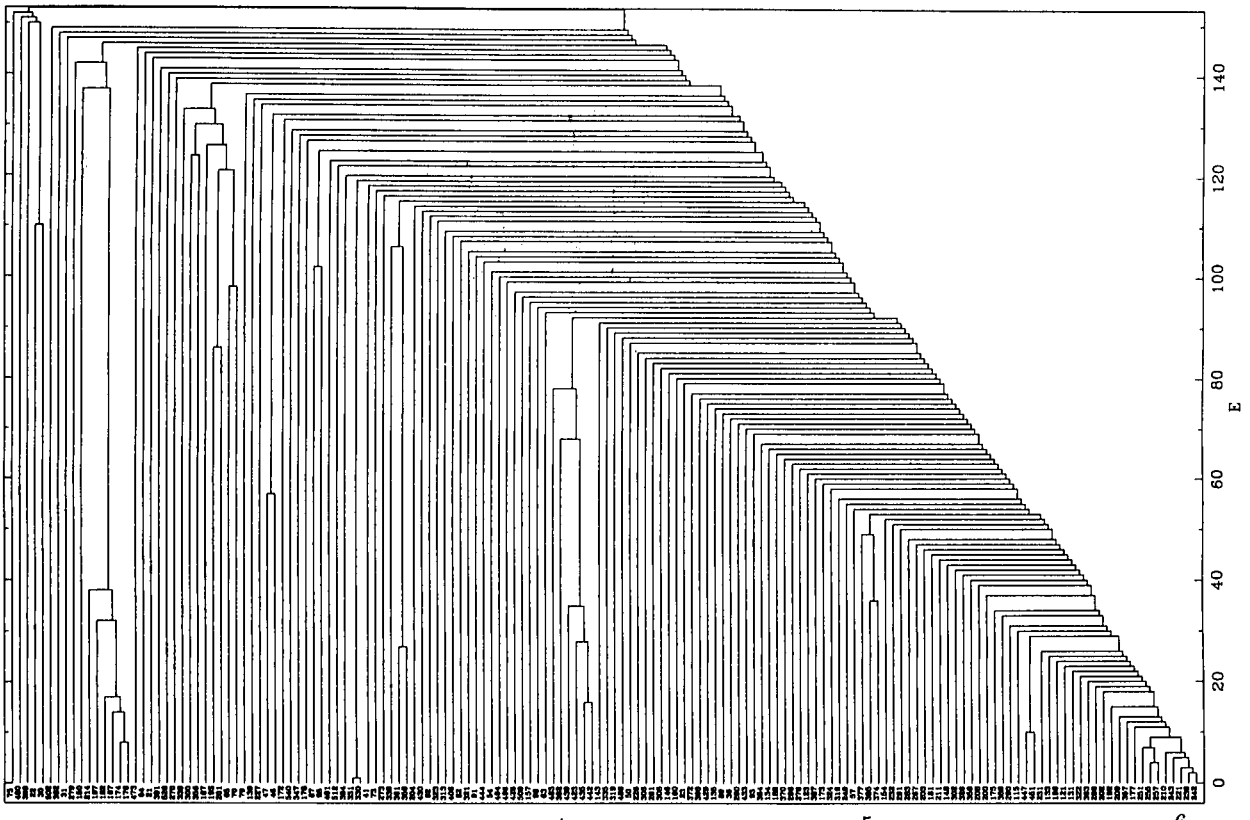

Group	1	2	3	4	5	6
<v> (km/s)	19319	14102	17914	15217	16104	16512
σ_v (km/s)	476	392	247	246	865	737

Figure 3. Result of the hierarchical test performed on the 154 brightest members of Abell 85, where E represents the binding energy of the system and the tiny numbers are the catalogue numbers for each galaxy. From left to right, groups 1 to 6 are indicated below the figure, as well as the average velocity and velocity dispersion of each group.

obtained in the interval 13,350 ≤ v ≤ 19,930 km/s, which will be taken as the criterion for galaxies to belong to Abell 85. This leads to a total number of *308 galaxies* with measured velocities belonging to Abell 85, making this velocity catalogue (hereafter the A 85 velocity catalogue) one of the richest ones for a single cluster.

The bi-weight mean velocity for this sample is 16,458 km/s, with a high velocity dispersion of 1185 km/s, in agreement with the existence of substructure.

The velocity of the cD galaxy is 16,734±48 km/s and 16,447±126 km/s as given by Beers et al. (1991) and Malumuth et al. (1992) respectively. We will use the Beers et al. value, which has the smallest error bar; this value is equal to the mean cluster velocity within error bars.

Search for Clustering Patterns

In order to search for substructure in Abell 85, we have performed on the A 85 velocity catalogue a hierarchical test based on the binding gravitational energy of galaxies (see Serna & Gerbal, 1996 for a full description of the method).

The result of such an analysis is displayed and reveals several interesting features. From left to right on Figure 3: Groups 1 and 3 are probably just isolated background galaxies (their spatial distribution shows no concentration), while Group 2 has a velocity close to the lower limit of that of the cluster and appears tight in projection. All the other galaxies can be considered to form the actual Abell 85 cluster, for which the velocity dispersion then becomes 760 km/s, a value more typical of rich clusters than the high value given above when analysing the whole A 85 velocity cata-

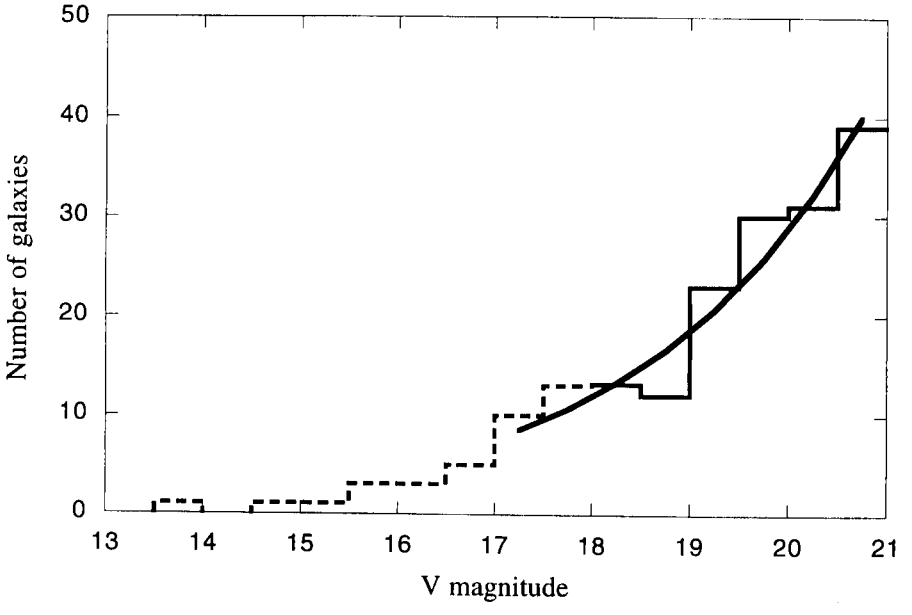

Figure 4. Luminosity function in the V band for the CCD catalogue (defined in text) and best fit with a power law of index $\alpha = -1.5 \pm 0.1$.

logue. Group 4 includes 6 galaxies close in projection (in particular 4 of them), Group 5 is a triplet very close in projection, and Group 6 is located at the bottom of the potential well, around the cD galaxy.

Luminosity Function in the V Band

The luminosity function in the V band shown in Figure 4 has been derived:

– directly, for the brightest galaxies ($V < 18$) with velocities belonging to the cluster;

– for fainter galaxies, for all the objects of our CCD photometric catalogue, to which we have subtracted the background counts in the V band taken from the ESO-Sculptor survey (Bellanger et al., 1995, Arnouts et al., 1996, see preprint by Lobo et al., 1996 for details on this subtraction).

The best fit is obtained for a power law of index $\alpha = -1.5 \pm 0.1$, similar to that obtained in central regions of clusters, such as e.g. in Coma, which we have re-analysed in detail recently (Biviano et al., 1996, Lobo et al., 1996 and references therein).

Conclusions

The combined data obtained with the MAMA measuring machine, CCD imaging and spectroscopy with MEFOS have led to one of the richest velocity catalogues for a single cluster. This will allow a detailed analysis of the physical properties of Abell 85, which will be compared to those derived from X-rays (Pislar et al., 1996).

Acknowledgements

We gratefully acknowledge A. Biviano for supplying us with his adaptive kernel programme, O. Le Fèvre for giving us his photometric analysis software, and A. Serna for giving us his hierarchical test programme.

CL is fully supported by the BD/2772/93RM grant attributed by JNICT, Portugal.

References

Arnouts S., de Lapparent V., Mathez G. et al. 1996, *A&AS* in press.
Beers T.C., Forman W., Huchra J.P., Jones C., Gebhardt K. 1991, *AJ* **102**, 1581.
Bellanger C., de Lapparent V., Arnouts S., et al. 1995, *A&AS* **110**, 159.
Biviano A., Durret F., Gerbal D., Le Fèvre O., Lobo C., Mazure A., Slezak E. 1996, *A&A* in press.
Gerbal D., Durret F., Lima-Neto G., Lachièze-Rey M. 1992, *A&A* **253**, 77.
Lobo C., Biviano A., Durret F., Gerbal D., Le Fèvre O., Mazure A., Slezak E. 1996, *A&A* submitted.
Malumuth E.M., Kriss G.A., Van Dyke Dixon W., Ferguson H.C., Ritchie C. 1992, *AJ* **104**, 495.
Murphy P. 1984, *MNRAS* **211**, 637.
Pislar V., Durret F., Gerbal D., Lima-Neto G., Slezak E., 1996, to be submitted to A&A.
Serna A., Gerbal D. 1996, *A&A* in press.
Slezak E. Durret F. Gerbal D. 1994, *AJ* **108**, 1996.

Florence Durret
e-mail: durret@iap.fr

Fishing for Absorption Lines with SEST

THE REDSHIFT OF THE GRAVITATIONAL LENS TO PKS 1830–211

T. WIKLIND (Onsala Space Observatory, Sweden)
F. COMBES (DEMIRM, Observatoire de Paris, France)

Background

Molecular gas is the cold and dense part of the interstellar medium (ISM) which is directly involved in the formation of stars. The possibility of studying this ISM component at high redshifts would give us an insight in the conditions for stellar formation when these may have been quite different from what is seen in present-day galaxies. It was therefore with great interest that astronomers greeted the news in 1991 that emission from the rotational J=3–2 line of carbon monoxide (CO) had been detected in the galaxy F10214+4724 at a redshift of $z = 2.29$ (Brown & Vanden Bout, 1991). A standard conversion factor between the integrated CO emission and the column density of H_2 implied a molecular gas mass of 2×10^{11} $M_\odot$, which meant that the molecular gas constituted a major part of the total mass of the galaxy. Three years later CO emission was detected in the Cloverleaf quasar at $z = 2.56$ (Barvainis et al., 1994). In this case it was known that the CO emission was magnified by gravitational lensing, making it impossible to derive the intrinsic H_2 mass. It is now clear that also F10214+4724 is a gravitationally lensed system (Matthews et al., 1994) and that the molecular gas mass is overestimated by a factor of 10 or more (Radford, 1996). Yet another gravitationally lensed galaxy has been detected by Casoli et al. (1996). They observed CO emission from a gravitational arc at $z \approx 0.7$. With a magnification factor of ~ 50, this is intrinsically a relatively inconspicuous galaxy.

Apart from these gravitationally lensed objects, there have been searches for CO emission in nonlensed systems at high redshifts, which have all been negative. In fact, there are no confirmed observations of CO emission in nongravitationally lensed objects at redshifts higher than $z \approx 0.3$. Hence, high-z galaxies, including those with detected CO emission, appear not to contain extremely high molecular gas masses. At most, they are similar to nearby examples of merger systems, such as Arp 220. Nevertheless, the lensed systems have shown that molecular gas which has undergone a substantial stellar processing does exist at high redshifts.

Gravitationally magnified CO emission is, however, not our only means to study molecular gas at high redshifts. Just as in the optical wavelength band, it is easier to detect molecular absorption lines than the corresponding emission lines and, with an appropriate alignment of an intervening galaxy and a background radio continuum source, it is possible to probe the molecular ISM at very large distances. This has been demonstrated by the detection of more than 40 different molecular transitions at redshifts ranging from $z = 0.25$ to $z = 0.89$ (Wiklind & Combes, 1994, 1995a, 1995b; Combes & Wiklind, 1995). Due to the greater sensitivity of absorption lines, it is possible to observe molecules other than CO. Paradoxically, this is easier to do for gas at large distances, since Galactic absorption almost always gets confused with emission.

Molecular Absorption Lines at Intermediate Redshifts

The first molecular absorption at a cosmologically significant distance was detected with the SEST telescope in December 1993, towards the BL Lac object PKS1413+135 (Wiklind & Combes, 1994). The CO($J = 1 \leftarrow 0$) transition was seen at a redshift of $z = 0.247$. The continuum radio source is completely obscured at optical wavelengths and coincides with an edge-on galaxy with the same redshift as the absorption. The redshift of the BL Lac itself is not known, but since the impact parameter between the radio core and the nucleus of the galaxy is $< 0.1''$ and since there are no indications of gravitational lensing effects, it

is likely that the absorbing gas resides in the host of the BL Lac object.

A second molecular absorption line system, this time at a redshift $z = 0.685$, was detected towards the radio source B0218+357 (Wiklind & Combes, 1995). B0218+357 has been identified as a gravitational lens on the basis of its radio morphology (cf. Patnaik et al., 1993). It consists of two compact flat-spectrum cores, separated by 0.34″ and a steep-spectrum ring. The absorption takes place in the lensing galaxy, where we have detected 15 different molecular transitions of molecules such as HCO^+, HCN, HNC, CN, H_2CO and CS (Wiklind & Combes, 1995; Combes & Wiklind, 1996). Surprisingly, we have been able to observe the isotopomers ^{13}CO and $C^{18}O$, while $C^{17}O$ remains below our detection limit. Together with a nondetection of molecular oxygen O_2, the molecular line data has allowed a stringent limit on the O_2/CO ratio, with implications for chemical models (Combes & Wiklind, 1995).

A third molecular absorption-line system was detected in June 1995 towards the background source B3 1504+377, at a redshift of $z = 0.673$. Similarly to PKS1413+135, a small impact parameter and the absence of gravitationally lensed images of the radio source implies that the absorption takes place in the host galaxy to B3 1504+377 (Wiklind & Combes, 1996b).

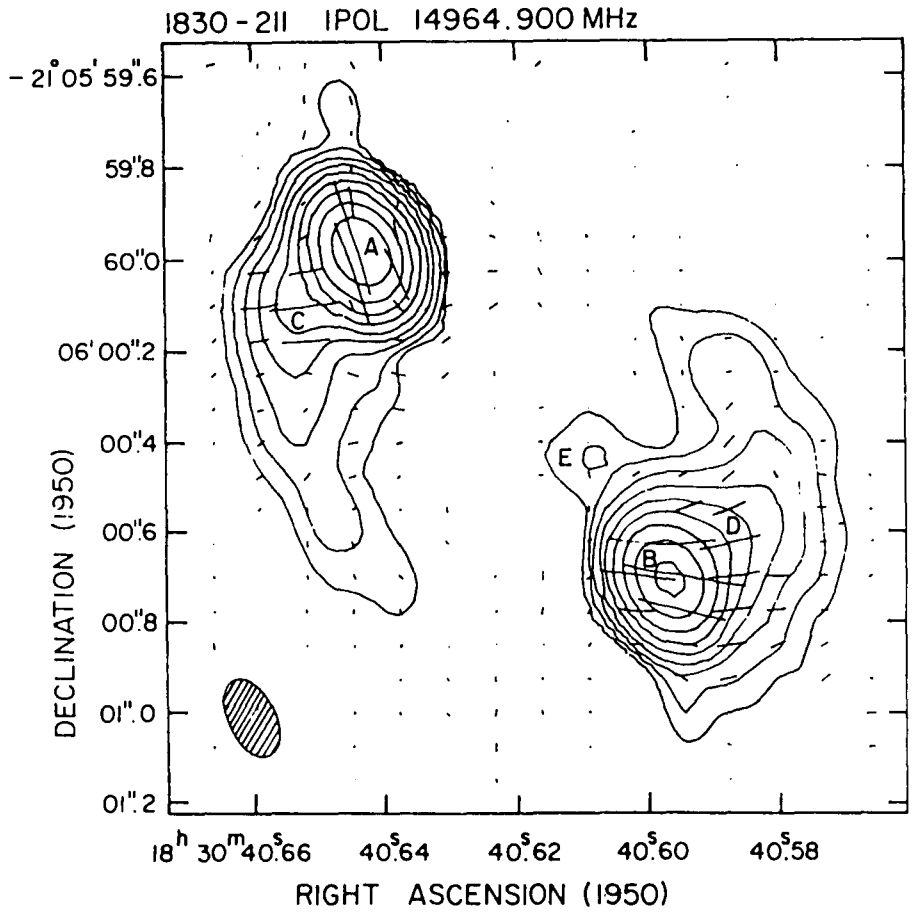

Figure 1: VLA image of PKS1830–211 at 15 GHz (from Subrahmanyan et al. 1990), showing contours of the flux and the electric field polarisation vectors.

Searching for More Molecular Absorption Line Systems . . .

We have also searched for molecular absorption lines associated with MgII and CIV absorption-line systems, as well as in the host galaxies of optically visible AGNs, without detecting any. The metal absorption-line systems are characterised by impact parameters (projected distance between the line of sight to the background AGN and the centre of an intervening galaxy) of tens of kpc and, due to the centrally concentrated molecular gas distribution found in nearby galaxies, it is not surprising that we find no molecular gas. The nondetections of molecular absorption at the redshifts of optically visible AGNs is readily understood as a selection effect; a molecular cloud in the line of sight is likely to cause several magnitudes of extinction, making the AGN virtually invisible at optical wavelengths. The three detected molecular absorption-line systems are characterised by a small impact parameter between a radio source and the centre of a galaxy which, albeit distant and faint, has been optically identified. The AGN associated with the radio source is not seen at optical wavelengths. The redshifts obtained from optical spectroscopy has been that of the intervening or associated galaxy.

While optical spectroscopy has a large instantaneous bandwidth, but limited spectral resolution, the contrary applies for millimetre wave spectroscopy. Measured in velocity, the bandwidth of a typical mm-wave receiving system is ~ 3000 km s^{-1}, while the resolution is ~1 km s^{-1}. This means that one needs to know the redshift of an absorbing galaxy to a relatively high accuracy in order to correctly tune the receivers. An alternative is to search for molecular absorption in a source with unknown redshift by sequential tuning of the receivers. From our experience with the known molecular absorption line systems, we know that it is not only CO which is likely to show strong absorption, but also HCO^+, HCN and HNC. Hence, by searching over the 3-mm band (80–115 GHz) we can cover the redshift intervals z = 0–0.44 and z = 0.55–3.32. The 'hole' at z = 0.44–0.55 can be filled by observing the 149–160 GHz band at λ2-mm (Table 1). The SEST telescope is ideal for such a search since it is equipped with new low-noise SIS receivers covering the 3- and 2-mm bands and has an instantaneous bandwidth of 1 GHz. Furthermore, the receivers can be tuned from the control room, making it possible to rapidly change the frequency. With a strong continuum source, i.e. 1–2 Jy, the whole 3-mm band can be searched in less than 12–20 hours. The additional search in the 2-mm band increases this time only slightly, as SEST supports a dual observing mode where the 3- and 2-mm receivers can be used simultaneously.

. . . and Finding One with Unknown Redshift

A small impact parameter and the absence of an optically visible AGN seems to be a prerequisite for detecting molecular absorption lines, making radio identified gravitational lenses with small image separation good candidates. One such object is the gravitational lens can-

TABLE 1: Redshift coverage of saturated molecular absorption lines.

Molecular transition	3-mm band (80–115 GHz)	2-mm band (149–160 GHz)
CO(1–0)	0.00–0.44	
HCO^+(2–1)	0.55–1.23	0.12–0.20
CO(2–1)	1.00–1.88	0.44–0.55
HCO^+(3–2)	1.31–2.34	0.67–0.80
CO(3–2)	2.00–3.32	1.16–1.32

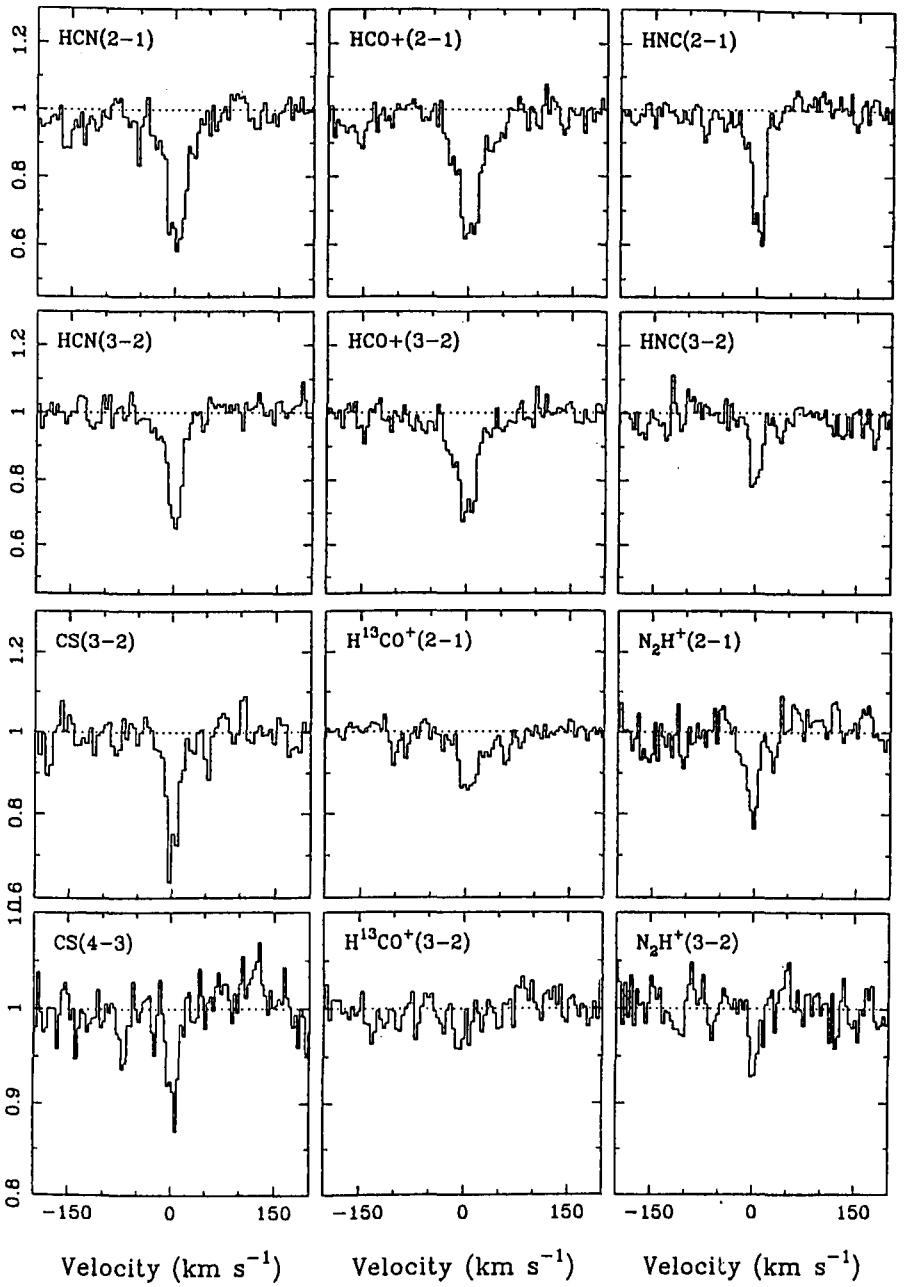

Figure 2: Absorption spectra from the lens to PKS1830–211 at z = 0.88582 observed with the SEST. The flux level has been normalised to unity and represents the flux from both images of the background radio source (which remains unresolved by the SEST telescope beam).

didate PKS1830–211. It is a strong radio source, with a radio morphology consisting of two compact components, separated by ~ 1″ and connected by an elliptical ring (Fig.1). The two components are parity-reversed images of a background quasar consisting of a core and a jet (Kochanek & Narayan, 1992; Nair et al., 1993). The extended feature of the lensed image makes PKS1830–211 ideally suited for modelling of the potential of the lensing galaxy and for deriving cosmographic parameters. One major drawback has been the unknown redshift of both the lens and the source. PKS1830–211 is located close to the Galactic Centre, at l = 12.2°, b = –5.7°, but the galactic extinction is moderate, with $A_V \approx 2.7^m$ (Subrahmanyan et al., 1990). Nevertheless, deep imaging in the BVRIK bands (Subrahmanyan et al., 1990; Djorgovski et al., 1992) has failed to detect an optical counterpart of neither the lens nor the background QSO. A recent attempt with the Keck telescope also failed (Djorgovski, private communication). Since PKS1830–211 is a strong source even at mm-wavelengths, with a flux ≥ 2Jy at λ3 mm, we decided to search for molecular absorption lines towards it, despite the unknown redshift.

We started our search in June 1995 and found the first absorption line after only a few hours of observation, at a frequency of 96.2 GHz. After confirming the detection, we observed at selected frequencies in the 3- and 2-mm band in order to establish the identity of the line. The candidate absorption line did not reach the zero level, but had a depth of ~ 35% of the continuum level. Our first interpretation was that the absorption was unsaturated. However, since the background source consisted of two components, separated by 1″, we could not exclude the possibility that the absorption was caused by molecular gas covering only one of them. It finally turned out that the absorption was caused by the HNC(2←1) line at a redshift of $z = 0.88582 \pm 0.00001$. This was established by detecting the J = 2←1 lines of HCN and HCO^+ as well as the J = 3←2 lines of HCN, HCO^+ and HNC. Subsequently we also observed absorption lines of CS(3←2), $N_2H^+(2\leftarrow1)$, $N_2H^+(3\leftarrow 2)$ and $H_2CO(2_{11} \leftarrow 1_{10})$. The detection of the N_2H^+ molecule suggested that the absorption of the more abundant molecules like HCN, HCO^+ and HNC were saturated, despite not reaching the zero level. We therefore tuned to the isotopic $H^{13}CO^+(2 \leftarrow 1)$. After some integration this transition was also detected, clearly showing that the $HCO^+(2\leftarrow1)$ line was heavily saturated. Some of the observed absorption profiles are shown in Figure 2.

The flux ratio between the two lensed images of the compact core represents different point-image magnifications. VLBI observations at λ2 cm gives a flux ratio of the NE and SW cores of 1.78 ± 0.10. If the molecular gas only covers one of the compact cores, the point-image magnification ratio is directly given by $R = (T_c/T_{abs}) - 1$, where T_c and T_{abs} are the total continuum flux and the depth of a saturated absorption line measured from the continuum level, respectively. Our molecular absorption-line data imply a point-image magnification ratio of 1.75 ± 0.15. From this we conclude that the SW core is obscured by molecular gas, while the NE component is not.

Utility of the Absorption Lines Towards PKS1830–211

The individual continuum fluxes coming from the NE and SW cores can be derived directly from a single spectrum of the saturated J=2←1 lines of HCN, HCO^+ or HNC. Since PKS1830–211 is known to have changed its millimetre continuum flux with a factor of two on a time scale of ~ 8 months (Steppe et al., 1993), these lines can be used as a sensitive probe of the time delay between the lensed images of the core. The lensed image of PKS1830–211 shows considerable structure at low radio frequencies (but not at millimetre wavelengths), making it possible to construct a detailed model of the gravitational potential of the lens. A measurement of the time delay therefore has the potential of giving an accurate value for the angular-size distance and, hence, a value for the Hubble constant. This may prove to be the most valuable result from the detection of molecular absorption lines towards this source.

An interesting application of redshifted molecular absorption lines in general comes from the fact that the excitation of the molecules might be dominated by the cosmic microwave background radiation. For dense gas this requires relatively high redshifts, but for diffuse gas, where collisions between molecules are infrequent, this can occur at intermediate redshifts. This latter situation seems to apply to the absorbing gas towards PKS1830–211. For the HCN, HCO^+ and HNC molecules we have derived an excitation temperature of 6–8 K. This is significantly higher than the expected temperature of the cosmic microwave background radiation, T_{CMB}, which at a redshift of $z = 0.89$ should be 5.16 K[1], but since these lines are heavily saturated they only give an upper limit to T_x. The unsaturated lines of CS, N_2H^+ and $H^{13}CO^+$, which directly give T_x, have an excitation temperature of only ~ 4 K. This is less than the expected temperature of the cosmic background radiation, but given the 3σ errors, the excitation temperatures are still consistent with a T_{CMB} at $z = 0.89$ of 5.16 K. The very low values of T_x show that the excitation of the molecular lines is dominated by the cosmic microwave background radiation and, given our observational uncertainties, we can derive a conservative upper limit to T_{CMB} of 6.0 K. Detection of more molecular absorption-line systems at similarly high, or higher, redshifts offers the possibility of observing the evolution of T_{CMB} as a function of redshift.

Although the excitation temperature of the molecular lines is low, the actual kinetic temperature of the gas may be considerably higher. The abundance ratio of the isomeric molecules HCN/HNC acts as a thermometer of the kinetic temperature; when this ratio is ~ 1, the gas has a T_k of approximately 15–20 K, whereas if the ratio is well in excess of 1, the temperature is 50–100 K. This effect stems from the way molecules are formed through gas-phase reactions. For our absorption lines towards PKS1830–211, we estimate the kinetic temperature to be around 16 K.

[1] In the big-bang theory, the temperature of the microwave background radiation scales as $T_{CMB} = T_{bg}(1+z)$, where T_{bg} is the temperature at $z = 0$.

References

[1] Barvainis et al. 1994, *Nature*, **371**, 586.
[2] Brown, R.L., Vanden Bout, P.A. 1991, *AJ* **102**, 1956.
[3] Casoli, F., Encrenaz, P., Fort, B., Boisse, P., Mellier, Y. 1996, *A&A*, L41.
[4] Combes, F., Wiklind, T. 1995, *A&A* **303**, L61.
[5] Combes, F., Wiklind, T. 1996, in *Cold Gas at High Redshifts*, eds. Bremer, M., Röttgering, H., van der Werf, P & Carilli, C., Kluwer.
[6] Djorgovski, S., Meylan, G., Klemola, A., Thompson, D.J., Weir, W.N., Swarup, G., Rao, A.P., Subrahmanyan, R. Smette, A. 1992, *MNRAS* **257**, 240.
[7] Kochaneck, C.S. Narayan, R. 1992, *ApJ* **401**, 461.
[8] Matthews, K., et al. 1994, *ApJ* **420**, L13.
[9] Nair, S., Narashima, D. Rao, A.P. 1993, *ApJ* **407**, 46.
[10] Patnaik, A.R., Browne, I.W.A., King, L.J., Muxlow, T.W.B., Walsh, D., Wilkinson, P.N. 1993, *MNRAS* **261**, 435.
[11] Radford, S.J.E. 1996, in *Cold gas at High Redshifts*, eds. Bremer, M., Röttgering, H., van der Werf, P & Carilli, C.L., Kluwer.
[12] Steppe, H., Paubert, G., Sievers, A., Reuter, H.P., Greve, A., Liechti, S., Le Floch, B., Brunswig, W., Menéndez, C. & Sanchez, S. 1993, *A&AS* **102**, 611.
[13] Subrahmanyan, R., Narasimha, D., Rao, A.P. Swarup, G. 1990, *MNRAS* **246**, 263.
[14] Wiklind, T. Combes, F. 1994, *A&A* **286**, L9.
[15] Wiklind, T. Combes, F. 1995, *A&A* **299**, 382.
[16] Wiklind, T. Combes, F. 1996a, *Nature* **379**, 139.
[17] Wiklind, T., Combes, F. 1996b, *A&A* in press.

Tommy Wiklind
e-mail: tommy@oso.chalmers.se

The Break-Up of Periodic Comet Schwassmann-Wachmann 3: Image Documents from La Silla Telescopes

H. BOEHNHARDT, Universitäts-Sternwarte München, Germany
H.U. KAEUFL, P. GOUDFROOIJ, J. STORM, ESO
J. MANFROID, University of Liège, Belgium
K. REINSCH, Universitäts-Sternwarte Göttingen, Germany

1. Science with an Ordinary Comet

Until recently comet 73P/Schwassmann-Wachmann 3 (hereafter SW3) was considered a rather ordinary comet and as not being worthwhile a dedicated observing programme. Therefore, not much more than orbital elements and brightness estimates were available when the European Space Agency ESA became interested in this object as a potential target for the next cometary mission ROSETTA. SW3 belongs to the family of Jupiter comets a group of comets with orbits substantially and repeatedly affected by Jupiter's gravitation. Indeed, it was Jupiter that brought SW3 into its present orbit: two encounters in 1965 and 1978 changed the perihelion distance and inclination of the comet's orbit from 1.02 to 0.94 AU and from 17.3 to 11.4°, respectively (Belyaev et al., 1986).

But what is the scientific interest in observing SW3 nowadays? The driver was ESA's selection of the comet as a back-up target for the ROSETTA mission. The design of the scientific experiments onboard ROSETTA and the planning of the mission operations require the knowledge of basic physical properties of the comet, such as the nuclear size, rotation, activity profile, chemistry, the production rates of gas and dust, etc. Addressing these mission-related parameters on the basis of observations, one simultaneously contributes to the characterisation of SW3 as a member of the Jupiter family comets. It is important to learn about the similarities and diversities among comets and comet families and to establish a classification scheme for these solar-system objects which are believed to represent the most pristine and unaltered remnants of the solar system nebula. In that way it may be possible to constrain the formation history and conditions of our planetary system and furthermore the development of comets since their formation in the interplanetary and interstellar environment around the Sun.

2. The Prelude Observations

As a potential ROSETTA target, comet SW3 was monitored more thoroughly than usual. Almost monthly, broadband filter imaging of SW3 was performed by

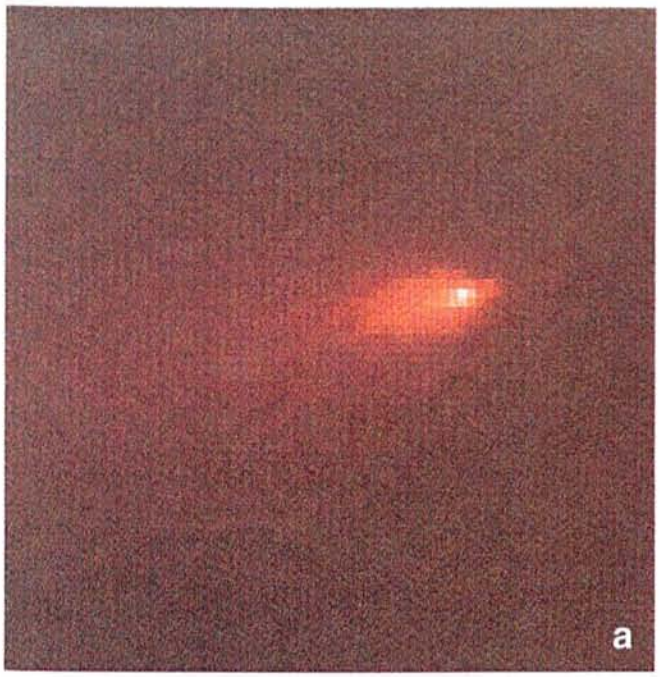

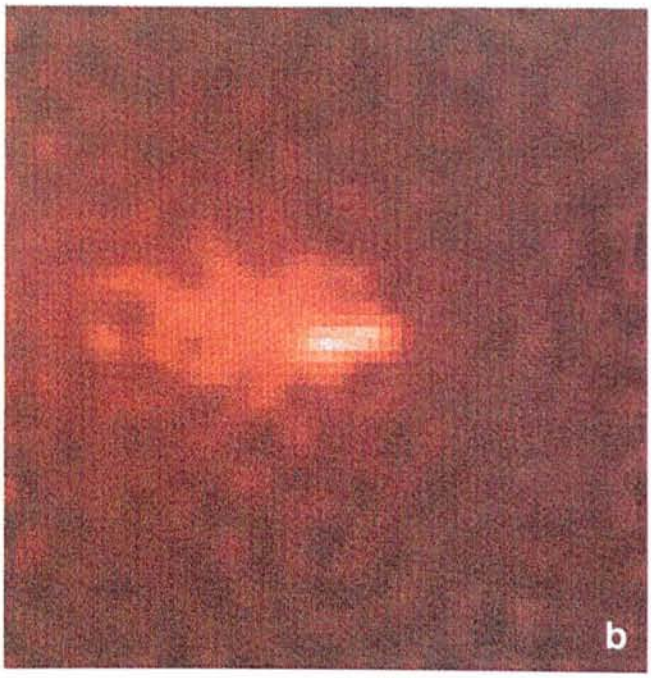

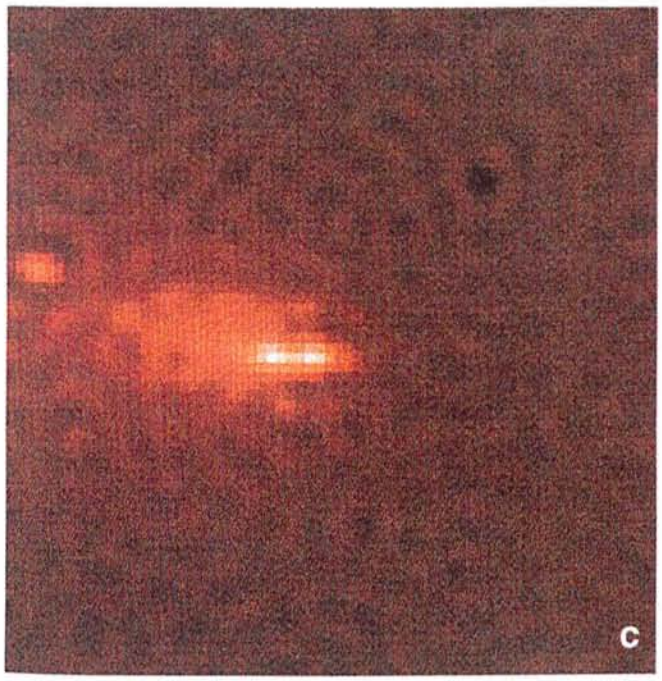

Figure 1a: SW3 on October 27, 1995. The 20-sec B-filter exposure was obtained by J. Manfroid (Liège) with the Dutch telescope at ESO-La Silla. This subframe of the central coma region was deconvolved by Richardson-Lucy algorithm. North is up and east to the left, the field of view is 22 × 22 arcsec.

Figure 1b: SW3 on November 27, 1995. The 120-sec B-filter exposure was obtained by K. Reinsch (Göttingen) with the 2.2-m telescope at ESO-La Silla. This subframe of the central coma region was deconvolved by Richardson-Lucy algorithm. Image orientation as in Figure 1a, the field of view is 19 × 19 arcsec.

Figure 1c: SW3 on December 2, 1995. The 120-sec R-filter exposure was obtained by J. Storm (ESO) with the Danish 1.5-m telescope at ESO-La Silla. This subframe of the central coma region was deconvolved by Richardson-Lucy algorithm. Image orientation as in Figure 1a, the field of view is 27 × 27 arcsec.

H. Boehnhardt and K. Birkle from late December 1994 until late June 1995 using telescopes at ESO La Silla and at the Calar Alto Observatory. During that period of time the comet behaved normally: a coma and tail were detected in late January 1995 when the comet was at 2.8 AU solar distance and developed as expected. The comet was brightening gradually until at least August 20, 1995, when it was estimated by a Japanese amateur astronomer at magnitude 13.

The first indication that something unusual happened to SW3 came from J. Crovisier and collaborators (1995, 1996) who detected a much higher OH production with the Nancay radio telescope on September 8–12, 1995, compared with that on September 1–5, 1995. Amateur astronomers reported the comet to be about 5 mag brighter than expected in late September 1995 (around 8 mag). This elevated coma brightness continued and still increased during October 1995 (SW3 then being brighter than 6 mag, i.e. more than 200 times brighter than normal at this distance). However, at that time the reason for this strong and continuous outburst of the comet was unclear.

3. The Break-Up of the Comet

A regular observing programme on SW3 by the first two authors of this paper was scheduled at ESO-La Silla for December 12–14, 1995. By means of simultaneous observations using the NTT plus EMMI for the visual wavelength range and the 3.6-m telescope plus TIMMI for the mid-IR range the gas and dust content in the comet should be characterised. Alerted by the reports on the SW3 outburst, the authors approached colleagues with a request for additional images of the comet before the beginning of their own observing campaign. As a result, exposures of SW3 were taken between late October and early December 1995. All these observations (including those taken after the break-up was detected – see below) had to be made under rather difficult conditions: since the comet's elongation from the Sun was only between 43 to 56°, these images were taken through high air masses (elevations from 35 down to 12°) and the daily observing window was rather short.

4. The ESO Image Gallery of the Break-Up

The break-up of the comet was detected by Boehnhardt and Kaeufl (1995) during their simultaneous observations at the NTT and 3.6-m telescopes. The R filter and 10-micron images revealed a total of four fragments in the coma (A,

B, C, F), but only three at either wavelength region (see Fig. 2). Two fragments (A and C), i.e., those at the extreme ends of the almost linear chain, seemed to be present both in the visual and IR wavelength range. The third companion, B in the visual and F in the infrared, were clearly different. Hence they produced significant signal levels only in the specific wavelength regions. The three-day observing run also revealed an increase in the distance between the fragments A, B and C and short-term variations in the brightness of their innermost regions.

The continuously increasing separation between the pieces A-C was confirmed by the follow-up observations scheduled on a short notice for the NTT on 7 and 31 January 1996 (see Fig. 3). By that time the fragments clearly had their own comae and tails embedded in a common sheath of material and the relative brightness of the companions may have stabilised.

Inspection of the earlier images of SW3 taken before the break-up detection in mid-December 1995 confirmed an extensive coma development. The central brightness peak in the coma was elongated in the east-west direction. However, applying the Richardson-Lucy deconvolution algorithm to the central coma region, the elongated peaks seen on November 28 and December 1–2, 1995 could be resolved into two separate fragments (see Fig. 1b,c). Evidently, the distance and the position angle of the two pieces changed during this 5-day interval. Despite all our efforts, we were unable to resolve the central coma peak in the late October to early November images (see Fig. 1a). However, the deconvolved images may indicate the presence of separate fragments already by that time.

5. Break-Up Scenarios

The ESO images of comet SW3 provide a unique documentation of the evolution of the SW3 fragments after the break-up. Using position measurements of the three condensations A, B, C, it is possible to derive solutions for the break-up sequence (for a theoretical background see Sekanina, 1982). An initial analysis of the ESO data (supplemented with those of other observers) performed independently by Sekanina and Boehnhardt & Kaeufl (1996) indicated a two-step break-up sequence, with the fragments A and B breaking off as a single body from the fragment C around October 24, 1995, while A and B themselves broke apart on December 1, 1995. In the meantime some more measurements became available and the earlier ones were remeasured in order to improve the position accuracy and to determine the intrinsic uncertainty of the values. Based upon these new data, improved solutions for the separation

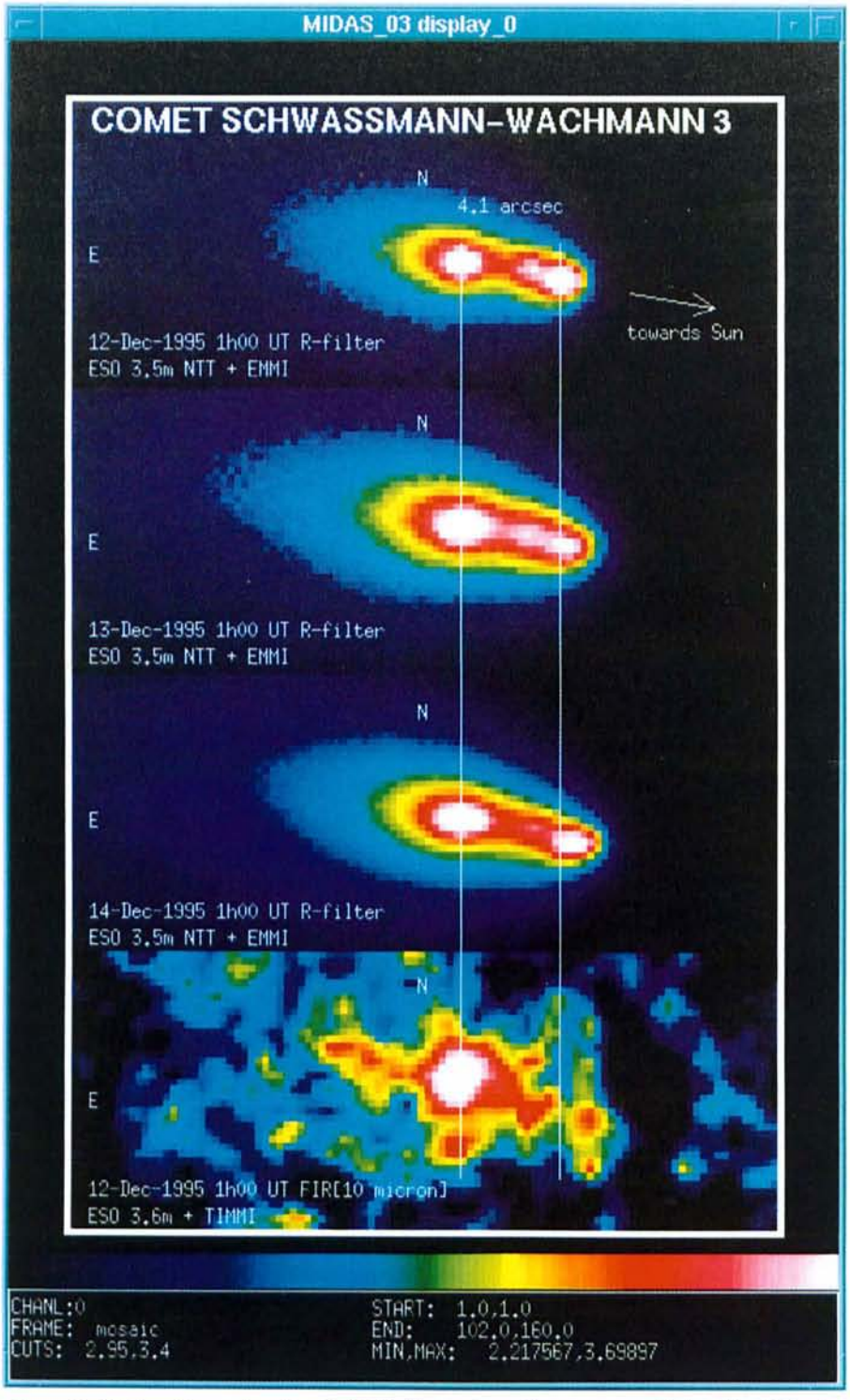

Figure 2: SW3 on December 12–14, 1995. The series of images was obtained by H. Boehnhardt (Munich) and H.U. Kaeufl (ESO) at the ESO NTT with EMMI and at the ESO 3.6-m telescopes with TIMMI. The upper three subimages show the relative motion and brightness variability of fragments A–C as seen in the visual wavelength range. The lower subimage gives the 10-micron view of the inner coma of SW3. Image orientation and scale is given in the figure, no image deconvolution applied.

sequence show B to have split from C before A separated from C, both events in late October and early November 1995 (Sekanina, private communication). One can exclude that the outburst of SW3 observed in September 1995 coincided with the break-up of the nucleus (Sekanina et al., 1996). Instead, we agree with Sekanina (1996) and Crovisier et al.(1996) in their conclusion that the outburst commenced more than one month before the nucleus splitting. Thus, the increased activity apparently represented a prelude to the dramatic break-up of SW3.

The existing observations do not provide a clear indication on the physical processes involved in the SW3 nucleus fragmentation. Possible scenarios are:

(1) The disruption of the surface crust over a large area caused by erupting pressurised gas under the surface layer

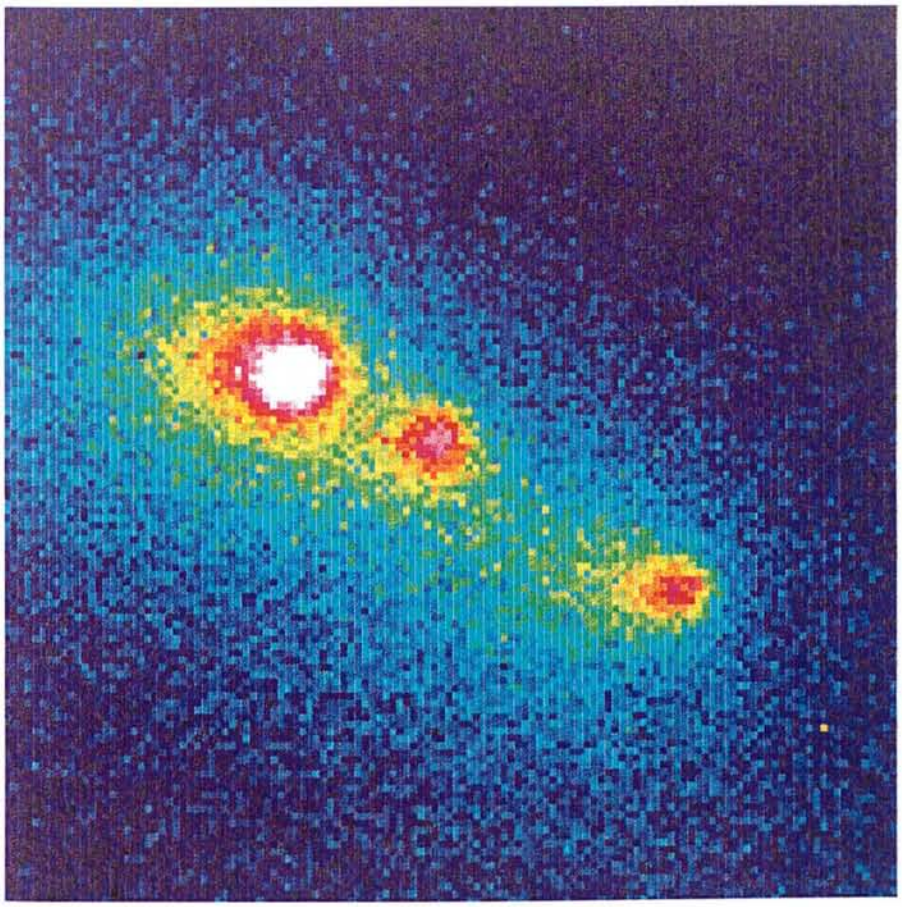

Figure 3: SW3 on January 31,1996. The 300-sec R-filter exposure was taken by P. Goudfrooij (ESO), H.U. Kaeufl (ESO) and H. Boehnhardt (Munich) with the ESO NTT plus EMMI. Image orientation as in Fig. 1a, the field of view is 34 × 34 arcsec, no image deconvolution applied.

of the nucleus as the comet approaches the Sun (the outburst of SW3 happened just 2–4 weeks before perihelion). Subsequently, the new and highly active regions release a large amount of gas and dust into the coma which simultaneously erodes the internal structure of the weakly bound comet body. As a result, major pieces can separate from the nucleus.

(2) A spin-up of the nucleus due to reaction forces from the outgassing results in new cracks in the surface due to a centrifugal stress in the nucleus. Hence, the gas and dust release increases which may both weaken the internal structure of the cometary body and may further accelerate the nucleus rotation. When the critical rotation rate is reached (order of a few hours; Sekanina, 1982), the comet begins to disintegrate.

(3) The impact of a major body on the nucleus severely damages the surface crust. The follow-up scenario of such an event resembles that described under (1). The impactor may have been a gravitationally bound fragment of the nucleus itself. Such companions are suspected to remain undetected in the proximity of the nucleus for very long times.

The enormous OH production observed in September and October 1995 (Crovisier et al., 1996) and the small nucleus size (our own unpublished observations indicate a nucleus radius of 1–1.5 km, see also Birkle and Boehnhardt, 1996) required almost the whole nucleus surface being active during the pre-splitting outburst. This constraint may be somewhat relaxed if one assumes a significant production of material from minor nucleus fragments released during the outburst. The detection of further fragments (for instance our IR fragment F or any of the additional ones reported by other observers, see IAU Circular 6301) could be evidence for the existence of numerous fragments around the nucleus.

6. SW3 and ROSETTA

The recent outburst and fragmentation of the SW3 nucleus may initiate new considerations about the role of the comet for the ROSETTA mission. Since this spacecraft project is very ambitious from the operational and scientific point of view (for instance continuous monitoring of the comet from circumnuclear orbit over about one year and two surface science packages to be landed on the nucleus), the splitting of SW3 presents new risks but also has some attractive aspects. The risks are the increased danger for the ROSETTA spacecraft from the debris around the nucleus and – even worse – the disappearance of the comet if a break-up should result in the object's disintegration. The positive aspect of this event is the implication that – if the nucleus of SW3 survives – fresh material from the nucleus interior becomes easily accessible on the surface. It is in the affected regions of the surface that the original and unmodified ingredients of the pre-solar nebula can be found (rather than on the largely evolved and processed surface crust of periodic comets that did not split). This perspective makes comet SW3 – at the moment – much more attractive for addressing fundamental questions of the solar-system formation by *in-situ* experiments than any other ROSETTA target.

7. Concluding Remarks

The splitting of SW3 in 1995 was another example of how brittle cometary nuclei are. Unlike in most previous events, however, the break-up of SW3 is well documented by high-quality ground-based observations, many of them carried out at ESO. SW3 represents an excellent candidate for a comprehensive analysis of cometary fragmentation, which could lead to a better understanding of the disintegration processes involved in the evolution of comets. An important unresolved key question both for the continuing break-up modelling and for the ROSETTA mission is the survival of the SW3 fragments. It will be addressed by further observations when the comet becomes visible again after its conjunction with the Sun.

Acknowledgements

The authors like to acknowledge very much the readiness of Dr. Kurt Birkle, MPI for Astronomy Heidelberg, Germany, to contribute observations of SW3 to the benefit of our SW3 programme. Dr. Zdenek Sekanina, JPL Pasadena, USA, provided very valuable comments and unique information for the interpretation of the SW3 nucleus splitting.

References

Belyaev, N.A., Kresak, L., Pittich, E.M., Pushkaev, A.N.: 1986, *Catalogue of Short-Period Comets*, Slovak Acad. Sciences, Bratislava.

Birkle, K., Boehnhardt, H.: 1996, *SuW* **34**, 782.

Boehnhardt, H., Kaeufl, H.U.: 1995, IAU Circ. 6274.

Crovisier, J., Biver, N., Bockelee-Morvan, D. et al.: 1995, IAU Circ. 6227.

Crovisier, J., Bockelee-Morvan, D., Gerard, E. et al.: 1996, *A&A*, submitted.

Sekanina, Z.: 1982, in Comets (ed. L.L. Wilkening), Univ. Arizona Press, 251.

Sekanina, Z., Boehnhardt, H., Kaeufl, H.U.: 1996, IAU Circ. 6301.

Hermann Boehnhardt
e-mail: hermann@bigbang.usm.uni-muenchen.de

The ESO Data Management Division

P. QUINN, ESO Data Management Division

Astronomers are currently at an important cross-road in their ability to gather information about the Universe. Firstly, computers and astronomical detectors have simultaneously increased in performance. Modern observatories using high-throughput, large-format detectors for imaging and spectroscopy are capable of producing tens of gigabytes of raw data every clear observing night. Although this allows rapid progress on observing programmes, the data rate and volume can easily saturate current network technologies and consume the disk space typically found on most workstations. Secondly, large telescopes in the 8–10-m class are going to be the workhorses of optical and IR astronomy well into the next century. These telescopes will be available to astronomers around the globe and competition for these expensive resources will be fierce. Observing programmes then have to be undertaken in the most efficient manner possible, minimising the effects of the weather in order to complete programmes in the shortest possible time.

Because of this "data deluge" and the need for maximum efficiency, astronomers are faced with the realisation that perhaps the classical observing cycle of trekking to the telescope and returning home with a tape of unprocessed data is no longer the most efficient or practical way to do astronomy. ESO astronomers stood at this cross-road and considered the options carefully when designing the Science Operation Plan for the VLT.

In this plan, ESO decided to enable the VLT to execute observing programmes in a service mode. Astronomers can specify programmes in a Phase I–Phase II proposal process and the resulting observations would be completed by ESO astronomers and technicians at the VLT when the conditions are most favourable for that programme. In this way, ESO astronomers would be as efficient and competitive as possible in completing the types of frontier programmes that will be common place on the VLT. Furthermore, ESO decided to meet the challenge of the data volume potential of the VLT by insisting that the VLT should be able to deliver calibrated data to the astronomer with a well-defined accuracy. This has two immediate benefits for the astronomer. Firstly the data processing and storage necessary to calibrate the data is provided by ESO which helps relieve the "deluge" significantly since most data reduction systems expand raw data by factors of 2–5 before calibration is complete. Secondly, by guaranteeing the calibration process to a given accuracy, ESO has to continuously monitor the applicability of calibration data and the performance of telescopes and instruments over long periods of time. The quality control of the calibration process will ensure the long-term usefulness of the data.

Once ESO adopted the principles of service observations and delivery of calibrated data for the VLT, it was obvious that the flow of data must be managed from start to end of the observing process. The ESO Data Management Division was formed to design and implement the Science Data Flow System for the VLT. Beginning in 1994, the division was formed from pre-existing groups at ESO whose responsibilities covered proposal submission, data archiving and the processing of ESO telescope data using the MIDAS system.

By the end of 1995, the division consisted of three main components: the Science Archive Group, the Data Pipeline Group and the User Support Group. Each of these groups addresses specific components in the Data Flow System (DFS).

The Design of the DFS

In early 1995, the Data Flow Working Group was formed to formulate the requirements on the DFS following the guidelines of the Science Operation Plan. The group consisted of astronomers, instrumentation and software experts from several ESO divisions under the leadership of Preben Grosbøl. Discussions within the group focused on the characterisation of the "observing cycle" from proposal entry to final archive of the data. This cycle was broken down into component processes and the outline of the DFS took shape. A fundamental concept that holds the component processes together is that of the Observation Block. This "quantum of data" in the data flow system is an object which contains the essential target and instrument information to define an observation of a single object. An Observation Block is defined by either a classical observer at the telescope or a service mode observer. Whether the observer uses service-mode capabilities or not, the Observation Block is intrinsic to the flow of data from place to place in the VLT operation. Preliminary design documents describing the services offered by each of the modules in the DFS and their interrelationships were drawn up and distributed by the middle of 1995. The basic modules in the DFS are:

(1) Programme Handling:	The electronic submission of Phase 1 proposals. Preparation of a 6-month schedule for service and classical mode observing sessions.
(2) Observation Handling:	Phase II proposals are prepared using software tools. Observation Blocks are created for each target. Medium-Term Scheduler system prepares a list of possible Observing Blocks to be executed for the next few nights. Short-Term Scheduler systems select the next Observation Block to be executed by the VLT Control System (VCS) based on environment and configuration data.
(3) Science Archive:	Provides on-line catalogue services to observers. Stores raw data passed by the VCS. Data distribution and archival research on VLT data.
(4) Pipeline:	Organise raw data and calibration information for analysis. Schedule calibration processing of data. Apply approved calibration recipes.
(5) Quality Control:	Maintain calibration plan for a given instrument and mode. Compare calibration data with simulators. Study long-term trends in calibration data. Assess quality of calibrated data with respect to standards.

ESO VLT Data Flow Subsystem Breakdown

Data Management Division, April 1996

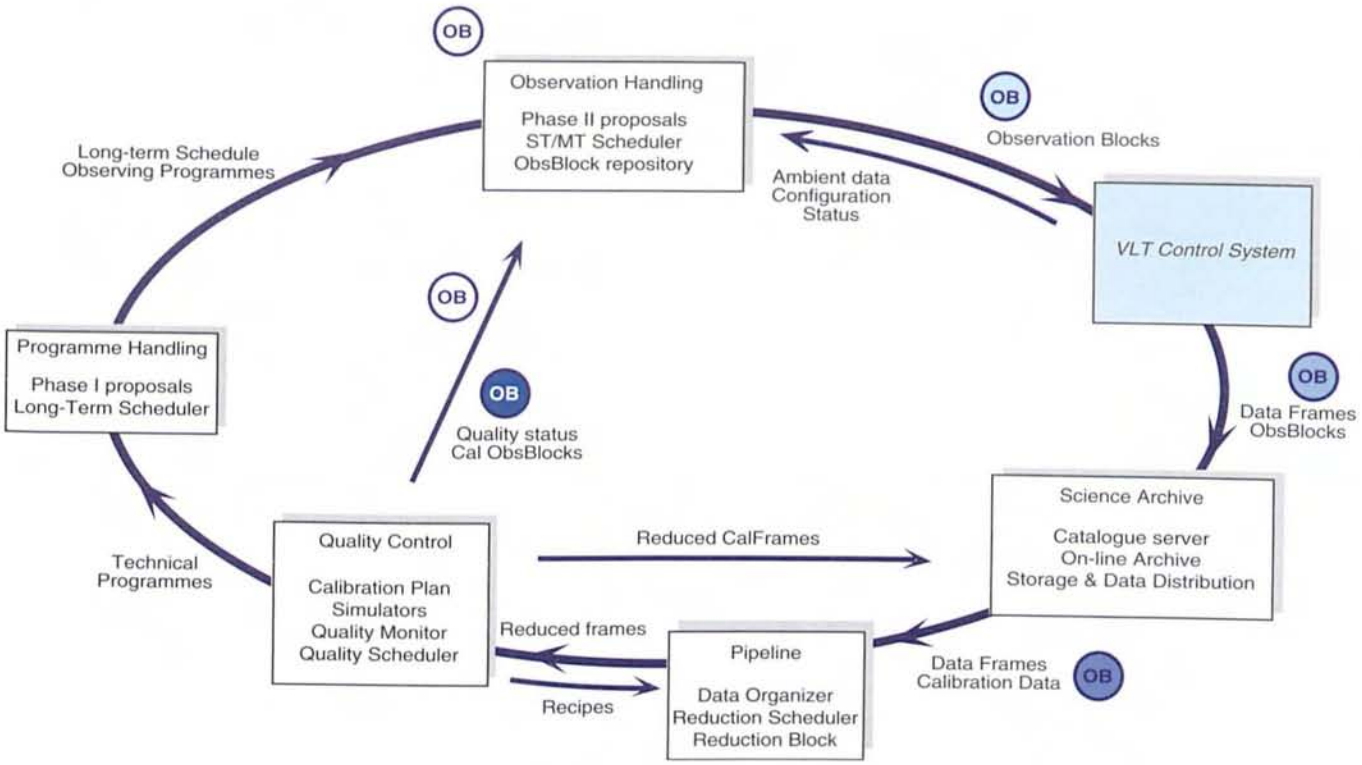

The DFS is the scientific operating system of the VLT. The VLT can be viewed as one machine with multiple components that interact. Unless the components of the VLT machine work together in an efficient manner, the scientific potential of the VLT will not be fully realised. With the DFS as a science operating system, the VLT machine can be scheduled and can make use of redundancy, pipeline and aggregation of resources to maximise throughput. In the design of the DFS, many opportunities exist to exploit the single machine vision of the VLT.

The concept of the DFS arrived late in the process of designing and implementing of the VCS. The VCS system is responsible for the control of the VLT Unit Telescopes and their associated instruments. This responsibility extends from low-level motor control to high-level assessments of the technical quality of data and its movement from instruments to storage. VCS was designed and partially implemented before concepts like Observation Blocks were introduced. It is therefore clear that the success of the DFS will depend critically on the close collaboration of software and system designers from DMD and the other ESO divisions. In September 1995, a Data Flow Project Team was formed by the Data Management Division to bring together astronomers and engineers from the VLT, Science and Instrumentation Division to address the many interfaces issues opened between the DFS and VCS. This Team has worked hard to crystallise the critical system interface issues and a number of collaborative software programmes are now under way between DMD and the VLT software group. A recent review of the status of VCS and DFS design in April 1996 (see this volume) pointed out the importance of the ongoing work of the Data Flow Project Team.

The development of a close collaboration and coupling between VCS and DFS will be aided and accelerated by the prototyping of DFS modules and VCS on the NTT. In July 1996, the NTT will be taken off the air for six months in order to install VLT-specific hardware and software for testing. From the beginning of 1997, the NTT will act like a single unit telescope. Several modules of the DFS, including the Observation Block System, will be extensively tested using SUSI as a trial instrument. All modules of the DFS will first be tested and modified within the NTT prototyping environment before going on a VLT unit telescope.

Data Pipeline Group

Under the leadership of Preben Grosbøl, the Data Pipeline Group is responsible for the final form of the DFS design as well as the implementation of the Pipeline and Quality Control modules of the DFS. Michèle Péron is the system designer for the DFS and is working to finalise the DFS design documents by the middle of 1996. Pascal Ballester, Klaus Banse and Carlos Guirao have responsibilities in Quality Control, Pipeline and system engineering respectively. The Data Pipeline Group is also responsible for the 95NOV release of MIDAS and the modification of MIDAS for use in the VCS. MIDAS will be used for NTT prototyping and will remain a valuable asset. Significant care has been taken to ensure that the design and high-level implementation of the Data Pipeline is independent of any specific data analysis system although MIDAS will be used for the low-level implementation on the first VLT instruments.

The VLT Science Archive

Miguel Albrecht leads the Science Archive Group which is responsible for the design and implementation of the archive. Currently the group operates the NTT archive and the European HST archive in collaboration with the Space Telescope European Co-ordinating Facility located within ESO. The VLT Science Archive will be distributed between Paranal and Garching and provide five types of services:

(a) Catalogue access for on-line and off-line needs,
(b) Storage of raw data from the VLT,
(c) Distribution of data to VLT users,
(d) Archive research on VLT and other data sets,
(e) Recalibration of raw data.

At the VLT, classical-mode astronomers and ESO staff will be able to ac-

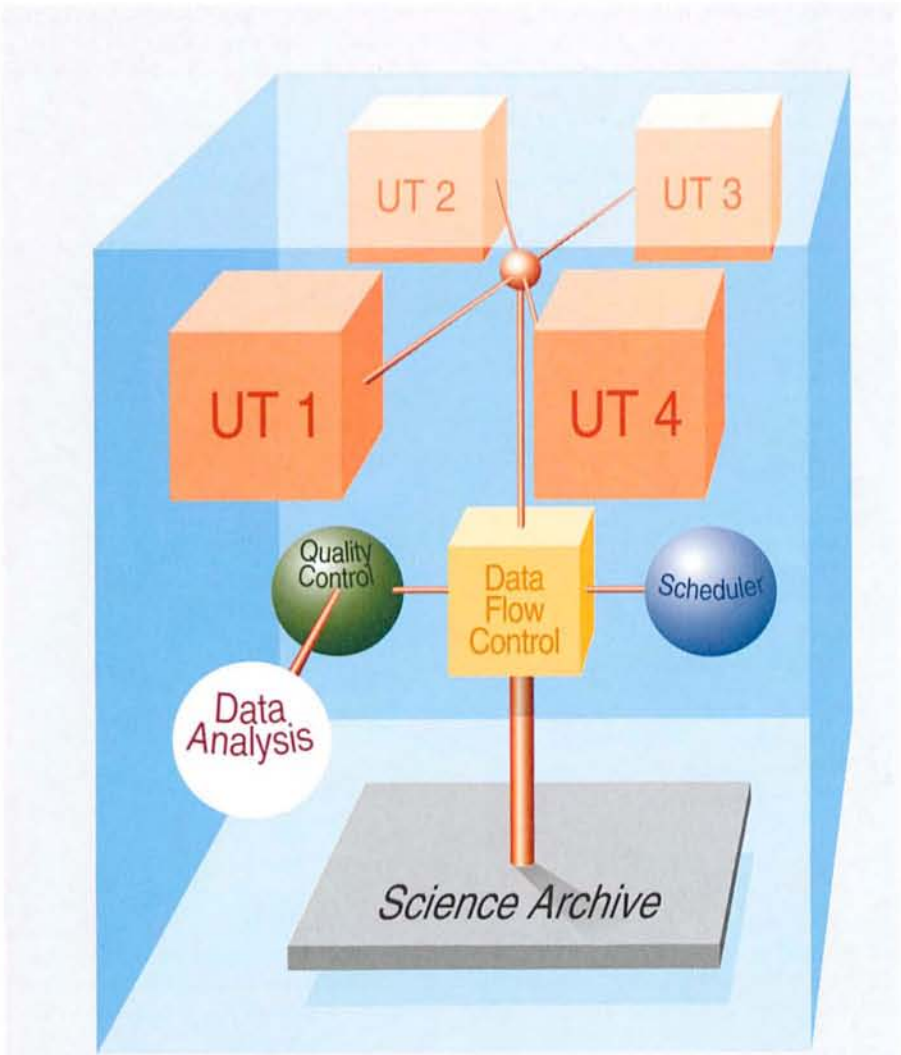

The VLT Machine

cess catalogue information for target acquisition and observation optimisation. Raw and calibrated data will be migrated from a data cache system to Garching for long-term archive and distribution to astronomers. Cache systems on Paranal and in Garching will be of the order of 1 terabyte in capacity. The main archive in Garching will have a capacity of order 100 terabytes and consist of mixed storage media for a variety of access needs. The archive will be connected to a DFS pipeline for recalibration of raw data as required since the archive will not store calibrated and derived data in the long term. A number of other archive resources, such as the HST database, will be available to VLT archival researchers. The availability of data from ground and space-based telescopes together with a software environment of tools for the manipulation of these "meta-data" resources will provide a powerful archival research environment. The design of the VLT Science Archive will be complete in 1996 and software systems will be prototyped on the NTT in early 1997. Archive specialists Fabio Sogni and Houri Ziaeepour form the current design team.

User Support

VLT users will need support in three main areas:

(a) Proposal preparation in Phase I and II,
(b) Calibration and analysis of VLT instrument data,
(c) Archival research.

The User Support Group, based in Garching, will address these needs via services offered on the World Wide Web. The group is also responsible for general ESO WWW services and intranet facilities. As part of the observation handling system, a software team in User Support is responsible for the design and implementation of the Short, Medium and Long Term Scheduling Systems. These systems will be constructed using the SPIKE engine developed at STScI for HST scheduling. A collaborative programme between DMD and STScI will deliver a prototype of the Short Term Scheduler for testing on the NTT in early 1997. A leader for the User Support group will be identified in June this year. Currently the group consists of Maurizio Chavan, Resy de Ruijsscher and Rein Warmels.

Other DMD Activities

In January 1996, ESO entered into a contract with Serco GmbH to provide Information Technology management for the operations at Garching. Serco operates a Help Desk to assist PC and workstation users with operational problems, upgrades and maintenance. The operation of the UNIX infrastructure and networking at ESO is also Serco's responsibility. Serco provides IT planning support to ESO as well as resources for short-term projects with fixed milestones and objectives. Joe Schwarz is the ESO manager of the Outsourcing Services Centre within the DMD and acts as ESO's single point of contact to the Serco operations.

An ongoing activity now under the responsibility of DMD is the Palomar Observatory Sky Survey II plate copy project. ESO has undertaken to provide the community with film copies of the IIIa-J, IIIa-F and IV-N plates from the Palomar Schmidt telescope as part of the second-generation sky survey. Positive glass copies of the original plates are made at ESO. These plates are then used for the film production and are also sent to STScI for digital scanning. The plate taking is approximately 80% complete in IIIa-J and IIIa-F and about 40% complete for the production of film copies. Jean Quebatte leads the photographic laboratory team of Peter Dorn and Gisela Strigl.

The Next 5 Years

The testing of prototypes for the DFS on the NTT in early 1997 marks the beginning of an important five year programme for the DMD. By the end of 1997 the DFS will need to support the test camera on UT1. User Support and Science Archive resources will be in place to support both classical and service mode observing proposals on the VLT in 1998. By the end of 1998, the DFS has to be fully operational to support the first VLT instrument operations. As new VLT instruments are designed and come on-line, a prototyping and commissioning process will involve specific support for all the available instrument modes within the DFS.

DMD will provide staff for the operation of the DFS on Paranal. Preparing and operating the scheduling system, Observation Block handling, pipeline processing, quality control of calibrations and archive operations will be carried out by DMD Data Flow Operations staff in collaboration with telescope operators, instrument scientists and staff astronomers.

The DFS is a critical component of the VLT machine that will have a fundamental bearing on the VLT's scientific productivity. The success of the DFS will depend as much on the astronomers that use it as the designers and maintainers of the system. The feedback of ideas and modifications from the user community must occur efficiently if the DFS is to provide astronomers with high-quality data products. Over the next years, DMD will host a series of workshops in which astronomers will be invited to participate in a broad range of discussions on the functionality and services offered by the DFS. These workshops will continue into the VLT operational era.

Peter Quinn
e-mail: pquinn@eso.org

DMD Major Milestones 1996–2001

1996 Q12
- Finalise DFS design/responsibilities/interfaces

Q34
- Science Archive design document
- Construct SUSI pipeline, OB/STS & Archive prototypes for NTT

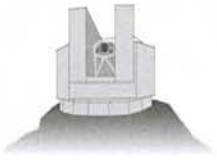

1997 Q12
- Operational prototypes on NTT, prototype development continues
- Data Flow Operations begin

Q34
- Phase I/II operational
- Test camera supported on Paranal
- UT1 integration

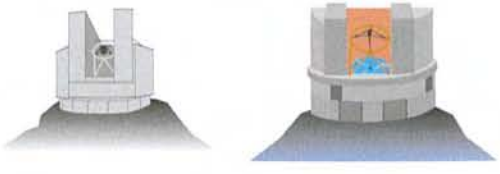

1998 Q12
- DFS instrument modules operational
- STS/MTS/LTS and user support services fully operational
- Science Archive operational

Q34
- Full DFS operational
- ISAAC & FORS1 integration

1999 Q12
- CONICA integration

Q34
- VLTI prototypes, UVIS integration

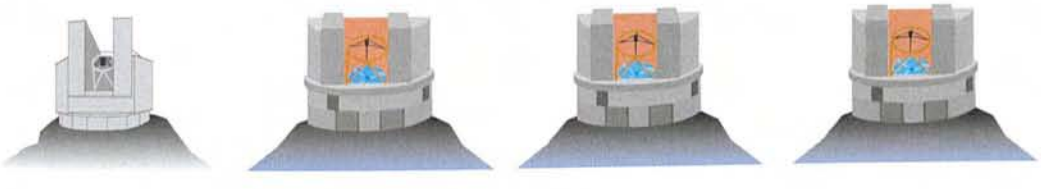

2000 Q12
- VISIR & FORS 2 integration

Q34
- FUEGOS integration

The Optical Detector Team WWW Pages

P. AMICO AND T. BÖHM, ESO

1. Introduction

ESO's Optical Detector Team (ODT) was formed in the first half of 1995 in order to improve the quality of ESO's optical detector systems. One of our first tasks was to improve communication of system performance to the ESO community. The World Wide Web (WWW) is the best avenue for this communication. Although some data had been posted on the Web, in the summer of 1995, this information was, in general, disorganised, incomplete and in some cases obsolete. Thus, we initiated the development of a new ODT *Web cluster*, a cohesive whole designed to maximise usability and completeness of information on optical detectors within the ESO Web. The deadline for going on-line was fixed for beginning of September 1995.

The design of our Web cluster was constrained by the following questions: Who is the typical user of ESO's Web? What kind of information does this user require? The typical user of the ODT WWW is an astronomer who is proceeding through the complete observation cycle: preparation of an observing proposal, preparation for an observing run, making the observations and finally, reducing the data. The information we need to provide must therefore address all CCD-related questions which could arise during this process:

- the list of optical detectors presently offered in combination with the different instruments and telescopes.
- *quick look* information on a specific detector, such as CCD type, pixel and detector size, quantum efficiency curves, read-out noise, conversion factor, dark current, and full frame readout time.
- advanced level information: linearity curves, cosmetic quality, charge transfer efficiency, available readout modes.
- general information on optical detectors, such as planned upgrades and detector history.
- on-line manuals.

To fully serve the purpose, the information on the Web must be kept up-to-date, be continuously available on the network, and it must be unambiguous. Ambiguity is avoided by designating the ODT Web cluster as the only source of information about optical detectors at ESO.

2. Structure and Content of the ODT Web Cluster

The World Wide Web offers much freedom in the way of structuring and presenting information. However, for the sake of efficiency, clarity and completeness of our Web cluster, we decided to

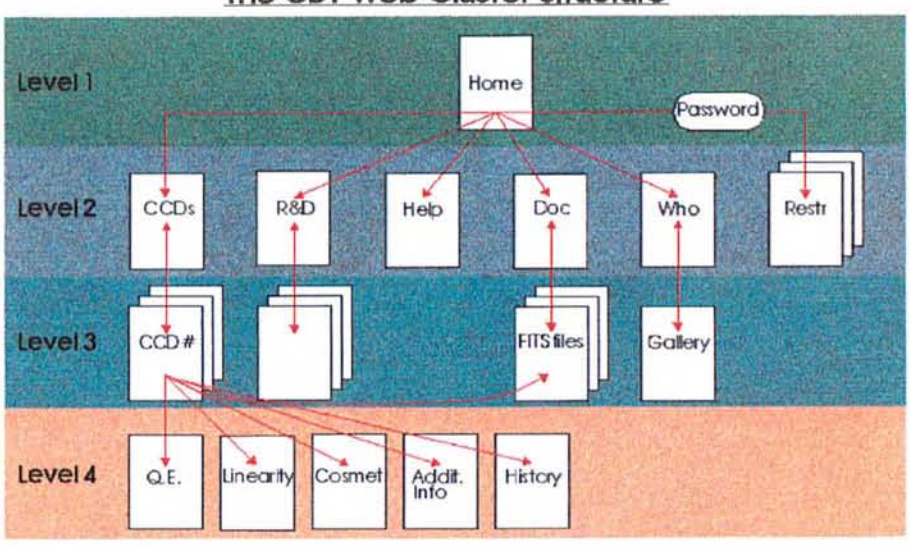

Figure 1: Diagram of the ESO-Optical Detector Team Web Cluster structure. The different levels can be identified by their corresponding background colour.

Figure 2: The ODT main index page. This page provides access to the different information and services.

organise it in a tree-like structure, limited to 4 hierarchical levels (Fig. 1) containing the following pages:

- Level 1 – ODT homepage (main index), see Figure 2.
- Level 2 – Information on CCDs at La Silla (present and past).
  - Research, developments and planned upgrades.
  - The helpdesk mailbox.
  - Document archive (FITS images and ps files).
  - Who is Who in the ODT.
  - ODT's internal Web area (restricted to ODT staff).
- Level 3 – Specific detector pages (see Fig. 3).
  - ODT activities.
- Level 4 – Advanced information on detectors.

The ODT Web cluster is linked to the ESO Web through the *Telescopes, Instrumentation and Detectors link* in the ESO portal. This structure is supported by navigation links, which allow the user to move to the upper adjacent level, the ODT homepage or the ESO portal.

The most relevant pages for the typical user are those containing technical information on CCDs in levels 3 and 4. These pages follow a well-defined structure, consisting of three main parts:

1. The upper part contains a table with the key characteristics of the CCD system. If variations of these values are discovered during routine tests, Web pages are updated within a few days of the test.

2. The middle part of the page contains a plot of the detector quantum efficiency and provides links to more detailed information on the linearity, cosmetic quality and an image archive, from which low-level flat fields and bias images can be retrieved in FITS format. These images are not meant to replace standard calibration images taken by the observer during the run, but allow a first estimation of the cosmetic quality of the CCD. (Clicking on the quantum efficiency curve gives access to a magnified version of the plot (also available in postscript format) and to a text table of q.e. data.

3. The third part of the page provides various services: access to advanced-level information (e.g.: (CTE, full well) for different read-out anodes, information on the history of the detector and a warning area for special comments and a mailbox report form.

The bottom of the page is reserved for the navigation area.

We have established a restricted area, accessible from the homepage by ODT members (password restricted), that the ODT is using as an *Intranet*. The ODT is using the Intranet to put all of our project information, scheduling plans and documentation on-line, so that team members working in Garching and Chile are literally "working from the same page".

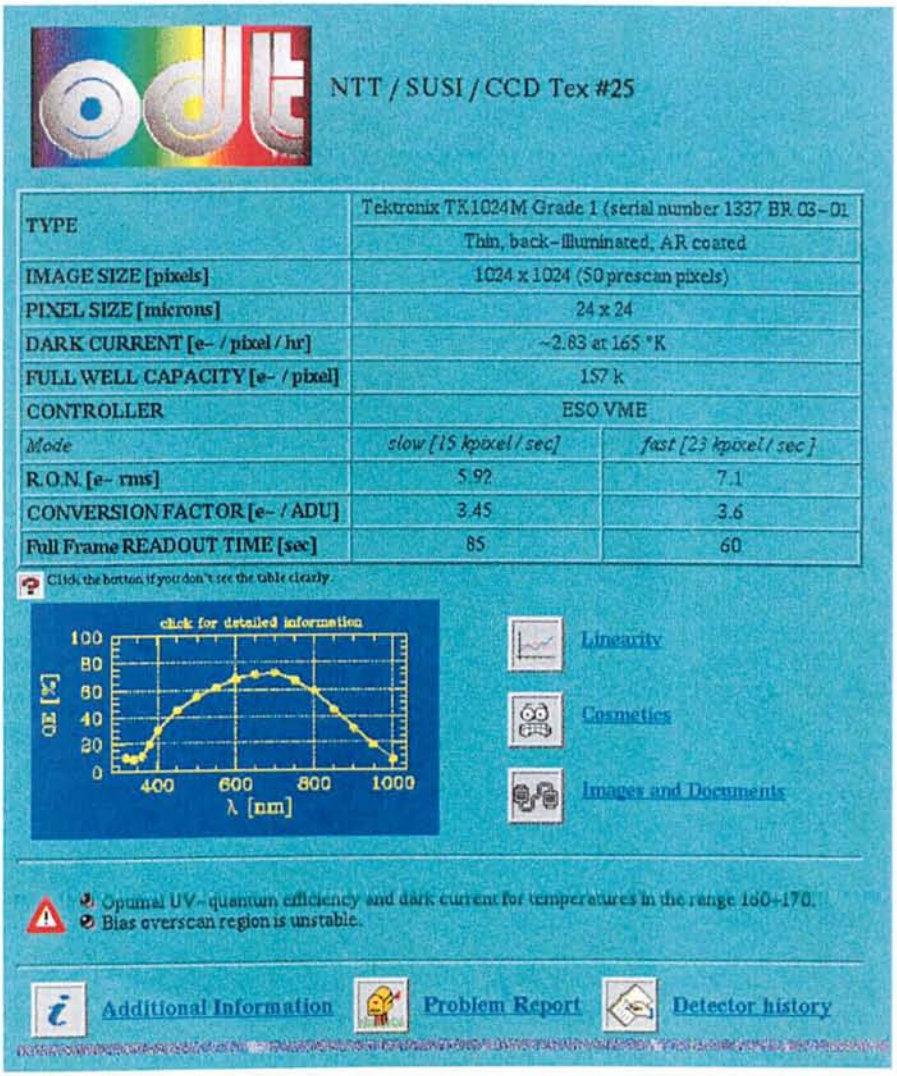

Figure 3: Example of the layout of a specific detector page (CCD #25 mounted on NTT with SUSI).

3. Layout and Styles

The graphical layout of a WWW page depends on the user browser and its settings. The layout of the ODT Web cluster is optimised for viewing with the Netscape Navigator version 1.1N (or greater). The pages are sized to A4 format in order to limit the use of scroll bars. The length of the blue marble bar shows the optimum page width. All pages are recognisable by the ODT logo, which is a spectrum with shaded letters "odt". The background colours of the pages are used to denote the level within the tree: light green (1), pastel blue (2), light blue (3) and light orange (4). Report/comment forms and special pages have a grey background.

4. ODT Helpdesk and Access Statistics

The ODT helpdesk provides a contact point for all users who need additional information or who have special requests. Access is made by sending e-mail to odteam@eso.org or using the report/comment forms that are within the ODT Web cluster. The incoming e-mail is checked daily by ODT members; we strive to respond to queries within one day.

We registered an average of 11,000 monthly accesses during the first six months on-line; 50% of these accesses are local.

5. General Remarks

The planning and implementation of the new ODT WWW cluster was led by ODT fellows in Garching with assistance from the optical detector engineers at La Silla. The response of the ESO community has been very encouraging and we have received many useful comments that have helped us to improve the quality of the pages. Providing high-quality information to the astronomical community is considered a top-priority task for the Optical Detector Team; regular updating and improvement of the Web cluster is part of this goal.

The ODT home page can be accessed at the following URL: "http://www.eso.org/odt".

Paola Amico
pamico@eso.org

The King of Sweden Visits ESO Exhibition

Four hundred years ago, it was the site of the leading observatory of the world and residence of the Danish astronomer Tycho Brahe. This year, during the final days of May, astronomers and engineers converged on the island of Hven on the occasion of the ESO/SPIE Conference on Optical Telescopes of Today and Tomorrow. The conference was part of a series of astronomy-related activities which take place this year on both sides of Øresund, the narrow stretch of water that separates Denmark and Sweden. Other events include an astronomy summer school, meetings for amateur astronomers as well as two exhibitions in Landskrona and Copenhagen. Both have been organised with the support of Copenhagen 96, the organisation responsible for the extensive activities in connection with Copenhagen being the European Capital of Culture 1996.

The exhibition in Landskrona is mainly a historical exhibition about Tycho Brahe. However, ESO and the VLT are presented in a section called "Tycho's Heritage". The exhibition was inaugurated on April 12 by His Majesty Carl XVI Gustav, King of Sweden. In the picture, Prof. Arne Ardeberg explains the working principle of the VLT to the King (at the centre) and his entourage. On the King's left is seen Ann Catrin Haglund, head of the regional authority, and Gösta Nilsson of the City of Landskrona.

The second exhibition opens at the Tycho Brahe Planetarium in Copenhagen in July this year. This is an ESO exhibition which has been prepared jointly by the planetarium, the Copenhagen University Observatory, Copenhagen Astronomical Society and ESO's Education and Public Relations Department.

C. MADSEN

ANNOUNCEMENTS

ESO Workshop on

Galaxy Scaling Relations: Origins, Evolution and Applications

ESO-Garching, 18–20 November 1996

Scaling relations between various galaxy parameters, such as the Tully-Fisher relation, the Faber-Jackson relation, and more recently the Dn-sigma relation and the Fundamental plane of early-type galaxies have been extensively studied in the local Universe. They are interesting both for investigating galaxy properties themselves and for their application to estimate distances of galaxies. With the arrival of the new generation of 8-m-class telescopes and the availability of HST imaging, it will be possible to measure scaling parameters of galaxies at high redshifts. The purpose of this workshop is to discuss our current knowledge of scaling relations in the local Universe and current and future attempts to measure and understand scaling relations at high redshift.

The meeting will cover the following main topics:

- Phenomenology of spiral, elliptical, and cD galaxy scaling relations, and their dependence on the environment
- Physical origin of the scaling relations
- The scaling relations at moderate and high redshifts
- Scaling relations as distance indicators
- Comparison with other distance indicators
- Peculiar Motions and implications to large-scale structure theories

Scientific Organising Committee: R. Bender (University of Munich), L. da Costa (ESO, Chair), M. Franx (Groningen), W. Freudling (ST-ECF), M. Haynes (Cornell), E. Huizinga (ESO), J. Mould (Mt. Stromlo), A. Renzini (ESO), S. White (MPA).

Contact Address:
Luiz da Costa
European Southern Observatory
Karl-Schwarzschild-Strasse 2, D-85748 Garching bei München, Germany
e-mail: scalwork@eso.org Fax: +49 89 320 06 480

Three Vacancies on La Silla for: Astronomer/Team Leader (CSO401), Infrared Astronomer (CSO402), Astronomer (CSO502)

Experience and knowledge: Several years of post-doctoral experience in the areas of high-dispersion optical spectroscopy, infrared imaging and/or spectroscopy, faint-object imaging and spectroscopy, or adaptive optics and proven capability of working in and/or leading multi-disciplinary teams. Good working knowledge of English and Spanish is essential.

Assignment: The La Silla Observatory operates on the basis of multi-disciplinary teams. There are four telescope teams to run the SEST sub-mm telescope, the 3.6-m and its Coudé Auxiliary Telescope (CAT), the New Technology Telescope (NTT) and the 2.2-m, ESO 1.5-m, Danish 1.5-m, Dutch 0.9-m, ESO 0.5-m and Schmidt telescopes. Each team consists of 10–15 persons including astronomers, technicians, engineers and night assistants. They are fully responsible for operations and are supported in the specialised technical areas by technicians and engineers from the so-called support teams (Optics, Detectors, IR, Mechanics, Electronics and Software). Each telescope team has 2 staff astronomers, as well as 2–3 post-doctoral fellows and 2–3 students. Staff astronomers and fellows share the responsibilities of instrument support acting as instrument scientists in charge of direct support to visiting astronomers at the telescope, documentation, upgrades, calibration plans and on-line data reduction facilities.

One of the staff astronomers on each team acts, on a rotating basis, as Team Leader and as such assumes the task of providing supervision and motivation to all the members of the team. Team Leaders are responsible for administrating the Team's budget and monitoring the performance of the team members. Team Leaders report to the Observatory Director and are members of the observatory management team. They receive managerial and administrative support from the observatory management for budgeting and personnel issues.

The available positions will fill vacancies in the 3.6m+CAT team, to support CASPEC, CES, TIMMI and/or ADONIS, in the NTT team to support SOFI and in the 2.2+1.5 team to support IRAC and/or EFOSC. Information about these instruments is available through the La Silla pages on the WWW.

Staff astronomers must be able to provide scientifically sound judgements on the many technical issues facing a modern observatory. ESO therefore requires, supports, and encourages staff astronomers to carry out dynamic and independent research programmes using La Silla telescopes, as well as facilities at other observatories. Active publication in leading journals is considered essential. Staff astronomers use up to 50% of their time on research, and are supported with excellent facilities and adequate travel grants to attend conferences, work with collaborators and visit other observatories.

Duty Station: La Silla staff astronomers are based at the ESO research and administrative centre in Santiago and are required to spend at least 105 nights per year at La Silla.

Contract: These positions are for an initial period of three years renewable for another three with the possibility for tenure after the fifth year.

Starting date: as soon as possible.

Remuneration: The remuneration for this post will be commensurate with the background, experience and family status. The basic monthly salary (tax-free) will not be less than DM 6,403. Furthermore, an expatriation allowance as well as some other allowances may be added.

Applications and three letters of recommendation should be submitted by September 15, 1996 to the:

European Southern Observatory, Personnel **(Ref.: Post No. & Title)**
Karl-Schwarzschild-Str. 2, 85748 Garching bei München, Germany

ESO Fellowship Programme 1997/98

The European Southern Observatory (ESO) intends to award up to six postdoctoral fellowships tenable at the ESO Headquarters, located in Garching near Munich, and up to two postdoctoral fellowships tenable at ESO's Astronomy Centre in Santiago, Chile.

ESO facilities include the La Silla Observatory in Chile, the VLT Observatory on Cerro Paranal, and the astronomical centres in Garching and Santiago. At La Silla, ESO operates eight optical telescopes with apertures in the range from 0.9 m to 3.6 m, the 15-m SEST millimetre radio telescope, and smaller instruments. First light for the first telescope of the Very Large Telescope (VLT) consisting of four 8-m telescopes is expected in the first quarter 1998. Both the ESO Headquarters and the Astronomy Centre in Santiago offer extensive computing facilities, libraries and other infrastructure for research support. The Space Telescope European Co-ordinating Facility (ST-ECF), located in the ESO Headquarters building, offers the opportunity for collaborations. In the Munich area, several Max-Planck Institutes and the University Observatory have major programmes in astronomy and astrophysics and provide further opportunities for joint programmes. In Chile, astronomers from the rapidly expanding Chilean astronomical community collaborate with ESO colleagues in a growing partnership between ESO and the host country's academic community.

The main areas of activity at the Headquarters and in Chile are:

- research in observational and theoretical astrophysics;
- managing and constructing the VLT;
- developing the interferometer and adaptive optics for the VLT;
- operating the La Silla Observatory;
- development of instruments for current ESO telescopes and for the VLT;
- calibration, analysis, management and archiving of data from the current ESO telescopes;
- fostering co-operation in astronomy and astrophysics within Europe and Chile.

In addition to personal research, fellows in Garching spend up to 25% of their time on the support or development activities mentioned above. These activities offer the opportunity to make short-term visits to the ESO sites in Chile and to develop in-depth knowledge of the operations of the observatory. In Chile, fellows and staff astronomers spend one week at ESO's Centre in Santiago, one week at La Silla Observatory and have the third week off. At La Silla, fellows help in supporting visiting astronomers, and participate in the development and maintenance of the telescopes and instruments. The fellowship programme in Chile offers a unique opportunity to learn and to participate in the process of observational astronomy while pursuing a research programme with state-of-the-art facilities.

Applicants should have a recent doctorate. The basic monthly salary will be not less than DM 5526 to which is added an expatriation allowance of 9–12% in Garching, if applicable, and up to 40% in Chile. The fellowships are granted for one year with the expectation of a renewal for a second year and, for Chile only, exceptionally a third year. Fellowships begin between April and October of the year in which they are awarded. Applications should be submitted to ESO not later than October 15, 1996. Applicants will be notified in December 1996 or soon thereafter. The ESO Fellowship Application Form must be used, which is available directly from ESO or from http://www.eso.org/adm/personnel/fellows. The applicant should arrange for three letters of recommendation from persons familiar with his/her scientific work to be sent directly to ESO. These letters should reach ESO not later than October 15, 1996.

Further inquiries, requests for application forms, and completed applications should be addressed to:

European Southern Observatory
Fellowship Programme
Karl-Schwarzschild-Strasse 2
D-85748 Garching bei München
Germany

Mr. Gerhard Bachmann Retired

After more than 25 years at ESO, most of that time as Head of Administration, Mr. Gerhard Bachmann retired on May 31, 1996, just after his 65th birthday on May 24. Mr. Bachmann was born in Berlin, began his professional career in the "Senatsverwaltung" of Berlin and became in 1963 assigned to the NATO Organisation in France and Luxembourg. He came to ESO in October of 1970 and was appointed Head of Administration in December 1972, succeeding Mr. J. Bloemkolk.

Throughout his time at ESO, Mr. Bachmann has greatly contributed to the success of the Organisation. Council Members and other officials of the Member States have repeatedly stated how impressed they were by his diplomatic abilities and his thorough knowledge of the interaction of science and politics in the field of astronomy. He played an important role in the negotiations with Chile and explored a closer co-operation with EU. Inside ESO, he has ensured the smooth running of the Organisation's Administration, making certain that ESO has avoided unnecessary bureaucracy, yet adhered strictly to the Rules and Regulations which govern this international organisation.

All of us at ESO wish Mr. Bachmann a happy and healthy retirement, much of which we understand he will spend in his beautiful house in the south of France.

New ESO Proceedings Available

The Proceedings of the OSA/ESO topical Meeting on

Adaptive Optics

(ESO Conference and Workshop Proceedings No. 54)

have been published. The 542-p. volume, edited by M. Cullum, is available at a price of DM 80.– (prepayment required).

Payments have to be made to the ESO bank account 2102002 with Commerzbank München, or by cheque, addressed to the attention of

ESO, Financial Services,
Karl-Schwarzschild-Strasse 2,
D-85748 Garching bei München, Germany

New ESO Preprints

(February – June 1996)

SCIENTIFIC PREPRINTS

1131. J.K. Kotilainen et al.: Near-Infrared Line and Continuum Imaging of the Nuclear Starburst Region NGC 1808. *A&A.*
1132. E. Giallongo et al.: The Proximity Effect, the UV Background and the statistics of the Lyman-Alpha Lines at High Resolution. *ApJ.*
1133. J.-L. Starck et al.: Astronomical Image Compression Based on Noise Suppression. *PASP.*

1134. R.A.E. Fosbury: Circumnuclear Activity. *Lecture Notes in Physics.* Springer.
1135. G. De Marchi and F. Paresce: Very Blue Stars and Mass Segregation in the Core of M15. *ApJ.*
1136. E.J. Wampler et al.: Deuterium and Ionic Abundances at High Redshift. Invited talk presented at Atami conference on "Origin of Matter and Evolution of Galaxies in the Universe '96", ed. T. Kajino, Y. Yoshii, S. Kubono (World Scientific, Singapore, 1996).
1137. C. Simpson et al.: Emission Line Ratios in a Radio-Selected Sample of AGN. *MNRAS.*
1138. D. Minniti et al.: Globular Clusters in the Inner Regions of NGC 5128 (Cen A). *ApJ.*
1139. J. Bally, J. Morse, Bo Reipurth: The Birth of Stars: Herbig-Haro Jets, Accretion and Protoplanetary Disks. *Science with the Hubble Space Telescope – II.* Space Telescope Science Institute, 1966. Eds. P. Benvenuti, F.D. Macchetto, E.J. Schreier.
1140. J.D. Kennefick, S.G. Djorgovski, G. Meylan: A Multicolor CCD Survey for Faint $z > 4$ Quasars. *AJ.*
1141. M. Villar-Martín, L. Binette, R.A.E. Fosbury: The Effects of Resonance Scattering and Dust on the UV Line Spectrum of Radio Galaxies. *A&A.*
1142. G.A. Wade et al.: A Magnetic Model for the Ap Star HD 192678. *AA.*
1143. Bo Reipurth, L.-Å. Nyman, R, Chini: Protostellar Candidates in Southern Molecular Clouds. *A&A.*
1144. Bo Reipurth, A. Pedrosa, M.T.V.T. Lago: Hα Emission in Pre-Main Sequence Stars – I. An Atlas of Line Profiles. *A&A.*
1145. D. Minniti, A.A. Zijlstra: Dwarf Galaxies also have Stellar Hallos. *ApJ* Letters.
1146. M. Turatto et al.: The Properties of the Peculiar Type Ia SN 1991bg. Analysis and Discussion of two Years of Observations. *MNRAS.*
1147. S. Randich, J.H.M.M. Schmitt, C. Prosser: Coronal Activity in the Coma Berenices Open Cluster. *A&A.*
1148. G.C. Van de Steene, K.C. Sahu, S.R. Pottasch: Optical Observations of Southern Planetary Nebula Candidates. *A&A.*
1149. V. Carbone, S. Savaglio: Multifractional Structure of Lyα Clouds: an Example with the Spectrum of QSO 0055–26. *MNRAS.*
1150: T. Böhm et al.: Azimuthal Structures in the Wind and Chromosphere of the Herbig Ae Star AB Aur. *A&A.*
1151: N. Nancy et al.: The Chamaeleon Infrared Nebula: a Polarization Study with High Angular Resolution. *ApJ* Letter.
1152. A. Iovino, R. Clowes, P. Shaver: A Large Sample of Objective Prism Quasar Candidates.
1153. M.R.S. Hawkins et al.: Two Variable Quasars at $z > 4$. *MNRAS.*
1154. M.-H. Ulrich and J. Rönnback: The Host of B2 0828+32, a Radio Galaxy with Two Sets of Radio Lobes. *A&A.*
1155. W.W. Zeilinger et al.: The Distribution of Ionized Gas in Early-Type Galaxies II. The Velocity Field of the Ionized Gas. *A&A.*
1156. A. Marconi et al.: Infrared and Visible Coronal Lines in NGC 1068. *A&A.*
1157. F. Comerón, J. Torra: The Galactic Distribution and Luminosity Function of Ultracompact HII Regions. *A&A.*

TECHNICAL PREPRINTS

70. D. Baade: The Operations Model for the Very Large Telescope. Invited talk given at the fall meeting of the Astronomische Gesellschaft in Bonn, September 1995, 18–23. To appear in R. Schielicke (ed.) *Reviews in Modern Astronomy,* Vol. 7. Springer.

PERSONNEL MOVEMENTS

International Staff (April 1 – July 31, 1996)

ARRIVALS

EUROPE

KÖNIG, Norbert (D), Head of Administration
TELANDER, Christine (S), Division Secretary (DMD)
ZIAIEPOUR, Houri (F), System Archive Engineer
EMSELLEM, Eric (F), Fellow
DUC, Pierre-Alain (F), Fellow
DROUET D'AUBIGNY, Christian (F), Coopérant

CHILE

PERSSON, Glenn (S), Paid Associate, SEST
SHETRONE, Matthew (USA), Fellow
TURATTO, Massimo (I), Paid Associate

TRANSFERS FROM GARCHING TO CHILE

PHAN, Duc Thanh (B), Software Engineer
CHIESA, Marco (I), Software Engineer

DEPARTURE

EUROPE

BACHMANN, Gerhard (D), Head of Administration
NASTVOGEL-WÖRZ, Michael (D), Software Support Engineer
DIERCKX, Peter (B), System Manager
JANSEN, Ronald (NL), Accounting Assistant
MAYR, Stephanie (D), Junior Analyst
PATAT, Ferdinando (I), Student

CHILE

KNEE, Lewis (CDN), SEST Fellow
RÖNNBACK, Jari (S), Fellow
GEOFFRAY, Hervé (F), Student
LEDOUX, Cédric (F), Coopérant

Local Staff Chile (April 1 – July 31, 1996)

ARRIVALS

GAJARDO, Maria Soledad (RCH), VLT Software Engineer
WENDEROTH, Erich (RCH), Instrument Operator

DEPARTURES

FERNÁNDEZ A., Juan (RCH), Cook
FERNÁNDEZ del R., Juan (RCH), Imports/Exports
AVILÉS, Roberto (RCH), Instrument Operator
ESPINOZA, Juan (RCH), Cook

ESO Proceedings Still Available

A number of proceedings published by ESO are still available. To permit you to complete the series or simply to inform you about any volume that you may have missed, we reproduce here a list of some of the more recent ESO proceedings.

No.	Title and year of publication	Price
40	High-Resolution Spectroscopy with the VLT, 1992	DM 45.—
41	Fourth ESO/ST-ECF Data Analysis Workshop, 1992	DM 25.—
42	Progress in Telescope and Instrumentation Technologies, 1993	DM 90.—
43	Astronomy from Large Data Bases II, 1993	DM 70.—
44	Science with the Hubble Space Telescope, 1993	DM 80.—
45	Structure, Dynamics and Chemical Evolution of Elliptical Galaxies, 1993	DM 90.—
46	Mass Loss on the AGB and Beyond, 1993	DM 70.—
47	Fifth ESO/ST-ECF Data Analysis Workshop, 1993	DM 30.—
48	ICO-16 Satellite Conference on Active and Adaptive Optics, 1994	DM 90.—
49	Dwarf Galaxies, 1994	DM 90.—
50	ESO/OAT Workshop "Handling and Archiving Data from Ground-based Telescopes", 1994	DM 35.—
51	Third CTIO/ESO Workshop on "The Local Group: Comparative and Global Properties", 1995	DM 50.—
52	European SL-9/Jupiter Workshop, 1995	DM 80.—
53	ESO/ST-ECF Workshop on "Calibrating and understanding HST and ESO instruments", 1995	DM 60.—
54	OSA/ESO Topical Meeting on "Adaptive Optics",1996	DM 80.—

ESO, the European Southern Observatory, was created in 1962 to . . . establish and operate an astronomical observatory in the southern hemisphere, equipped with powerful instruments, with the aim of furthering and organising collaboration in astronomy... It is supported by eight countries: Belgium, Denmark, France, Germany, Italy, the Netherlands, Sweden and Switzerland. It operates the La Silla observatory in the Atacama desert, 600 km north of Santiago de Chile, at 2,400 m altitude, where fourteen optical telescopes with diameters up to 3.6 m and a 15-m submillimetre radio telescope (SEST) are now in operation. The 3.5-m New Technology Telescope (NTT) became operational in 1990, and a giant telescope (VLT = Very Large Telescope), consisting of four 8-m telescopes (equivalent aperture = 16 m) is under construction. It is being erected on Paranal, a 2,600 m high mountain in northern Chile, approximately 130 km south of Antofagasta. Eight hundred scientists make proposals each year for the use of the telescopes at La Silla. The ESO Headquarters are located in Garching, near Munich, Germany. It is the scientific, technical and administrative centre of ESO where technical development programmes are carried out to provide the La Silla observatory with the most advanced instruments. There are also extensive facilities which enable the scientists to analyse their data. In Europe ESO employs about 200 international Staff members, Fellows and Associates; at La Silla about 50 and, in addition, 150 local Staff members.

The ESO MESSENGER is published four times a year: normally in March, June, September and December. ESO also publishes Conference Proceedings Preprints, Technical Notes and other material connected to its activities. Press Releases inform the media about particular events. For further information, contact the ESO Information Service at the following address:

EUROPEAN
SOUTHERN OBSERVATORY
Karl-Schwarzschild-Str. 2
D-85748 Garching bei München
Germany
Tel. (089) 320 06-0
Telex 5-28282-0 eo d
Telefax (089) 3202362
ips@eso.org (internet)
ESO::IPS (decnet)

The ESO Messenger:
Editor: Marie-Hélène Demoulin
Technical editor: Kurt Kjär

Printed by
Druckbetriebe Lettner KG
Georgenstr. 84
D-80799 München
Germany

ISSN 0722-6691

Contents

TELESCOPES AND INSTRUMENTATION

SCIENCE WITH THE VLT/VLTI

REPORTS FROM OBSERVERS

OTHER ASTRONOMICAL NEWS

ANNOUNCEMENTS